Laser-induced non-thermal processes

Wolfgang Kautek

University of Vienna
Department of Physical Chemistry
A-1090 Vienna, Austria

wolfgang.kautek@univie.ac.at

Outline

- Excitation mechanisms of solids
- Metals: Two-temperature model
  - Fundamentals: Influence of density of states
  - Thin films
  - Metal ablation
  - Hot electron electrochemistry
- Dielectrics: Multiphoton and Avalanche Ionization
  - Dielectric ablation
  - Coulomb explosion
  - Non-thermal melting, X-ray
- Role of Defects
- Applications

Outline

- Excitation mechanisms of solids
- Metals: Two-temperature model
  - Fundamentals: Influence of density of states
  - Thin films
  - Metal ablation
  - Hot electron electrochemistry
- Dielectrics: Multiphoton and Avalanche Ionization
  - Dielectric ablation
  - Coulomb explosion
  - Non-thermal melting, X-ray
- Role of Defects
- Applications

Overview of Laser Matter Interaction

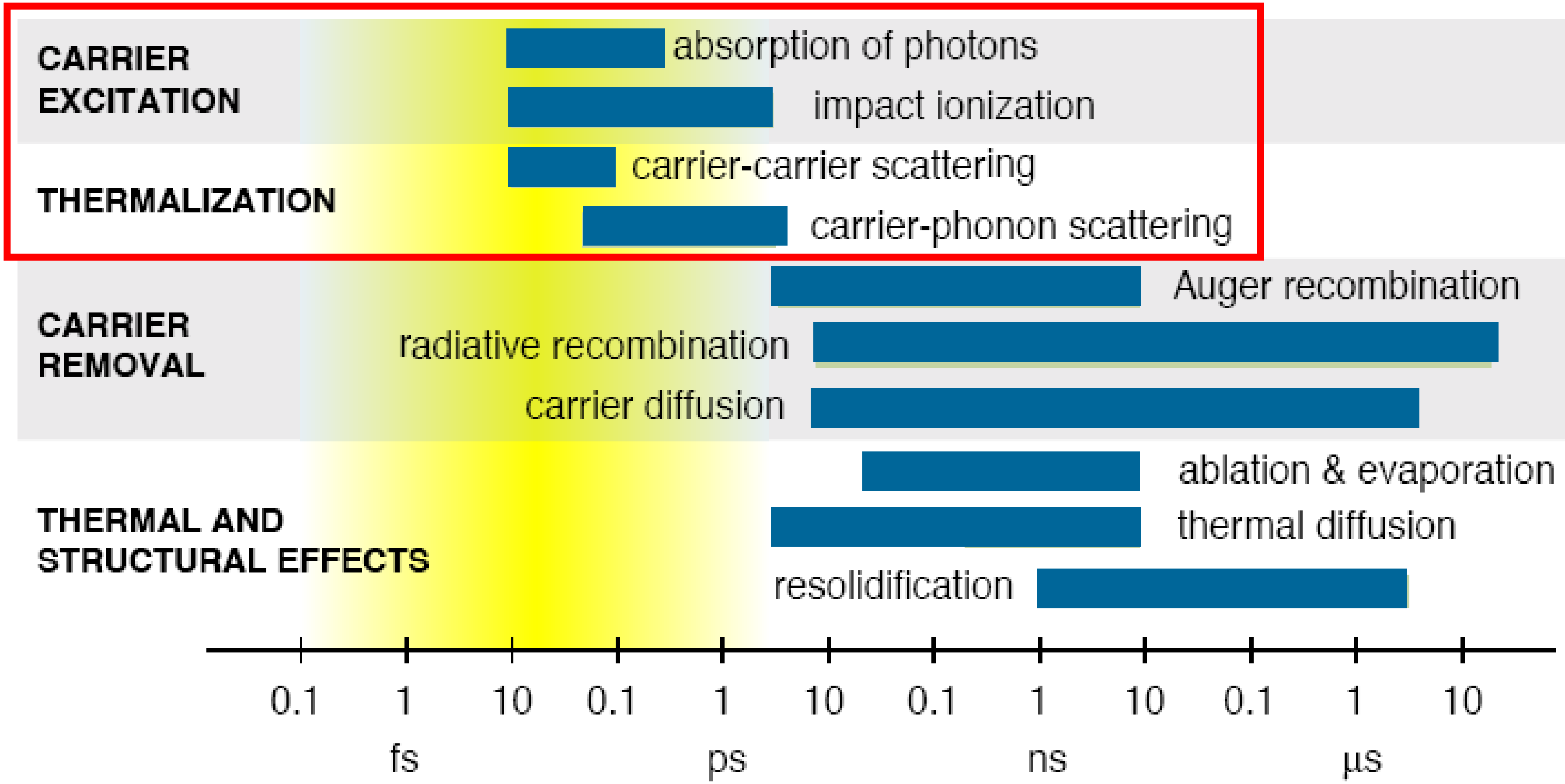

Accord. To E. Mazur

Exciting carriers in metals

Keldysh parameter $$\gamma = \frac{\omega}{e}\sqrt{\frac{m_e c n \varepsilon_0 E_g}{I}} << 1$$

ω: laser frequency
I: intensity
m_e: electron effective mass
e: electron charge
c: speed of light
n: refractive index
ε_0: permittivity of free space
E_g: is the bandgap

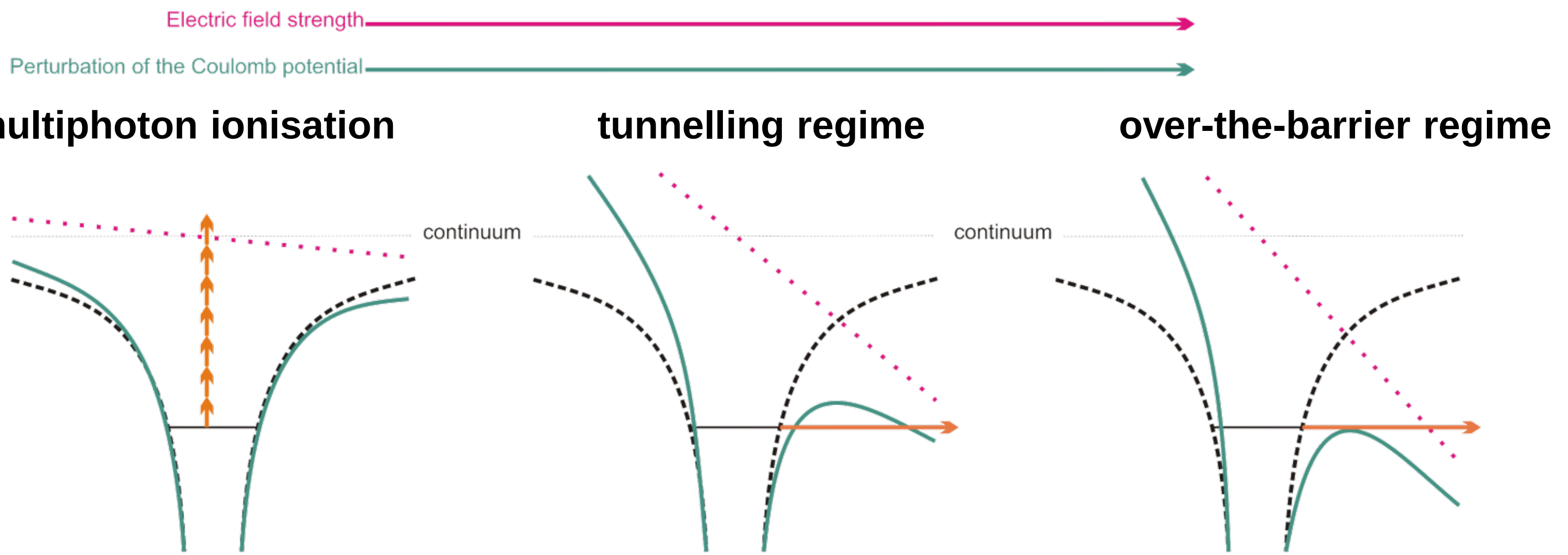

L. V. Keldysh, Sov. Phys. JETP 20 (1965) 1307.
W. Kautek and M. Forster, Springer Series in Materials Science 135 (2010) 89-214.
W. Kautek and O. Armbruster, Springer Series in Materials Science 191 (2014) 43-66.

Exciting carriers in semiconductors / dielectrics

Keldysh parameter $$\gamma = \frac{\omega}{e}\sqrt{\frac{m_e c n \varepsilon_0 E_g}{I}} >> 1$$

ω: laser frequency
I: intensity
m_e: electron effective mass
e: electron charge
c: speed of light
n: refractive index
ε_0: permittivity of free space
E_g: is the bandgap

Exciting carriers in semiconductors / dielectrics

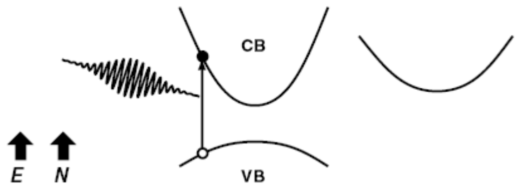

(a) *single photon absorption — direct*

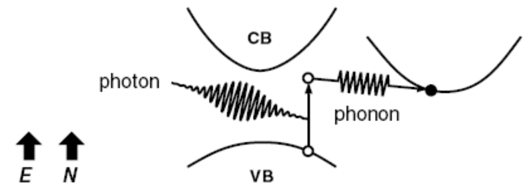

(b) *single photon absorption — indirect*

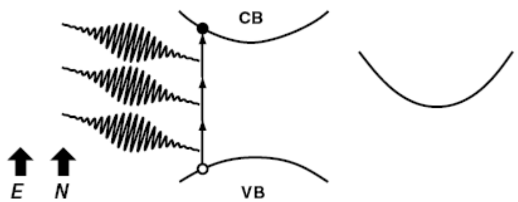

(c) *multi-photon absorption*

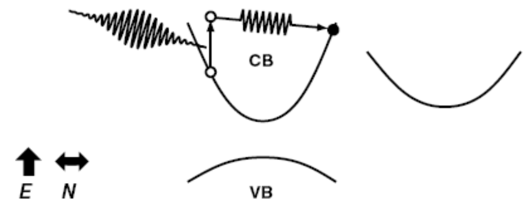

(d) *free-carrier absorption*

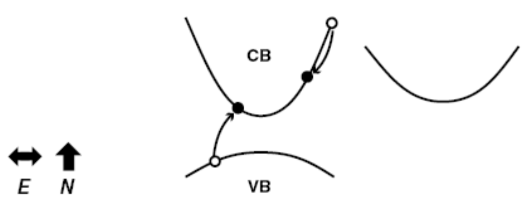

(e) *impact ionisation*

Accord. to E. Mazur

Mechanisms for exciting carriers in a semiconductor / dielectric

Carrier Redistribution, Thermalisation and Cooling

carrier distribution following laser excitation but before scattering

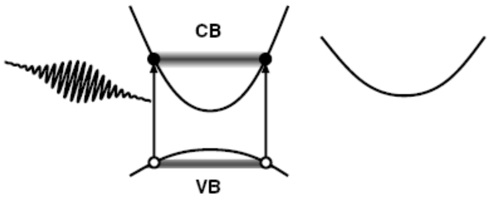

(a) *before scattering*

thermalised carrier distribution created by **carrier-carrier scattering**

$$\mathbf{k}_1 + \mathbf{k}_2 = \mathbf{k}'_1 + \mathbf{k}'_2$$

$$E(\mathbf{k}_1) + E(\mathbf{k}_2) = E(\mathbf{k}'_1) + E(\mathbf{k}'_2)$$

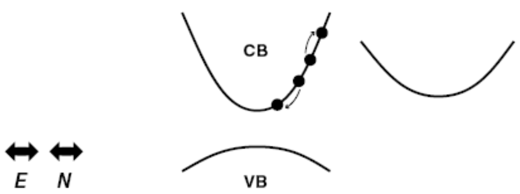

(a) *carrier-carrier scattering*

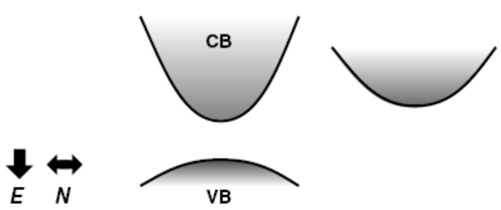

(b) *after scattering*

Accord. to E. Mazur

Overview of Laser Matter Interaction

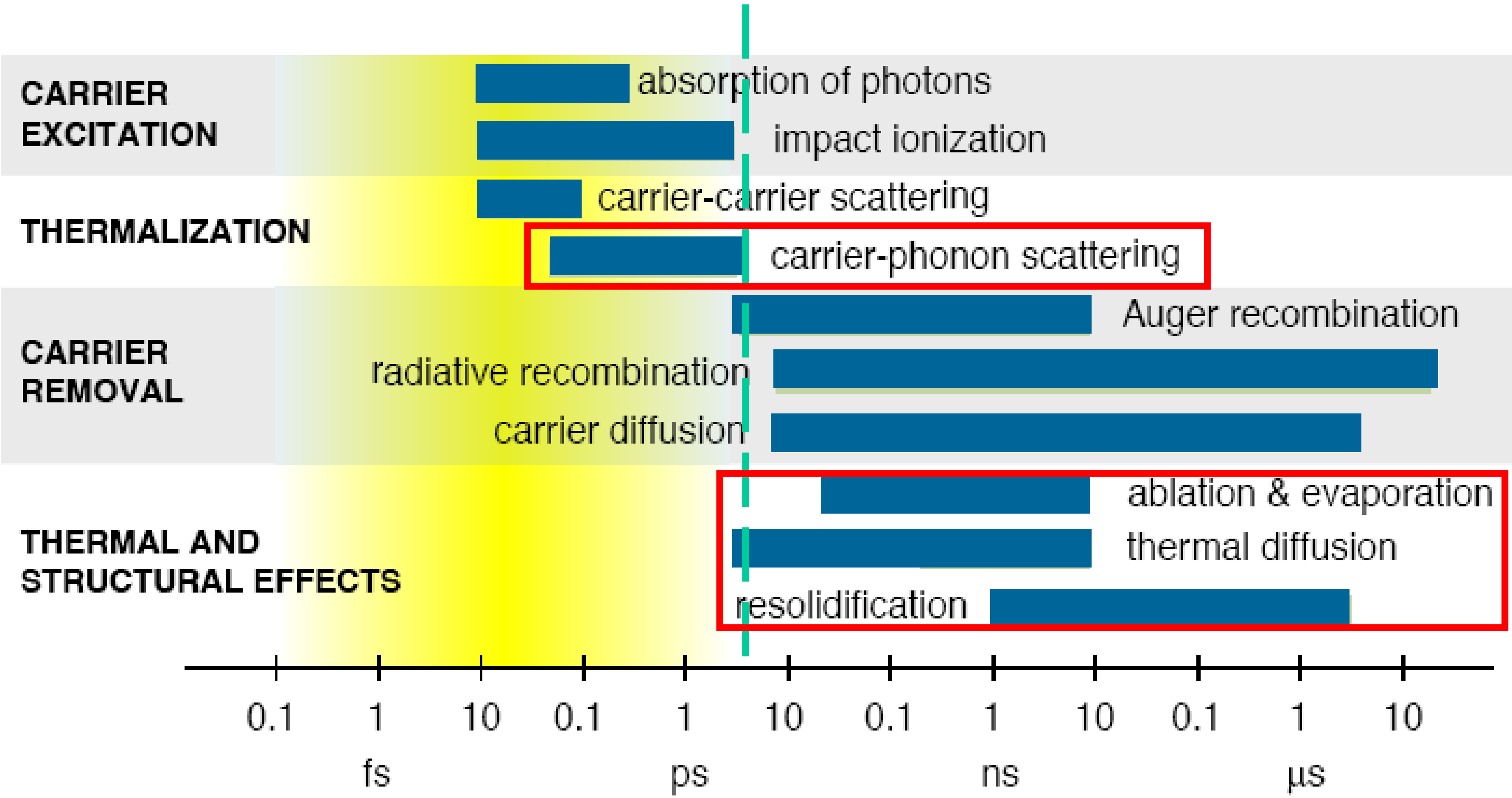

Accord. To E. Mazur

Wolfgang Kautek

Outline

- Excitation mechanisms of solids
- Metals: Two-temperature model
  - Fundamentals: Influence of density of states
  - Thin films
  - Metal ablation
  - Hot electron electrochemistry
- Dielectrics: Multiphoton and Avalanche Ionization
  - Dielectric ablation
  - Coulomb explosion
  - Non-thermal melting, X-ray
- Role of Defects
- Applications

2 Temperature Model (TTM)

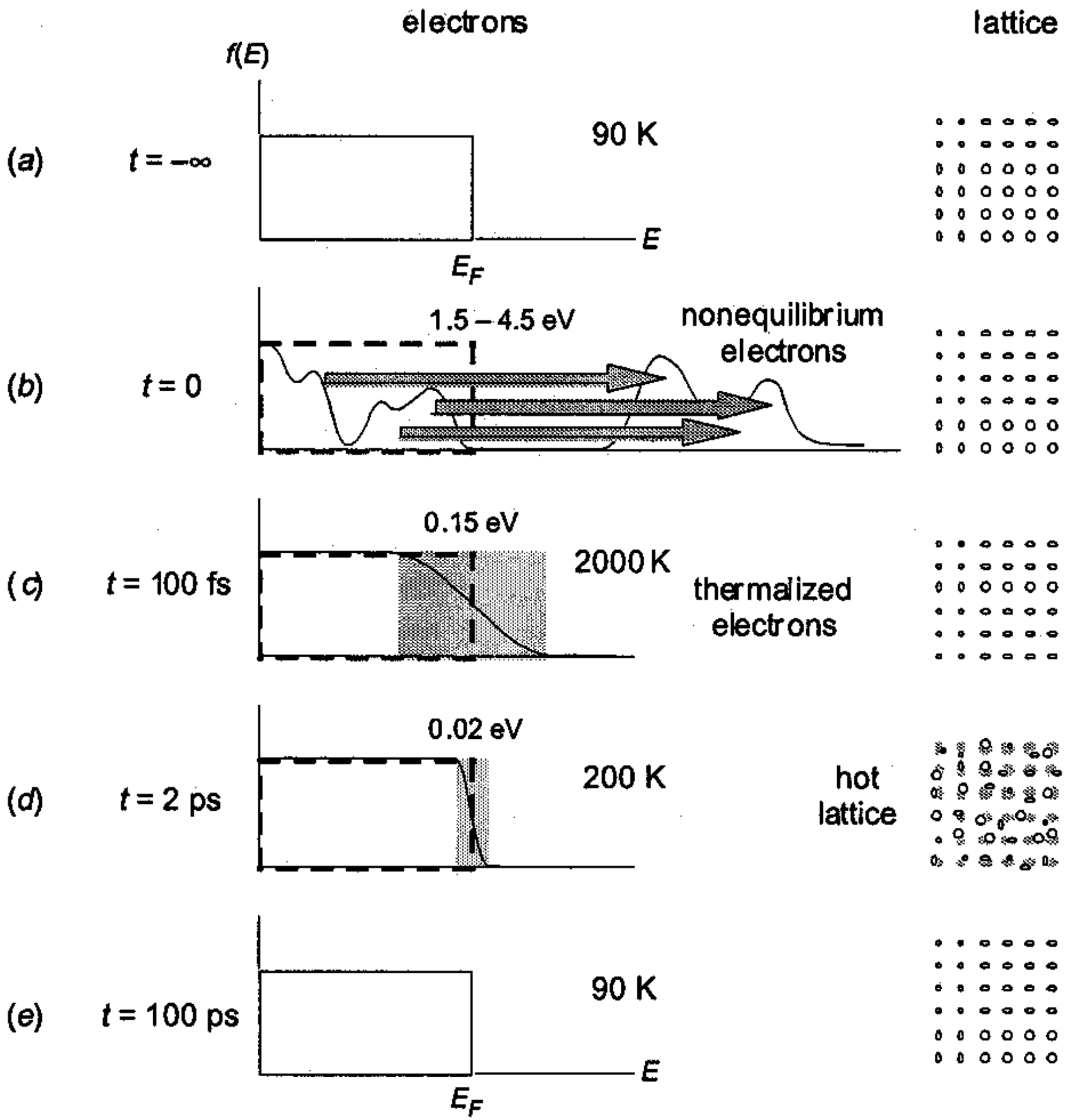

2 Temperature Model (TTM)

electrons — lattice

$$C_e(T_e)\frac{\partial T_e}{\partial t} = \nabla[K_e(T_e,T_l)\nabla T_e] - G(T_e)(T_e - T_l) + S(\vec{r},t)$$

$$C_l(T_l)\frac{\partial T_l}{\partial t} = \nabla[K_l(T_l)\nabla T_l] + G(T_e)(T_e - T_l),$$

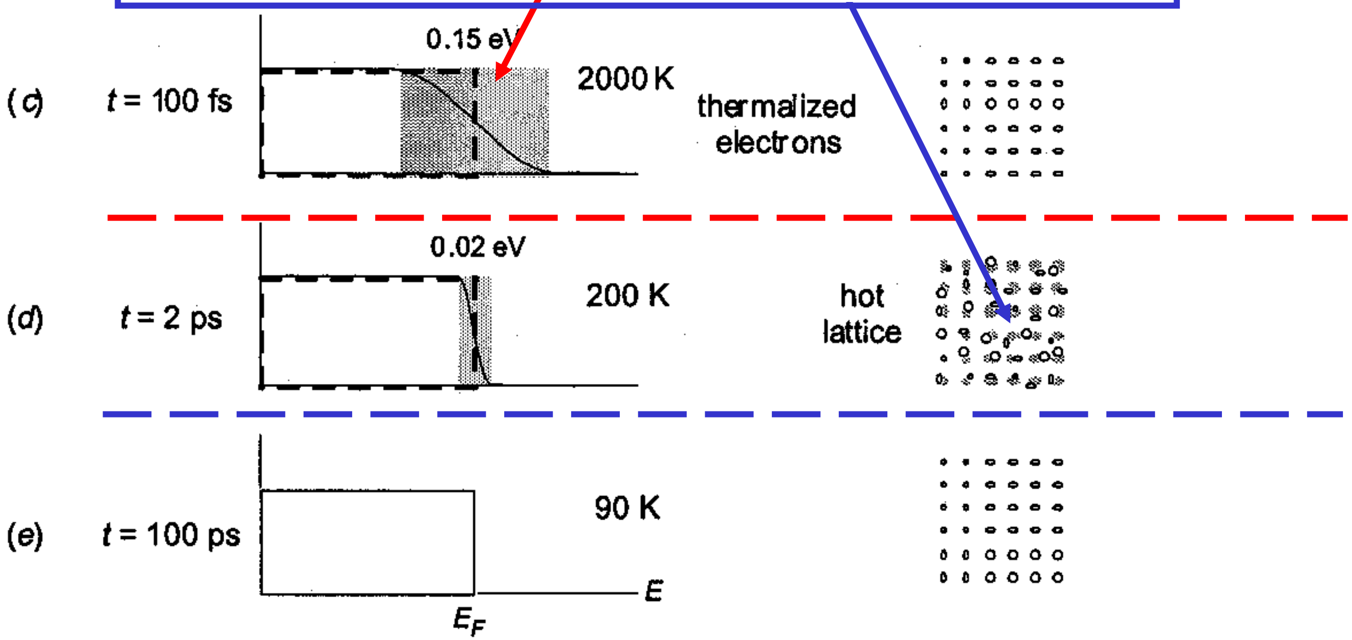

Relaxation phases following optical excitation of metals

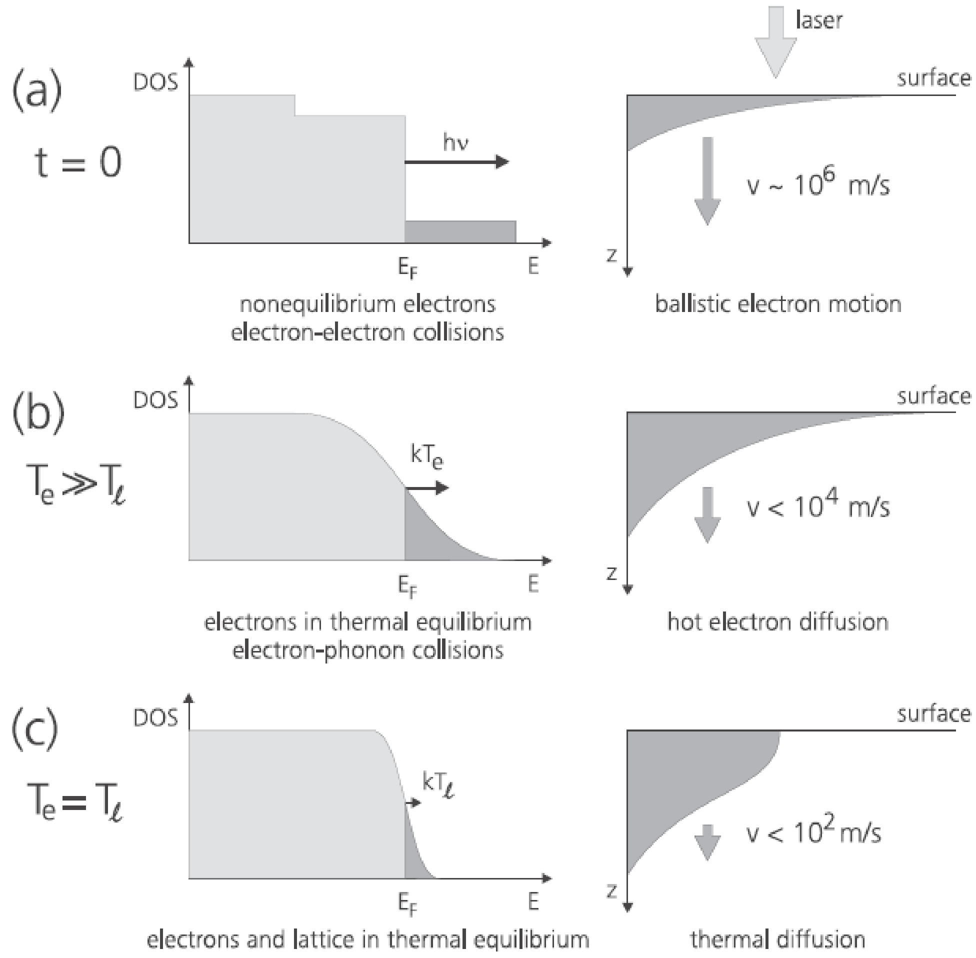

$$l_T \approx \sqrt{D\tau_l}$$

S.-S.Wellershoff, J. Hohlfeld, J. Güdde, E. Matthias, Appl. Phys. A 69, S99–S107 (1999)

2 Temperature Model (TTM)

electrons lattice

$$C_e(T_e)\frac{\partial T_e}{\partial t} = \nabla[K_e(T_e,T_l)\,\nabla\, T_e] - G(T_e)(T_e - T_l) + S(\vec{r},t)$$

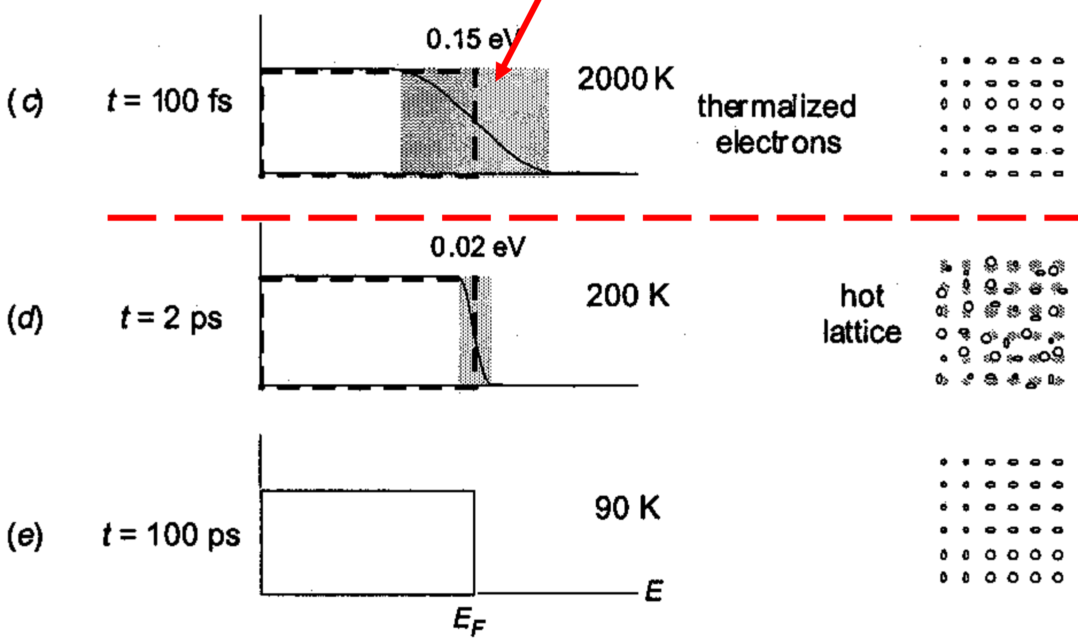

2 Temperature Model:
Hot electron balance

$$C_e(T_e)\frac{\partial T_e}{\partial t} = \nabla[K_e(T_e,T_l)\,\nabla\,T_e] - G(T_e)(T_e - T_l) + S(\vec{r},t)$$

C:	heat capacities
K:	thermal conductivities
$G(T_e)$:	electron-phonon coupling factor
$S(r,t)$:	source term of local energy deposition by the laser pulse

Does this hold also for ultrashort timescales?

Z. Lin, L.V. Zhigilei, V. Celli, PHYSICAL REVIEW B 77, 075133 (2008)

2 Temperature Model : Hot electron balance

Electron heat capacity

High T_e:

$$C_e(T_e) = \int_{-\infty}^{\infty} \frac{\partial f(\varepsilon, \mu, T_e)}{\partial T_e} g(\varepsilon)\varepsilon d\varepsilon$$

$g(\varepsilon)$: electron DOS at the energy level ε

μ: chemical potential at T_e

$f(\varepsilon,\mu,T_e)$: Fermi distribution function $f(\varepsilon,\mu,T_e)=\{\exp[(\varepsilon-\mu)/k_BT_e]+1\}^{-1}$

Low T_e:

$$C_e(T_e) = \gamma T_e$$

γ: electron heat capacity constant $\gamma = \pi^2 k_B^2 g(\varepsilon_F)/3$

$\gamma = \pi^2 n_e k_B^2 / 2\varepsilon_F$

$g(\varepsilon_F)$: electron DOS at the Fermi level

Z. Lin, L.V. Zhigilei, V. Celli, PHYSICAL REVIEW B 77, 075133 (2008)

2 Temperature Model: Hot electron balance

$$C_e(T_e)\frac{\partial T_e}{\partial t} = \nabla[K_e(T_e,T_l)\,\nabla\,T_e] - G(T_e)(T_e - T_l) + S(\vec{r},t)$$

C:	heat capacities
K:	thermal conductivities
G(T_e):	electron-phonon coupling factor
S(r,t):	source term of local energy deposition by the laser pulse

Does this hold also for ultrashort timescales?

Z. Lin, L.V. Zhigilei, V. Celli, PHYSICAL REVIEW B 77, 075133 (2008)

2 Temperature Model : Hot electron balance

Electron-phonon coupling factor

$$\left.\frac{\partial E_e}{\partial t}\right|_{ep} = G(T_l - T_e), \quad G = \frac{\pi^2}{6}\frac{m_e C_s^2 n_e}{\tau(T_e) T_e}$$

m_e: effective electron mass

C_s: speed of sound

n_e: number density of the electrons

$\tau(T_e)$: electron relaxation time defined as the electron-phonon scattering time, $\tau_{e\text{-}ph}$

Z. Lin, L.V. Zhigilei, V. Celli, PHYSICAL REVIEW B 77, 075133 (2008)

Aluminium

**Electron DOS &
Fermi distribution function**

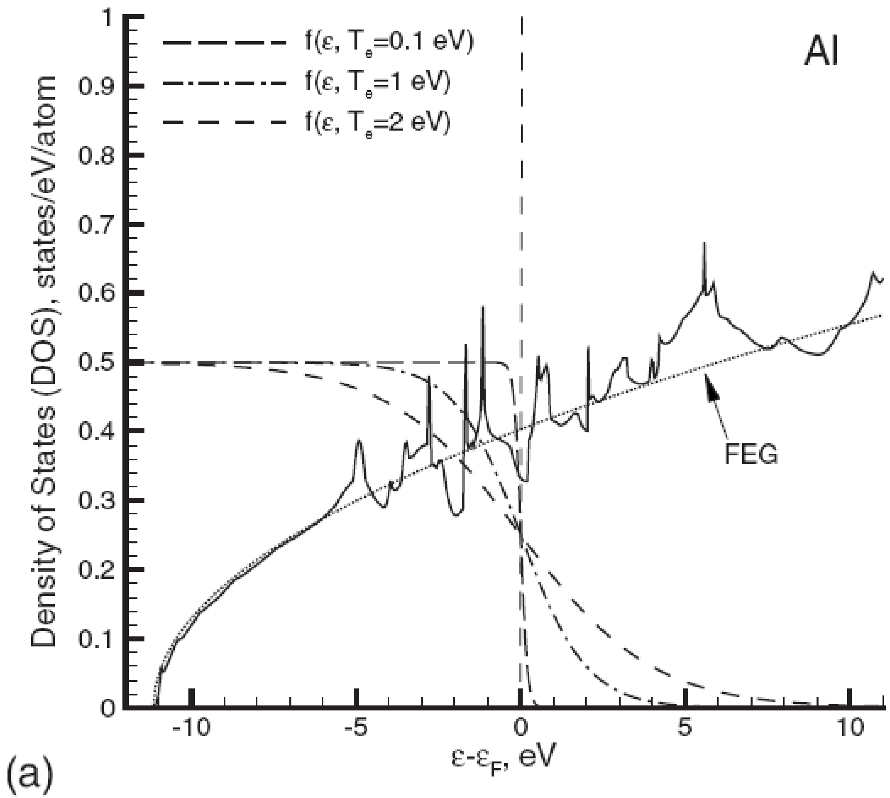

Electron-phonon coupling factor

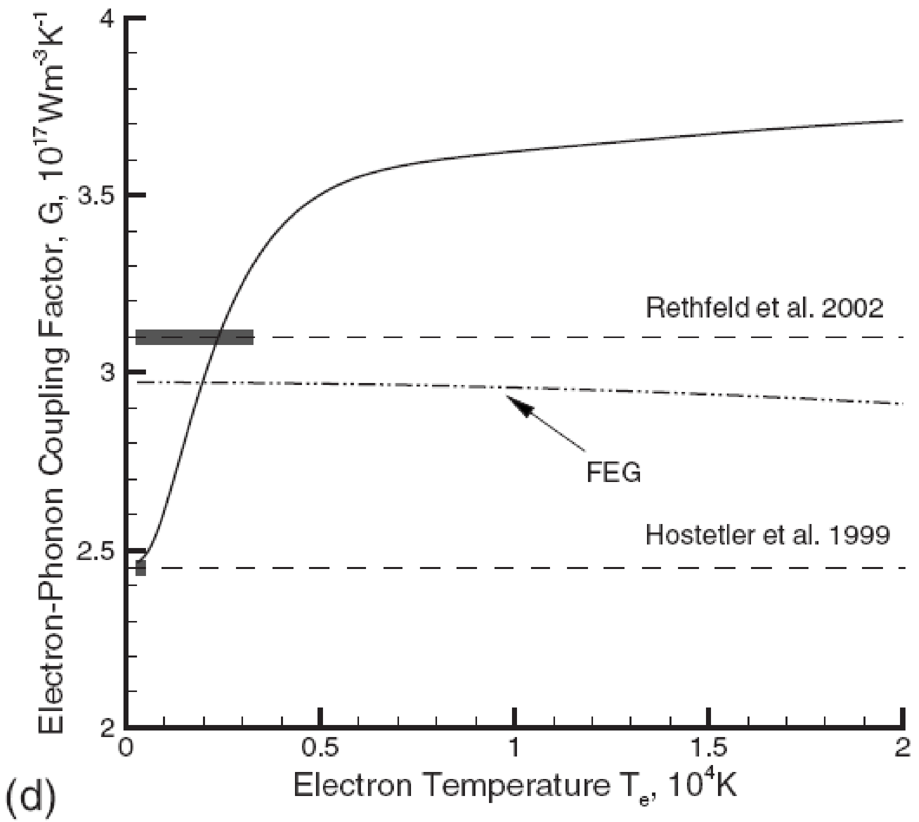

Z. Lin, L.V. Zhigilei, V. Celli, PHYSICAL REVIEW B 77, 075133 (2008)

Aluminium

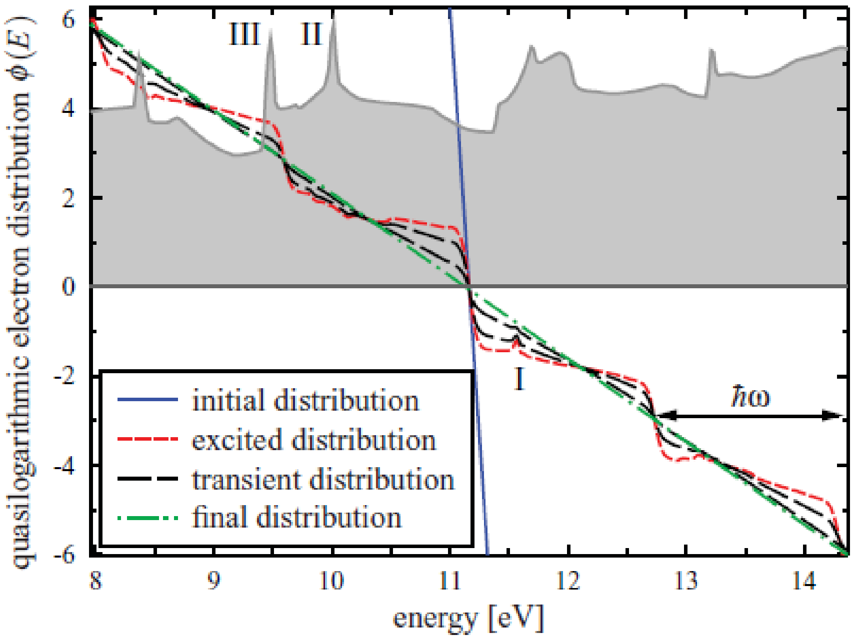

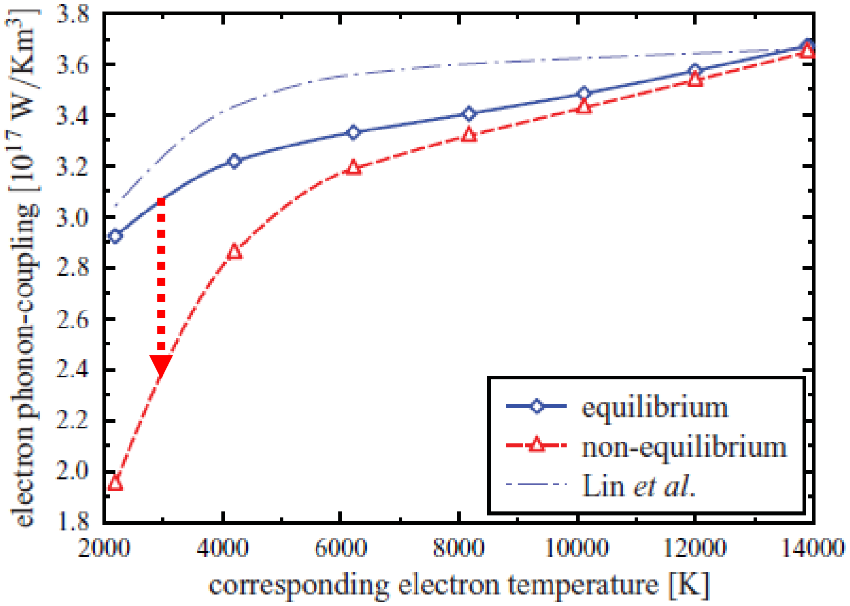

- Density of states reflected in non-equilibrium distribution
- Electron-phonon coupling depends on T_e
- Non-equilibrium **decreases** coupling

B.Y. Mueller and B. Rethfeld, PRB 87, 035139 (2013); Lin et al., PRB 77 075133 (2008); Rethfeld et al., PRB 65 214303 (2002)

Gold

Electron DOS & Fermi distribution function

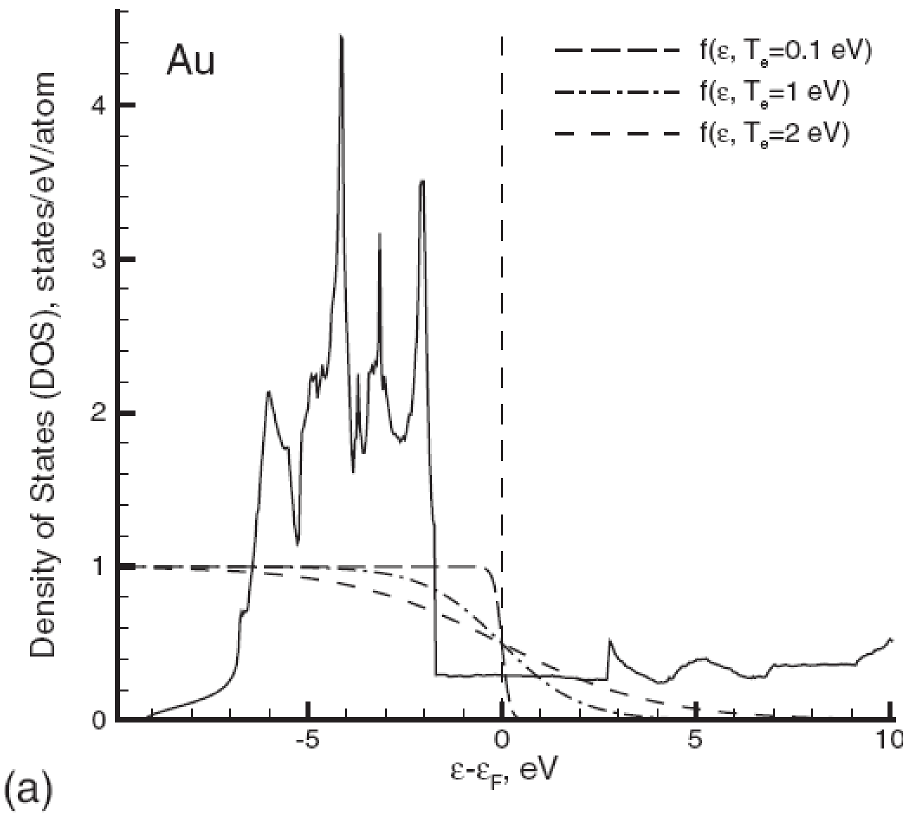

Electron-phonon coupling factor

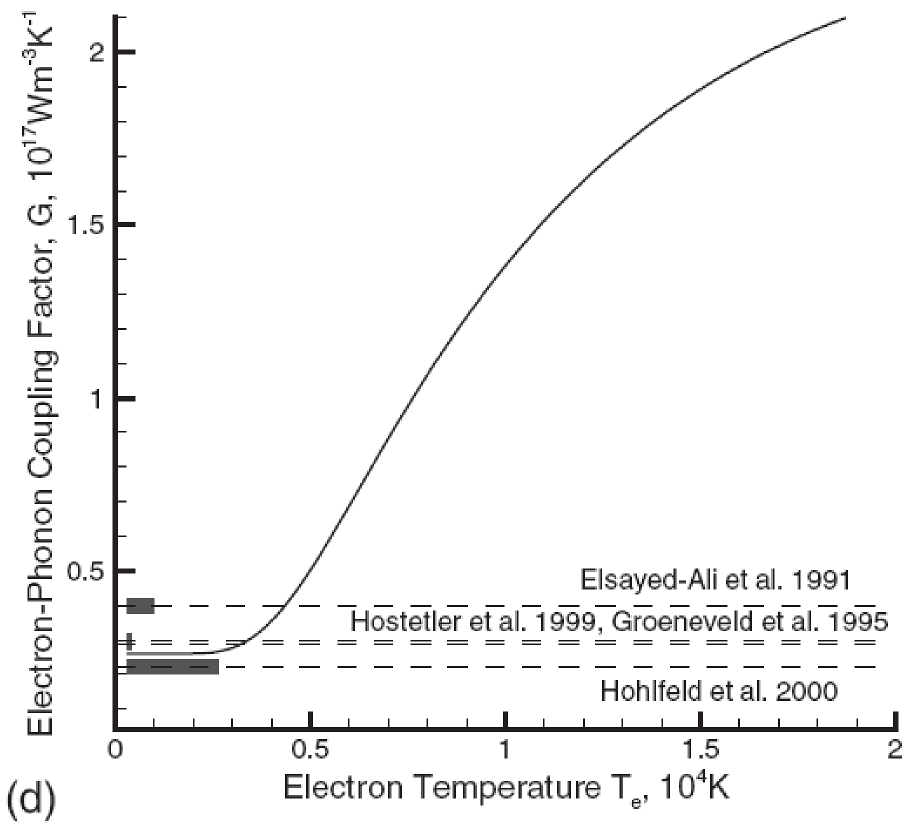

Z. Lin, L.V. Zhigilei, V. Celli, PHYSICAL REVIEW B 77, 075133 (2008)

Gold

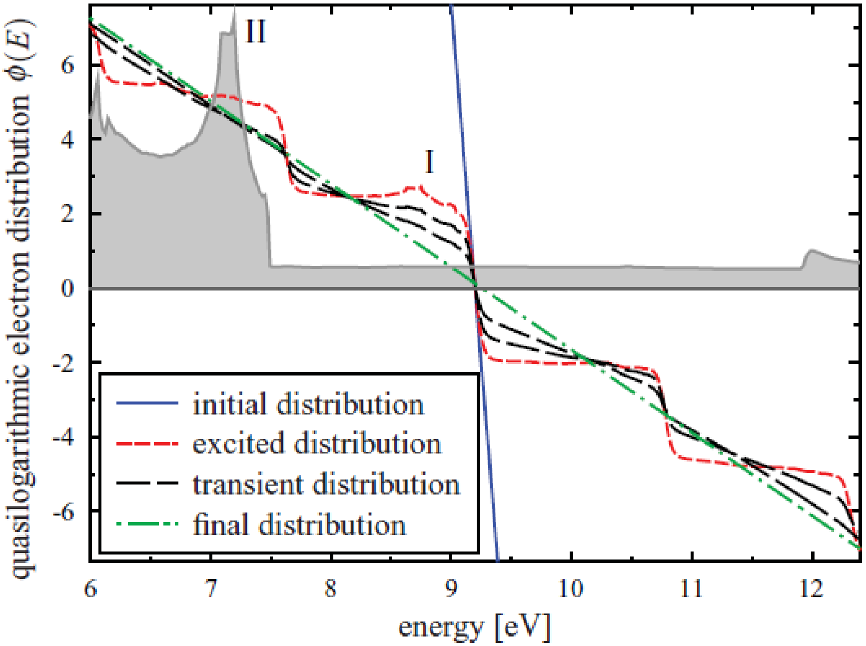

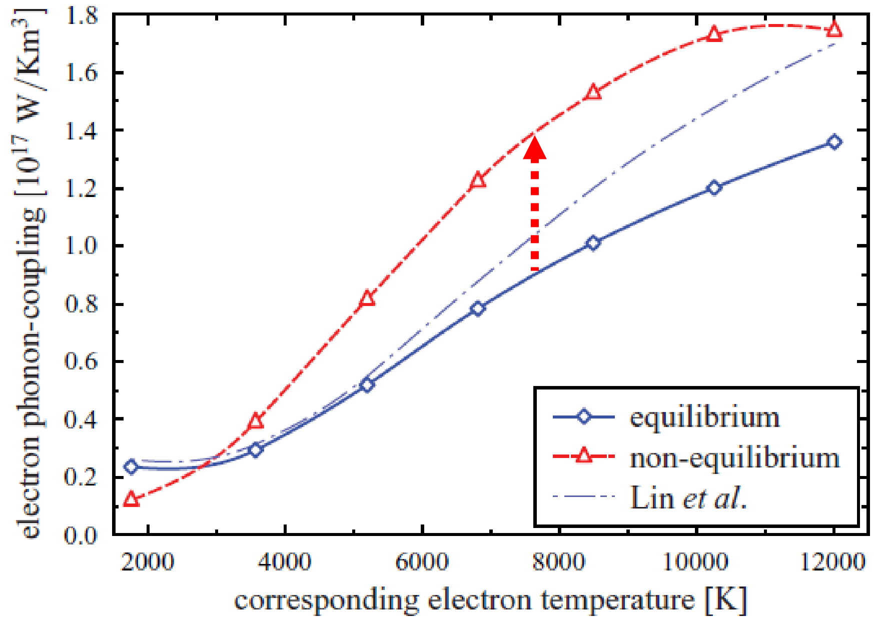

- Density of states reflected in non-equilibrium distribution
- Electron-phonon coupling depends on T_e
- Non-equilibrium **increases** coupling

B.Y. Mueller and B. Rethfeld, PRB 87, 035139 (2013); Lin et al., PRB 77 075133 (2008)

Nickel

Electron DOS & Fermi distribution function

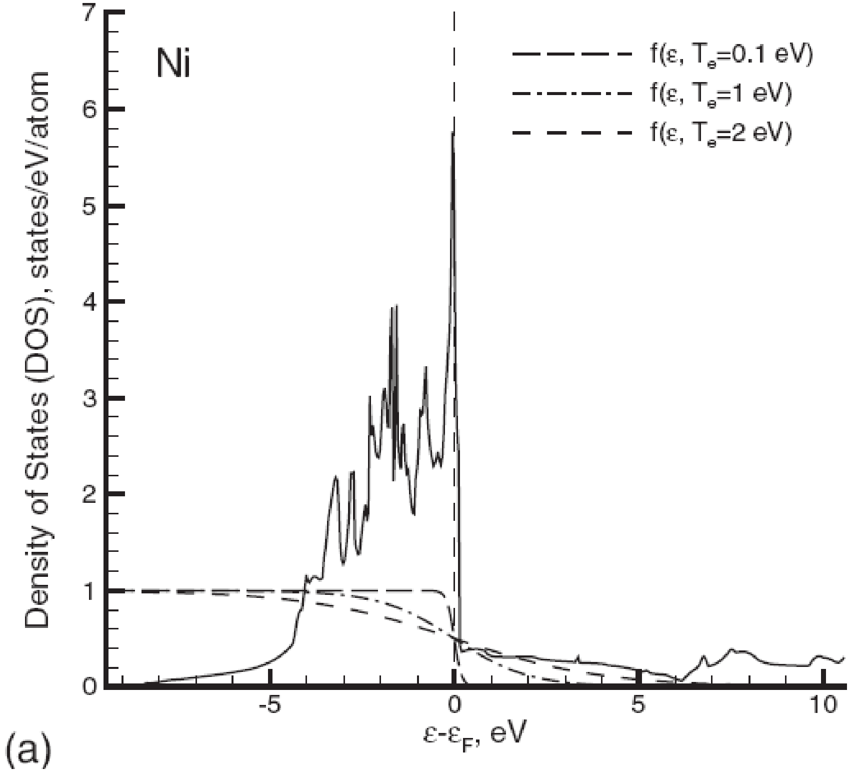

Electron-phonon coupling factor

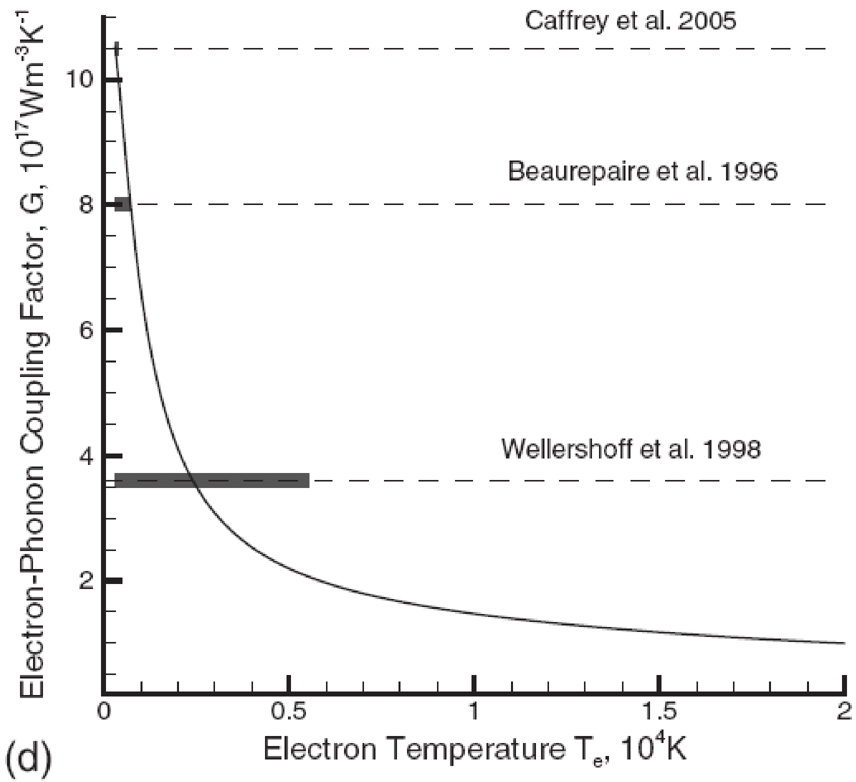

Z. Lin, L.V. Zhigilei, V. Celli, PHYSICAL REVIEW B 77, 075133 (2008)

Titanium

Electron DOS & Fermi distribution function

Electron-phonon coupling factor

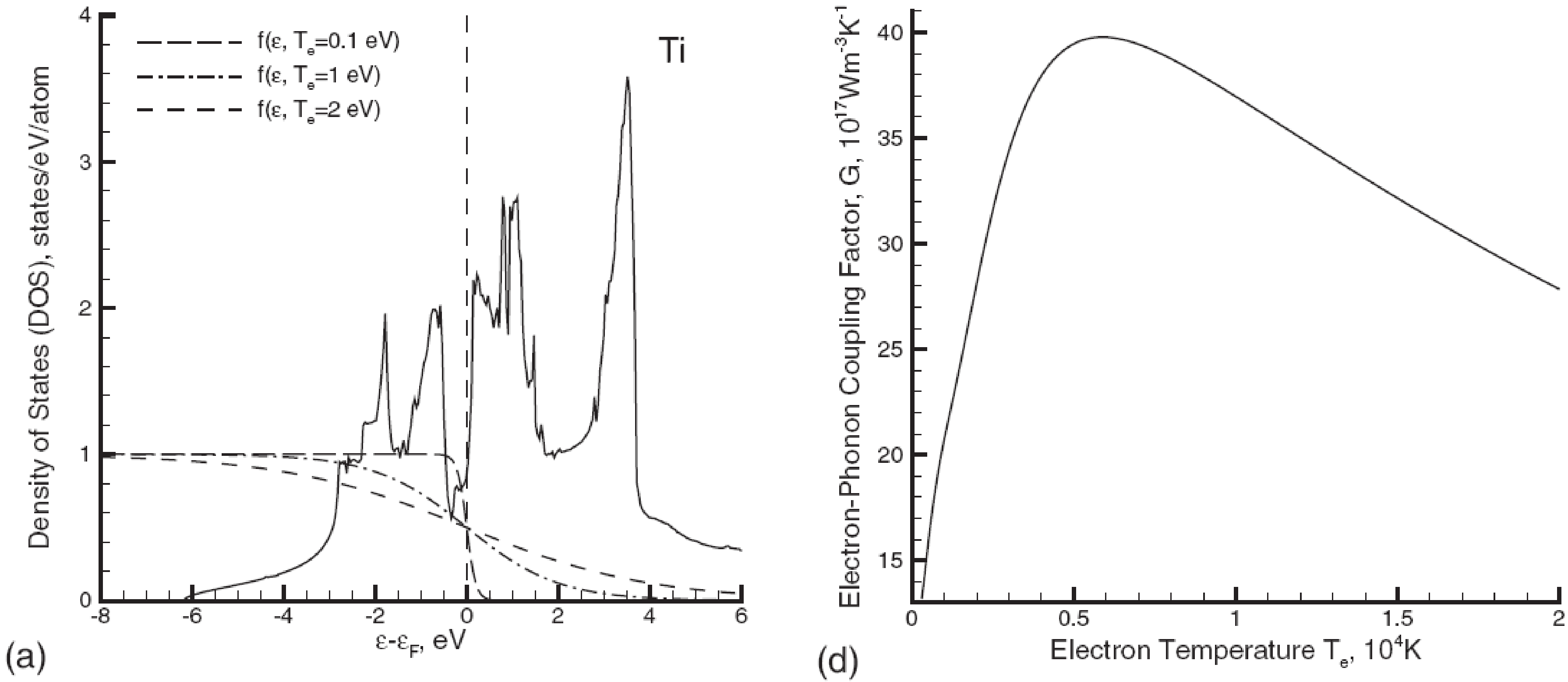

Z. Lin, L.V. Zhigilei, V. Celli, PHYSICAL REVIEW B 77, 075133 (2008)

Conclusions from strong electron-phonon nonequilibrium

- **Al:** Free Electron Gas (FEG) provides a good description of the temperature dependence of the **electron heat capacity**, but **fails** to predict a **40% increase** in the **electron-phonon coupling** with increasing electron temperature.

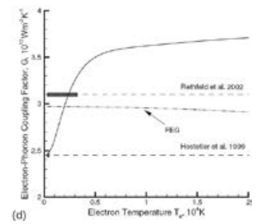

- **Au: electron heat capacity** and **electron-phonon coupling** factor are strongly **enhanced** by the **thermal excitation of *d* band electrons** at electron temperatures exceeding several thousand Kelvins

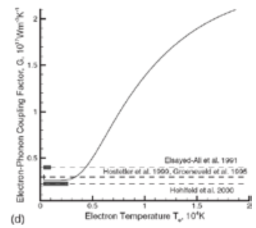

- **Ni: Fermi level at** high density of states at **edge of the *d* band** results in the opposite trend when the thermal excitation of *d* band electrons leads to a **decrease in the electron-phonon coupling** factor and large **negative deviations of the electron heat capacity** from the linear dependence on the electron temperature

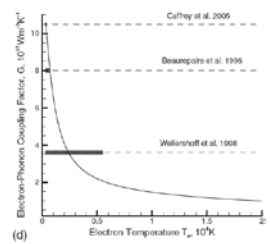

- **Ti: Fermi level in the middle of a partially filled *d* band**, in a local dip in the electron DOS, results in **complex nonmonotonic dependences** of the thermophysical properties on the electron temperature.

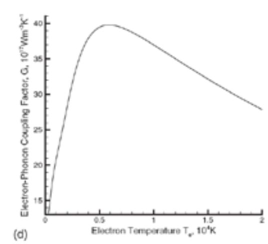

Z. Lin, L.V. Zhigilei, V. Celli, PHYSICAL REVIEW B 77, 075133 (2008)

Hot electron electrochemistry induced by fs laser pulses

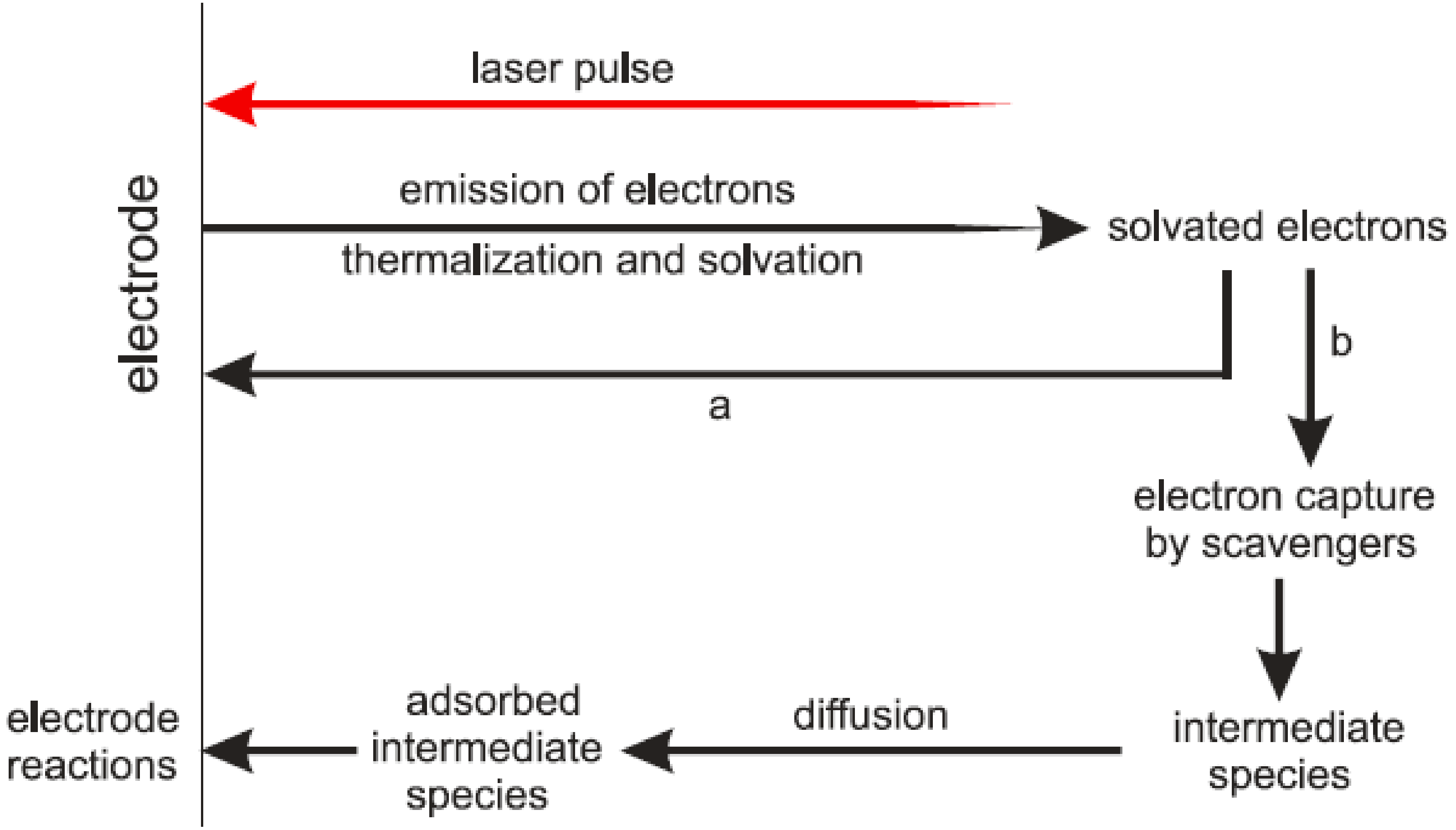

O. Armbruster, H. Pöhl, W. Kautek, in publication

Emission and Detection of Hot Electrons: Charging of Electrochemical Double Layer

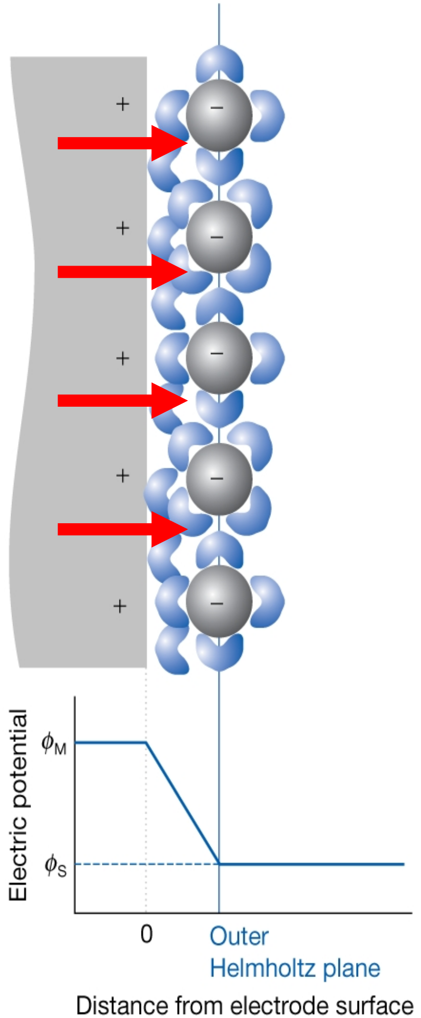

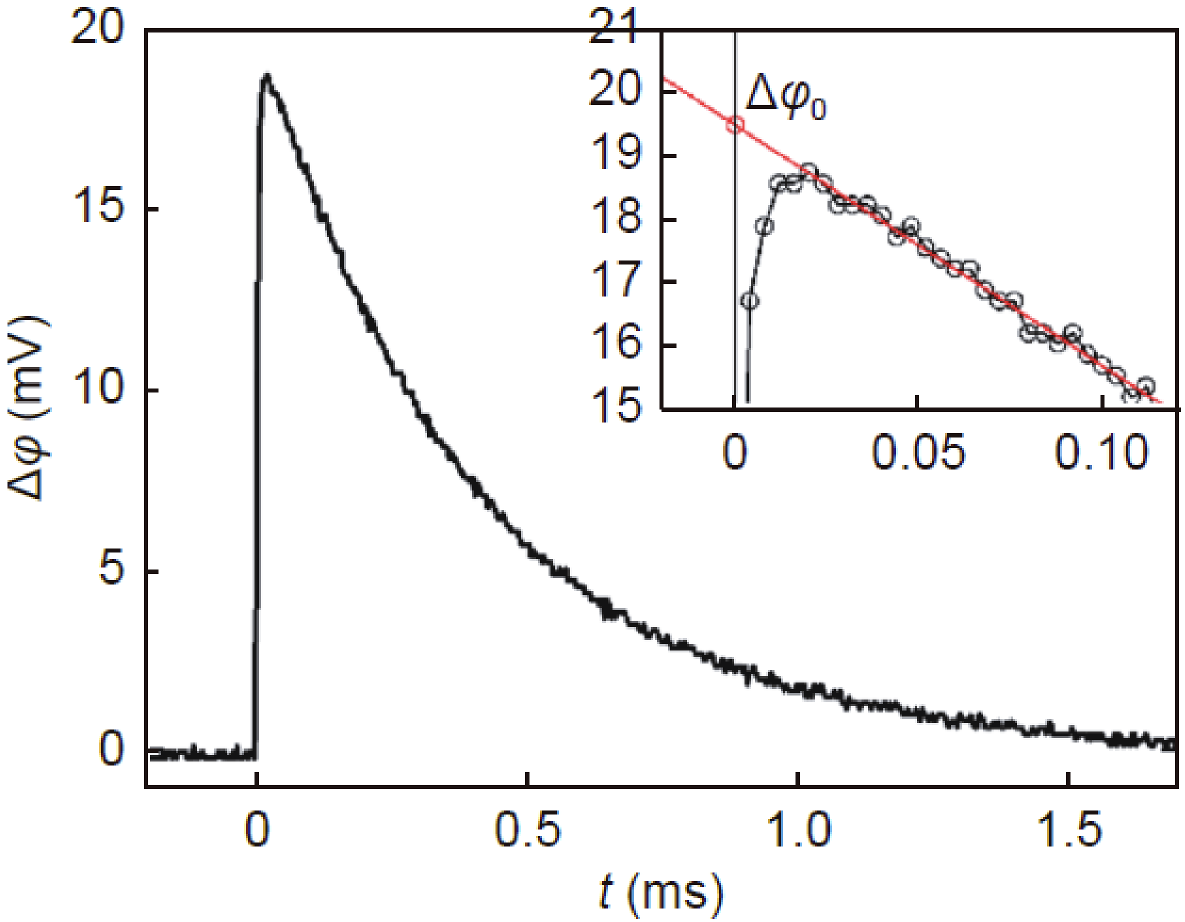

O. Armbruster, H. Pöhl, W. Kautek, Opto-Electron. Adv. 6 (2023) 220170

Hot electron electrochemistry induced by fs laser pulses

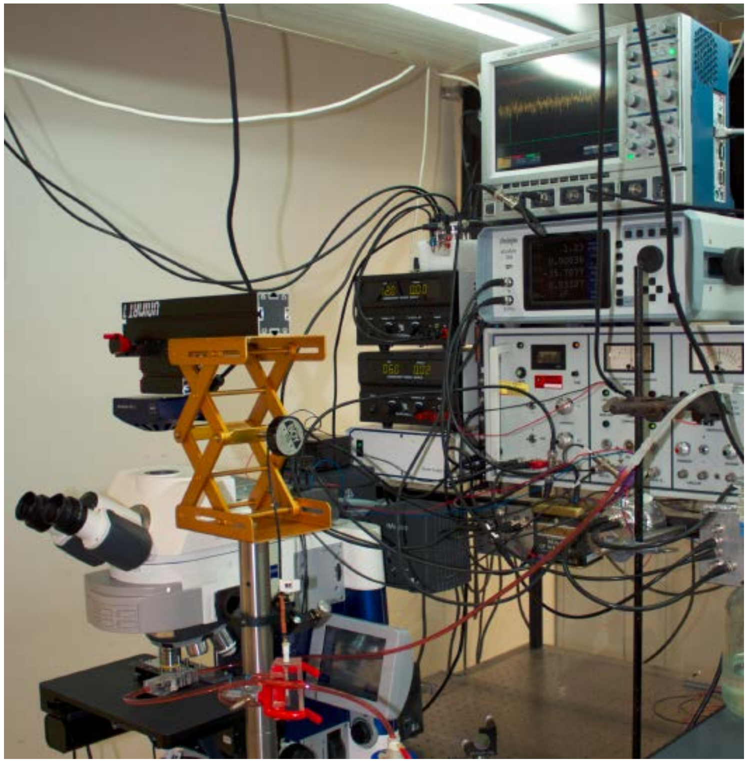

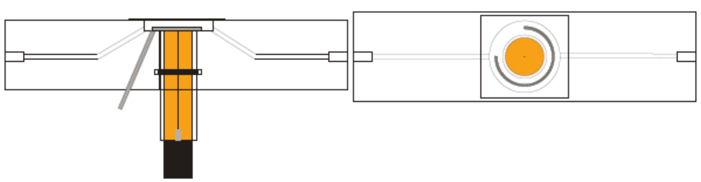

ΔU-transients

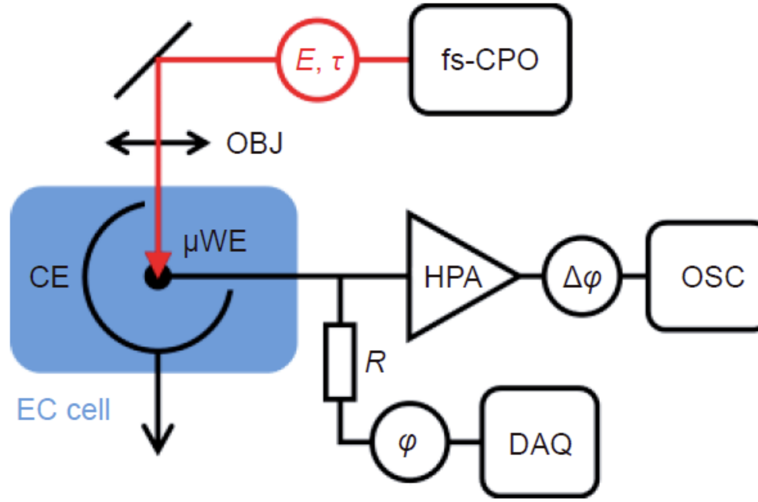

Impedance spectroscopy

O. Armbruster, H. Pöhl, W. Kautek, Opto-Electron. Adv. 6 (2023) 220170

electronic emission from metal into solution

Emitted charge density *q* vs. laser peak intensity *I* and electrode potential U_{DC}

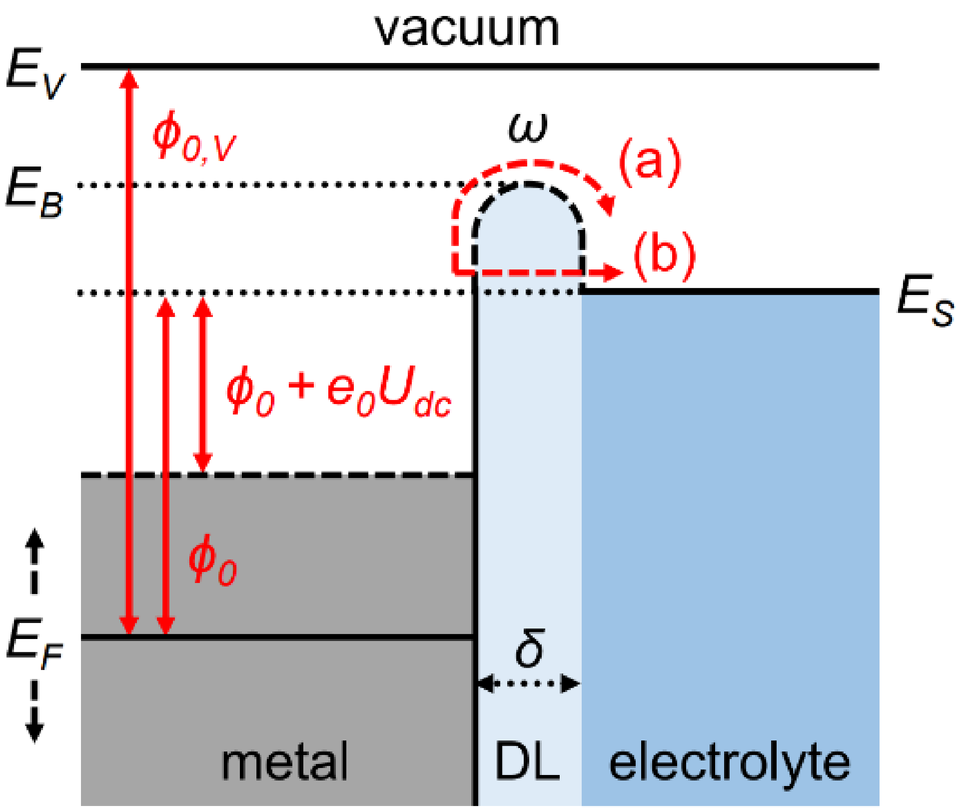

E_V: vacuum energy level

E_F: Fermi level of the metal

E_S: electronic level in solution

$\varphi_{0,V}$: work function from metal into vacuum

φ_0: unbiased work function from metal into solution

U_{dc}: applied electrochemical potential

e_0: elementary charge

A. Naghilou, O. Armbruster, and W. Kautek,
in "Handbook of Laser Micro- and Nano-Engineering", Ed. K. Sugioka, Springer International Publishing, Cham 2021, p. 61-82

Electronic Fermi-Dirac Distribution on the Metal and Density of States (DOS) of H_3O^+ and H_{ad}

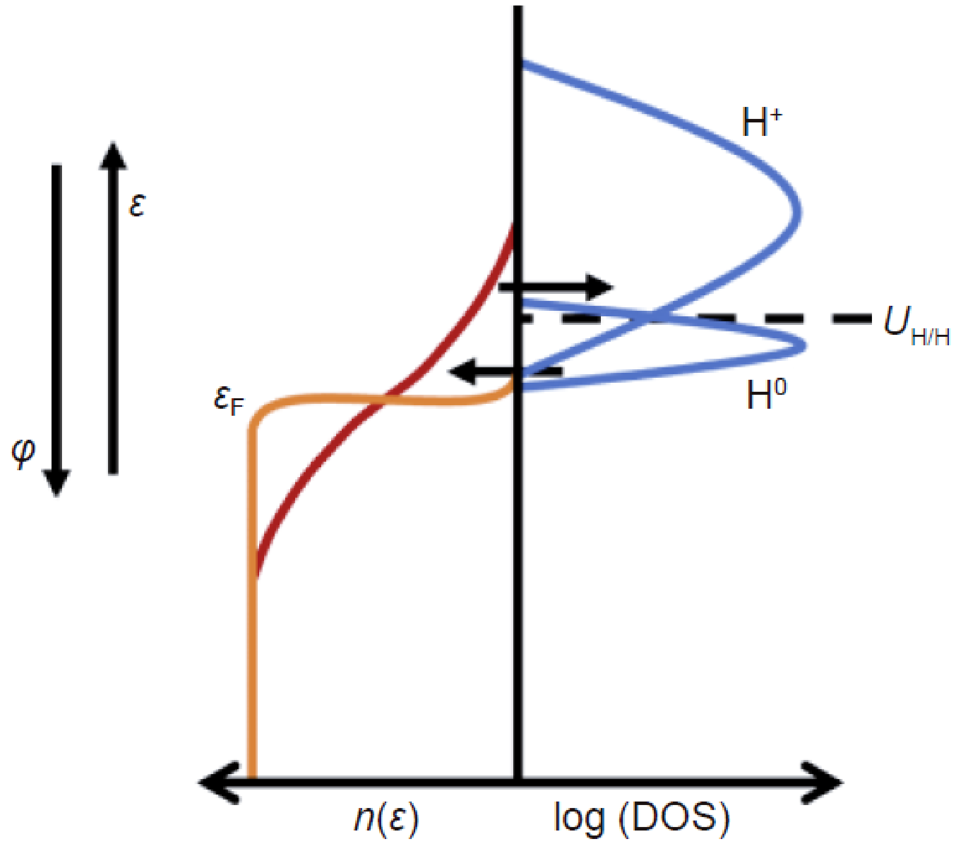

$2\ H_3O^+ + e^- \leftrightarrow H_{ad} + H_2O$

Tafel reaction

$2\ H_{ad} \leftrightarrow H_2$,

Heyrovsky reaction

$H_3O^+ + e^- + H_{ad} \leftrightarrow H_2 + H_2O$

O. Armbruster, H. Pöhl, W. Kautek, Opto-Electron. Adv. 6 (2023) 220170

Hot electron electrochemistry (H^+ reduction)

Emitted charge *Q* vs. laser peak intensity *I* and electrode potential U_{DC}

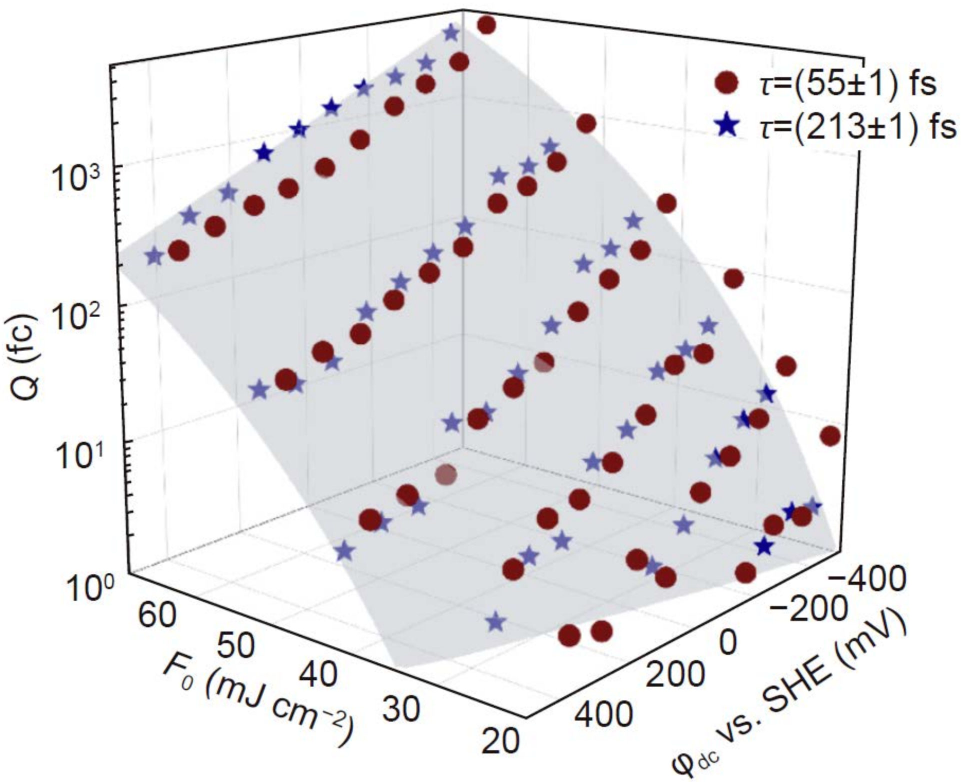

- Tafel relationsship
- Strong dependence on fluence (hot e^- density)
- Independent of τ_l ($< \tau_{e\text{-}h}$)

O. Armbruster, H. Pöhl, W. Kautek, Opto-Electron. Adv. 6 (2023) 220170

Pulse Laser Electrochemistry: Cold and Hot Electrons

ns-Lasers: Temperature jump

- Disordering the structure of adsorbed water dipoles (Entropy)
- Potential change (Nernst)
- Depassivation
- Desorption (Contaminants, inhibitors, etc.)

fs-Lasers: hot electron pulses

- ps current pulses, $j \sim 10^6$ A cm^{-2}
- Trigger intermediate electrochemistry
- Electrochemistry of dry electrons

A.G. Krivenko, V.A. Benderskii, J. Krüger, W. Kautek, Russian J. Electrochem. 33 (1998) 1068

Thin Films

Time dependence of electron and lattice temperatures

Bulk

Thin film

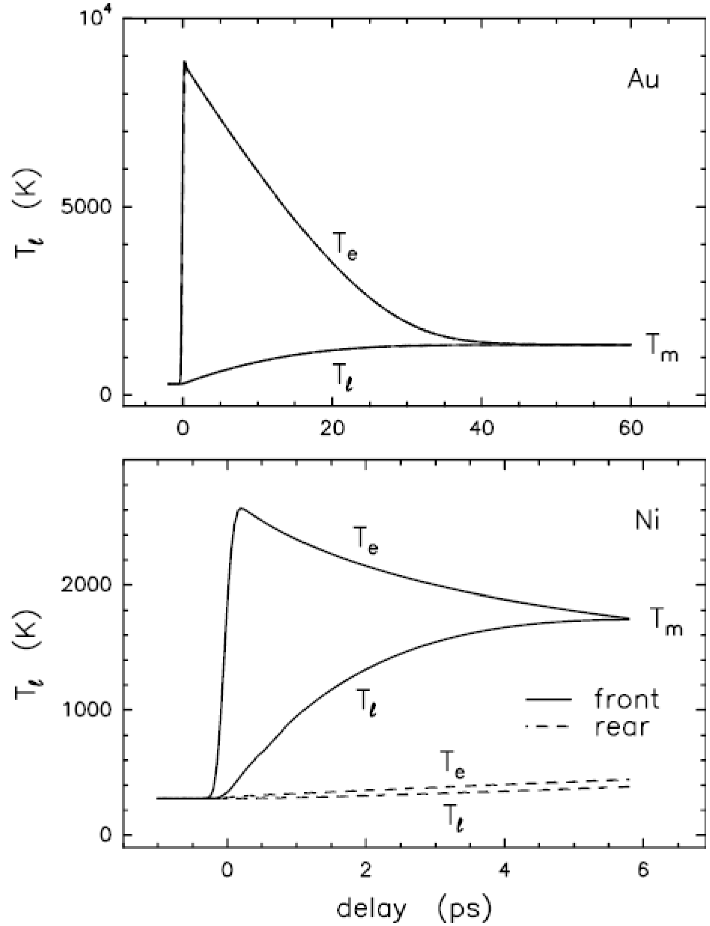

100-nm films
single 200-fs
400-nm laser pulse
23 mJ=cm²

S.-S.Wellershoff, J. Hohlfeld, J. Güdde, E. Matthias, Appl. Phys. A 69, S99–S107 (1999)

Thickness dependence of damage thresholds

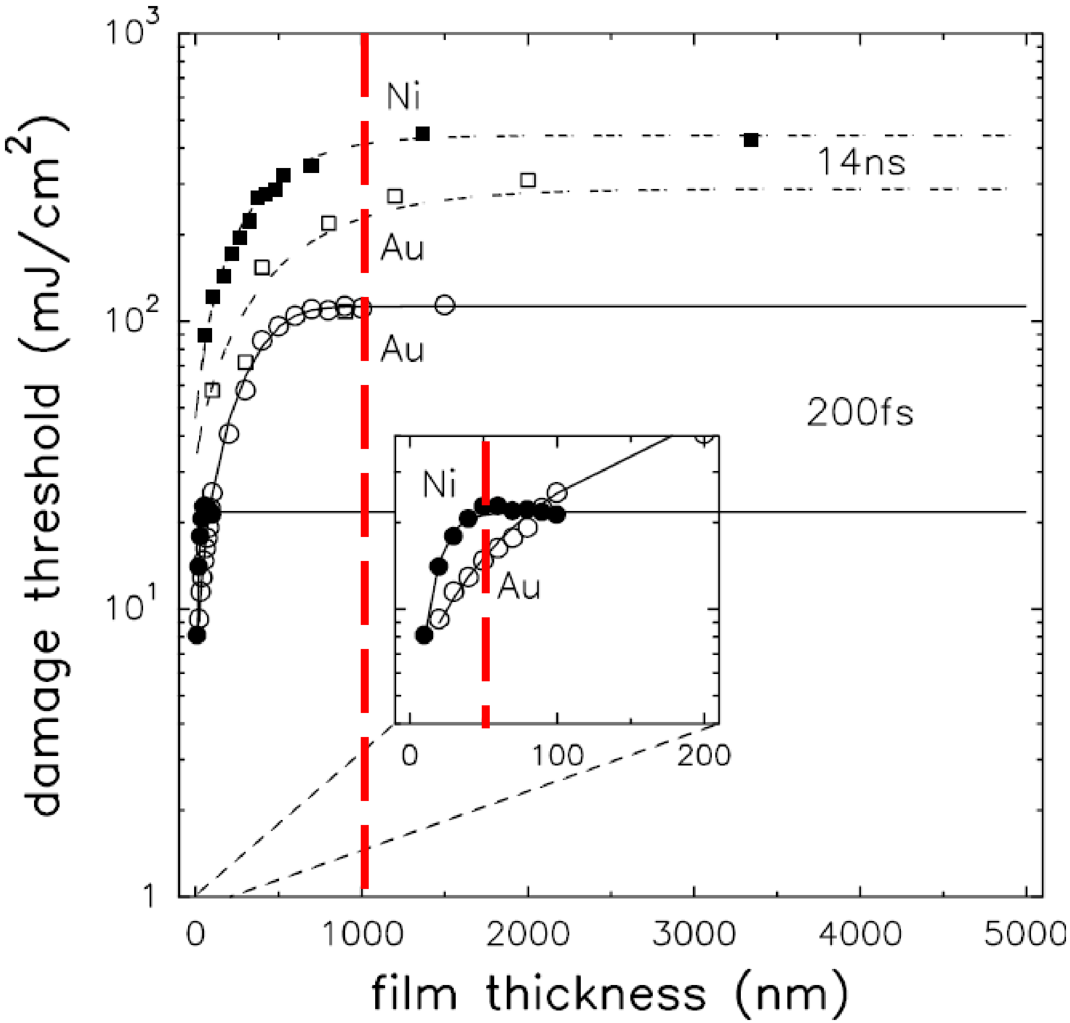

$$l_T \approx \sqrt{D\tau_l}$$

S.-S.Wellershoff, J. Hohlfeld, J. Güdde, E. Matthias, Appl. Phys. A 69, S99–S107 (1999)

DLC and C_xN_y thickness dependence of damage thresholds

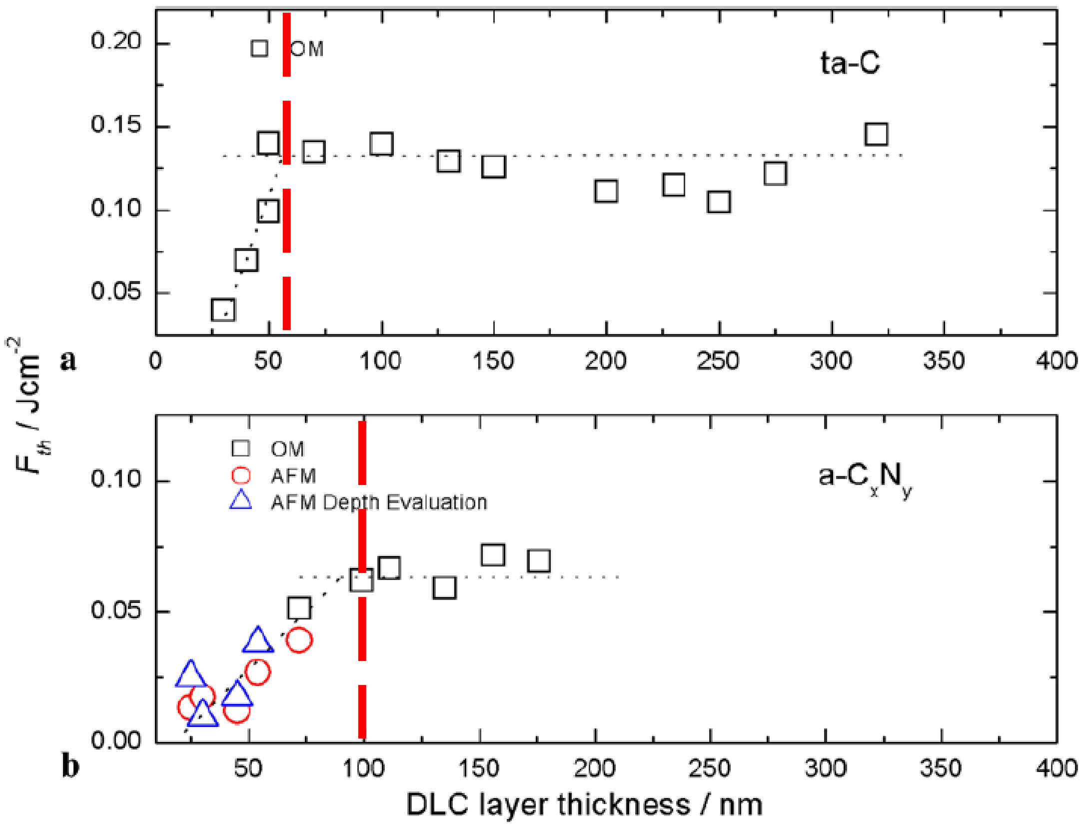

- α_{eff} in a-C_xN_y ~ 110 nm in accordance with **two-photon absorption**
- **Ballistic hot electrons** and
- **heat diffusion length** are negligible.

$$l_{tot} = \alpha_{eff}^{-1}$$

M. Forster, L. Égerházi, C. Haselberger, C. Huber, W. Kautek, Appl. Phys. A (2011) 102: 27–33

Thickness dependence of damage thresholds

$$l_{\text{tot}} = \alpha_{\text{eff}}^{-1} + l_{\text{ball}} + l_T$$

- **Threshold** depends on the **film thickness** whenever this is smaller than the range of **electronic energy transport**.
- **Importance of electron–phonon coupling** is reflected by the great difference in electron diffusion depths of **noble and transition metals**.
- **Noble metals**: **electron diffusion** **is the dominant process. Transient optical properties** and **ballistic energy transport** must be accounted for.
- **Transition metals**: **Ballistic transport negligible**.

S.-S.Wellershoff, J. Hohlfeld, J. Güdde, E. Matthias, Appl. Phys. A 69, S99–S107 (1999)

Outline

- Excitation mechanisms of solids
- Metals: Two-temperature model
  - Fundamentals: Influence of density of states
  - Thin films
  - Metal ablation
  - Hot electron electrochemistry
- Dielectrics: Multiphoton and Avalanche Ionization
  - Dielectric ablation
  - Coulomb explosion
  - Non-thermal melting, X-ray
- Role of Defects
- Applications

Coulomb Explosion

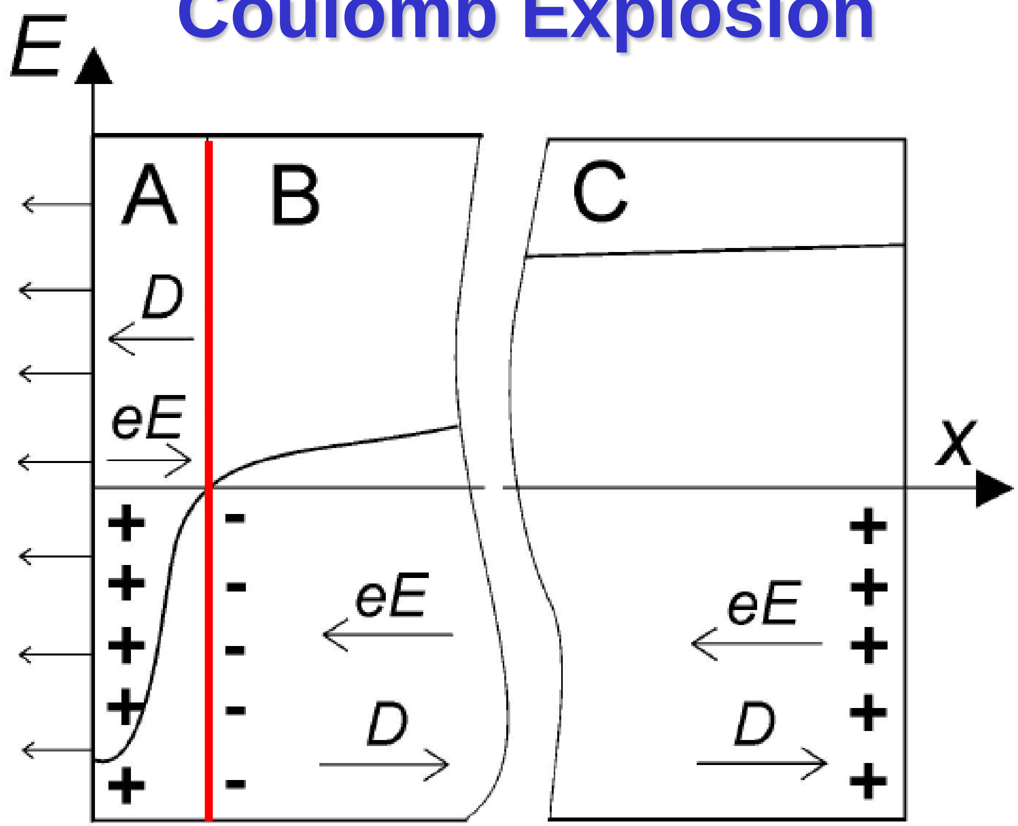

- A: surface region depleted of electrons, electric drag force *eE* dominates electron diffusion *D* toward the depleted region.
- B: electric field is small, a region with negative charging is formed.
- C: reduced positive charge

N.M. Bulgakova, R. Stoian, A. Rosenfeld, I.V. Hertel, W. Marine, E.E.B. Campbell, Appl. Phys. A 81, 345–356 (2005)

Coulomb Explosion

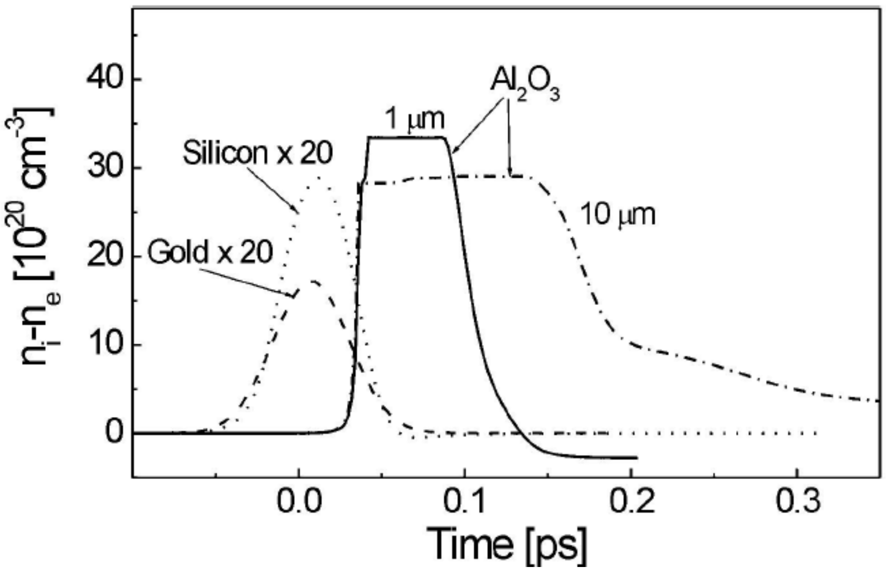

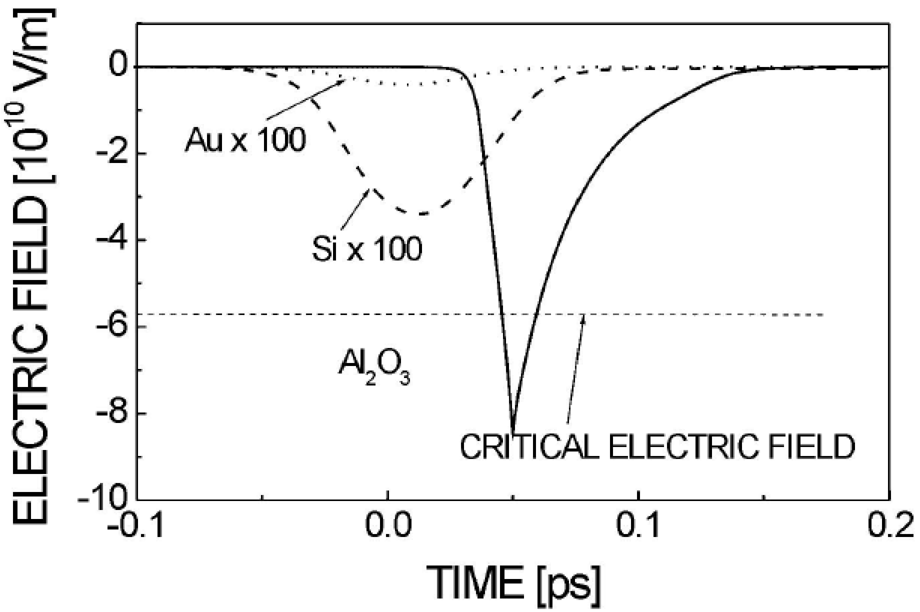

- Charging of **dielectric** surfaces causes a sub-picosecond electrostatic rupture of the superficial layers, i.e. Coulomb explosion (CE)
- Strongly **inhibited** for **metals and semiconductors** as a consequence of superior carrier transport properties

N.M. Bulgakova, R. Stoian, A. Rosenfeld, I.V. Hertel, W. Marine, E.E.B. Campbell, Appl. Phys. A 81, 345–356 (2005)

Dielectric:
Heat affected Zone and threshold fluence

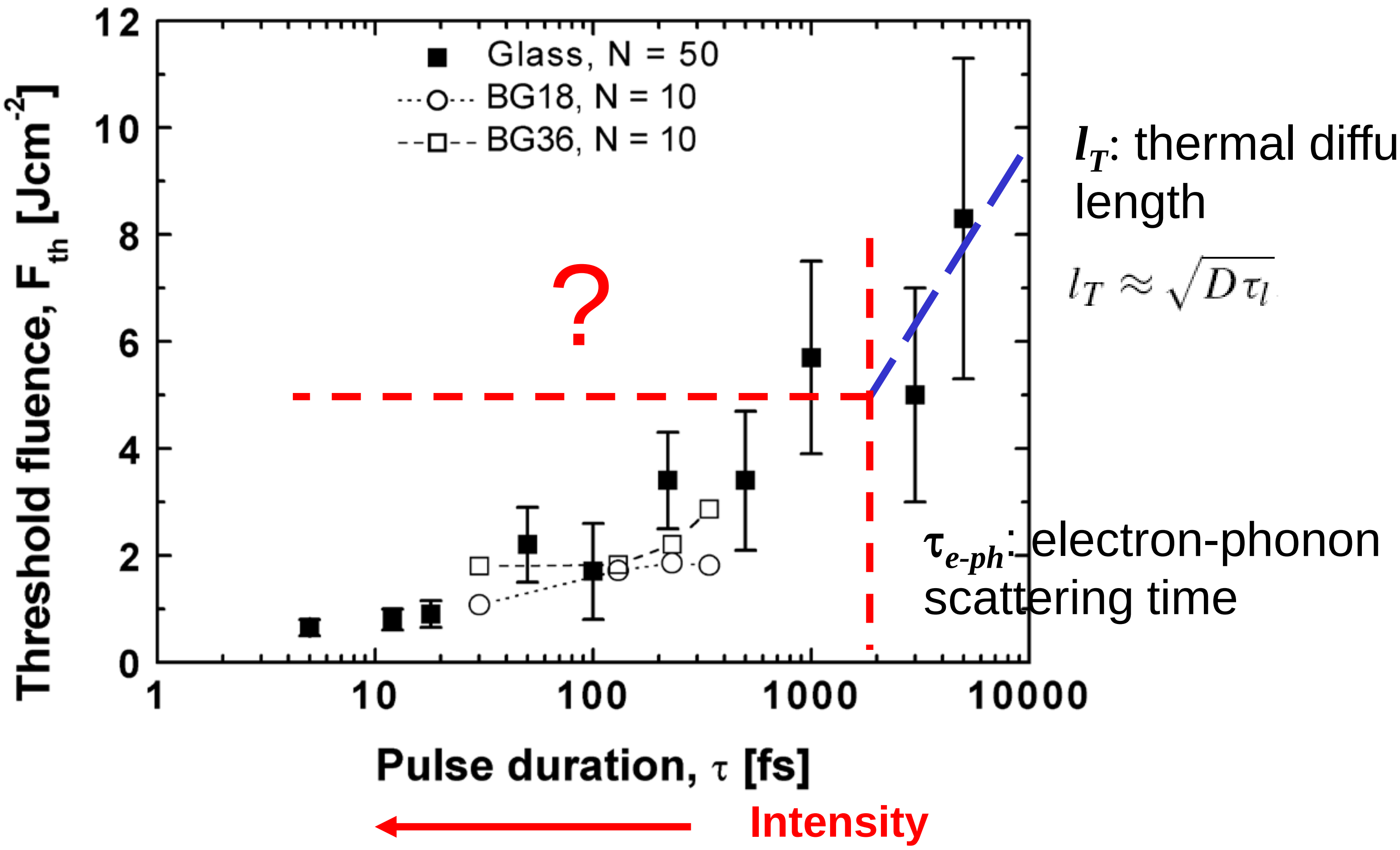

l_T: thermal diffusion length

$$l_T \approx \sqrt{D\tau_l}$$

J. Krüger, M. Lenzner, S. Martin, M. Lenner, C. Spielmann, A. Fiedler and W. Kautek, *Appl. Surf. Sci.* 208-209, p. 233, 2003.

Below the Electron-Phonon Relaxation Time: Heat Affected Zone = const. !!!???

Fused silica, λ = 780 nm, N = 80

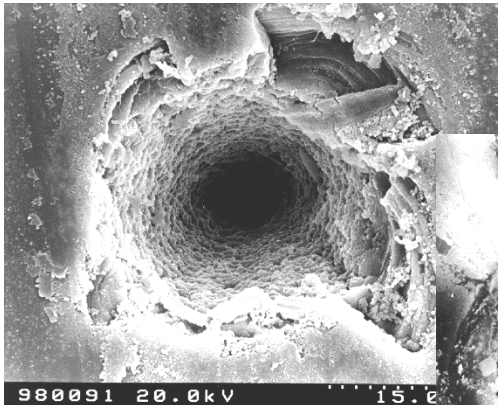

τ = 3 ps
(F = 19.9 Jcm^{-2})

τ = 220 fs
(F = 10.7 Jcm^{-2})

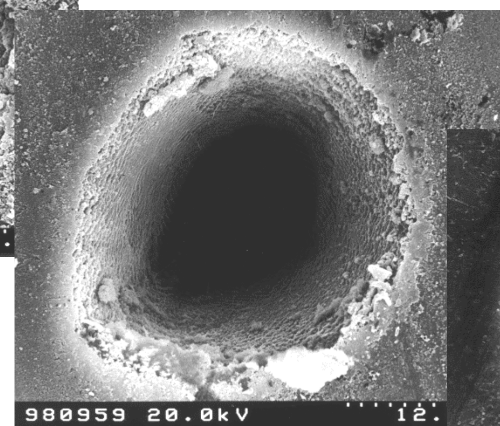

τ = 20 fs
(F = 11.1 Jcm^{-2})

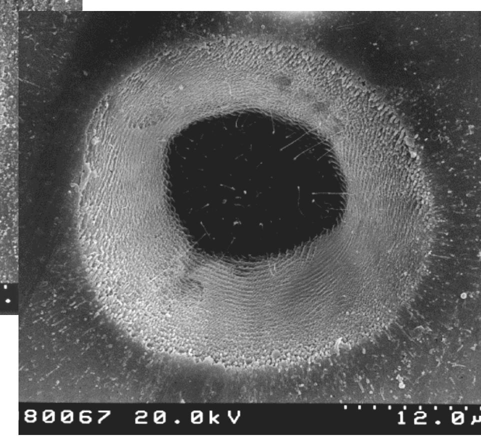

τ = 5 fs
(F = 6.9 Jcm^{-2})

M. Lenzner, J. Krüger, W. Kautek, and F. Krausz, Appl. Phys. A 68 (1999) 369.
"Precision laser ablation of dielectrics in the 10-fs regime".

Femtosecond Optical Breakdown in Dielectrics: 1997

2018 Nobel Prize

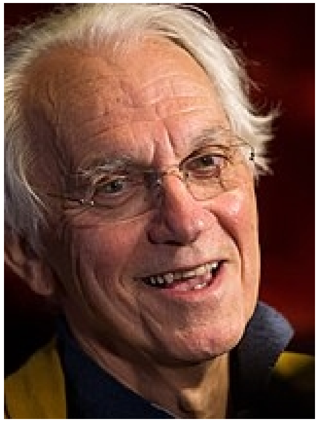

Gerard Mourou, ENSTA, Paris, F

2023 Nobel Prize

Ferenc Krausz, Max-Planck-Institut für Quantenoptik, Garching, D

VOLUME 80, NUMBER 18 PHYSICAL REVIEW LETTERS 4 MAY 1998

Femtosecond Optical Breakdown in Dielectrics

M. Lenzner,[1] J. Krüger,[2] S. Sartania,[1] Z. Cheng,[1] Ch. Spielmann,[1] G. Mourou,[3] W. Kautek,[2] and F. Krausz[1]
[1]*Abteilung Quantenelektronik u. Lasertechnik, Technische Universität Wien, Gusshausstrasse 27, A-1040 Wien, Austria*
[2]*Laboratory for Thin Film Technology, Federal Institute for Materials Research and Testing, D-12200 Berlin, Germany*
[3]*Center for Ultrafast Optical Science, University of Michigan, 2200 Bonisteel Blvd., Ann Arbor, Michigan 48109-2099*
(Received 17 December 1997)

We report measurements of the optical breakdown threshold and ablation depth in dielectrics with different band gaps for laser pulse durations ranging from 5 ps to 5 fs at a carrier wavelength of 780 nm. For $\tau < 100$ fs, the dominant channel for free electron generation is found to be either impact or multiphoton ionization (MPI) depending on the size of the band gap. The observed MPI rates are substantially lower than those predicted by the Keldysh theory. We demonstrate that sub-10-fs laser pulses open up the way to reversible nonperturbative nonlinear optics (at intensities greater than 10^{14} W/cm^2 slightly below damage threshold) and to nanometer-precision laser ablation (slightly above threshold) in dielectric materials. [S0031-9007(98)05969-9]

Dielectrics: Collisional and multiphoton ionization: rate equation approximation

MPI — Avalanche — Losses

$$\frac{\partial N(t)}{\partial t} = P(I) + \beta N(t) - \gamma N^2(t) - \zeta N(t)$$

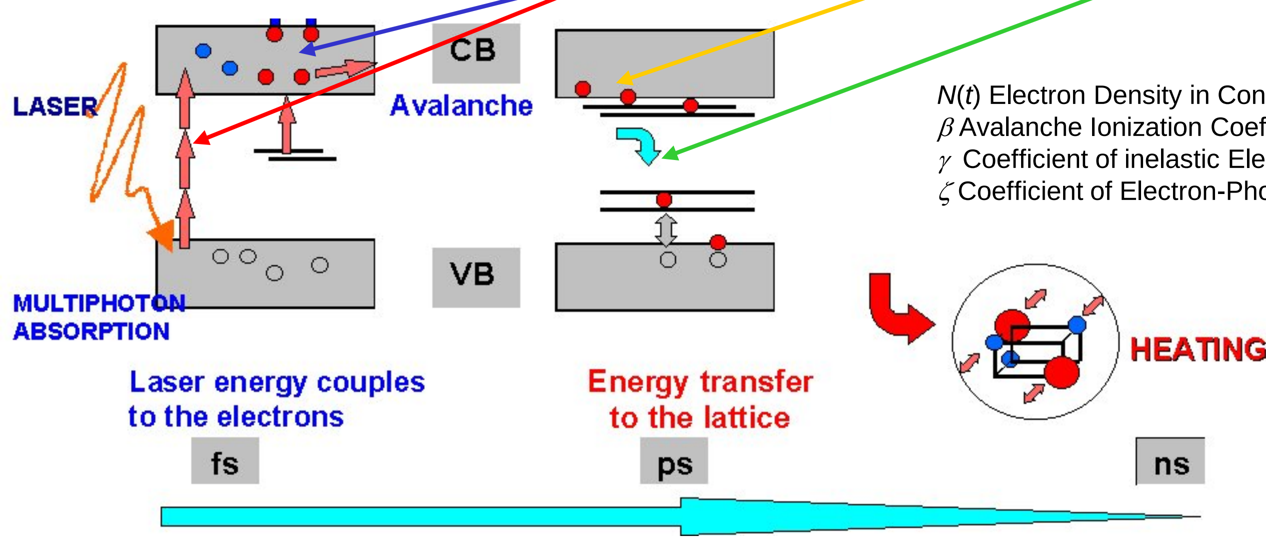

$N(t)$ Electron Density in Conduction Band
β Avalanche Ionization Coefficient
γ Coefficient of inelastic Electron-Electron Scattering
ζ Coefficient of Electron-Phonon Scattering

Accord. to Stoian, 2002

Non-thermal melting

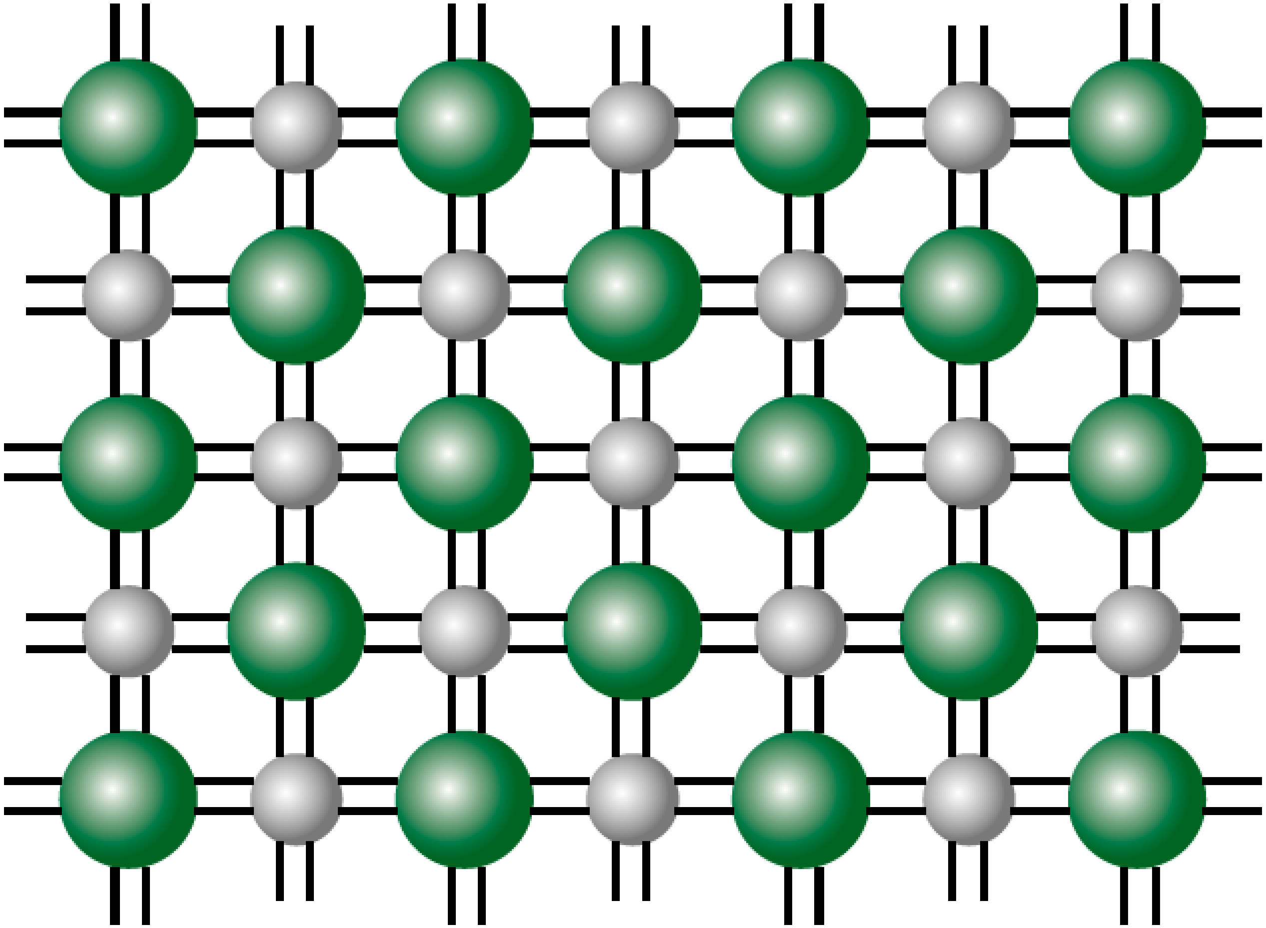

Accord. To E. Mazur

Non-thermal melting

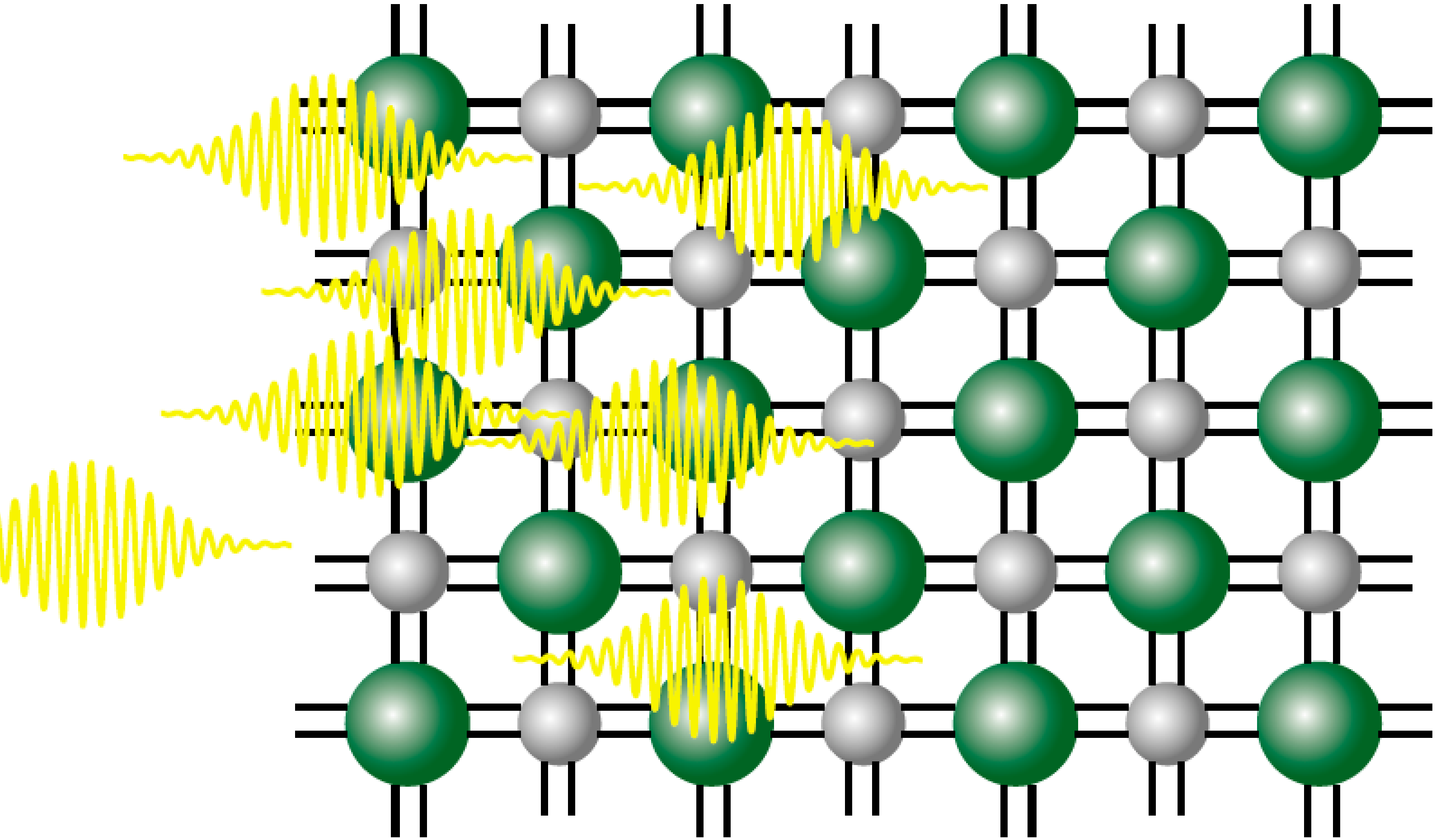

Accord. To E. Mazur

Non-thermal melting

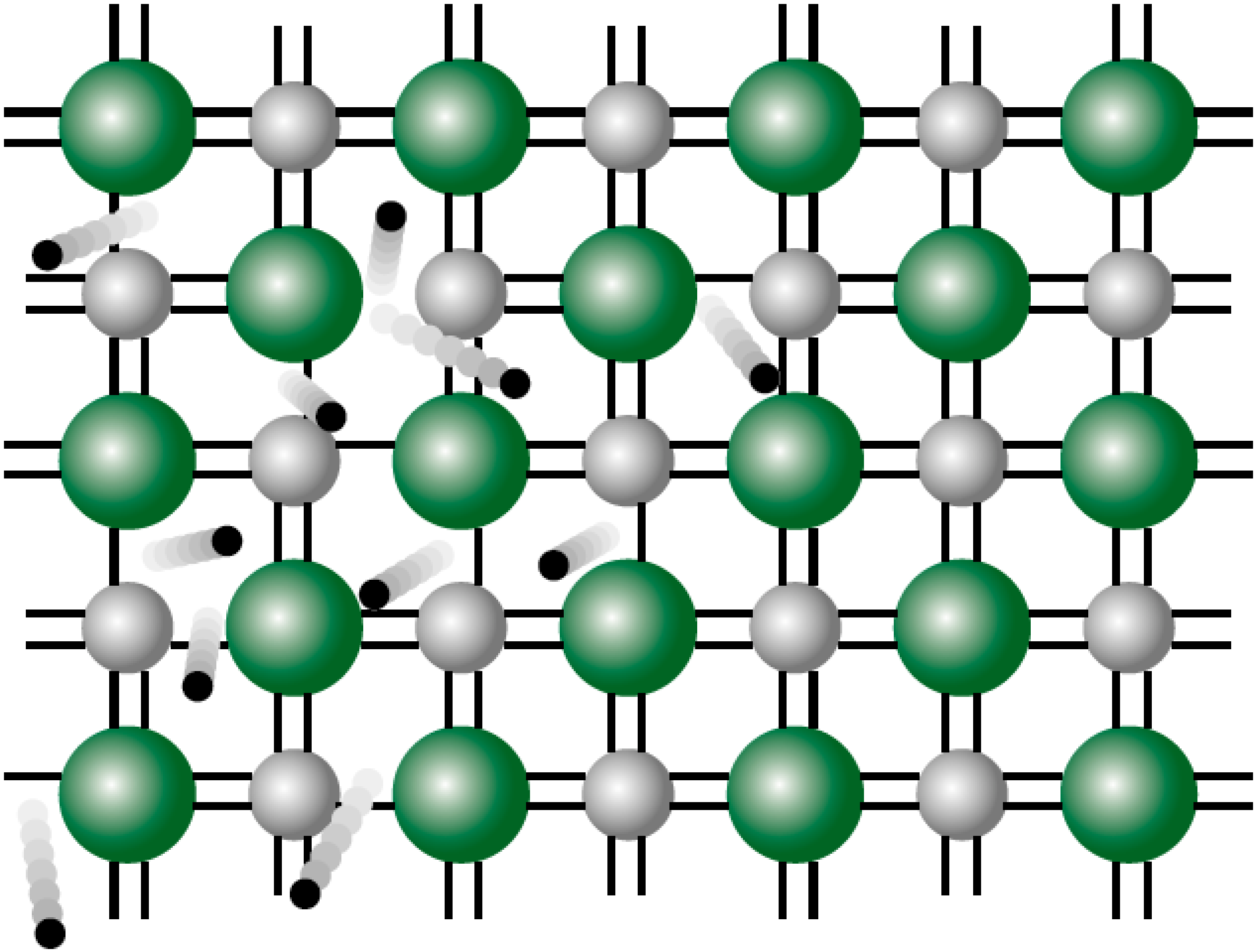

Accord. To E. Mazur

Non-thermal melting

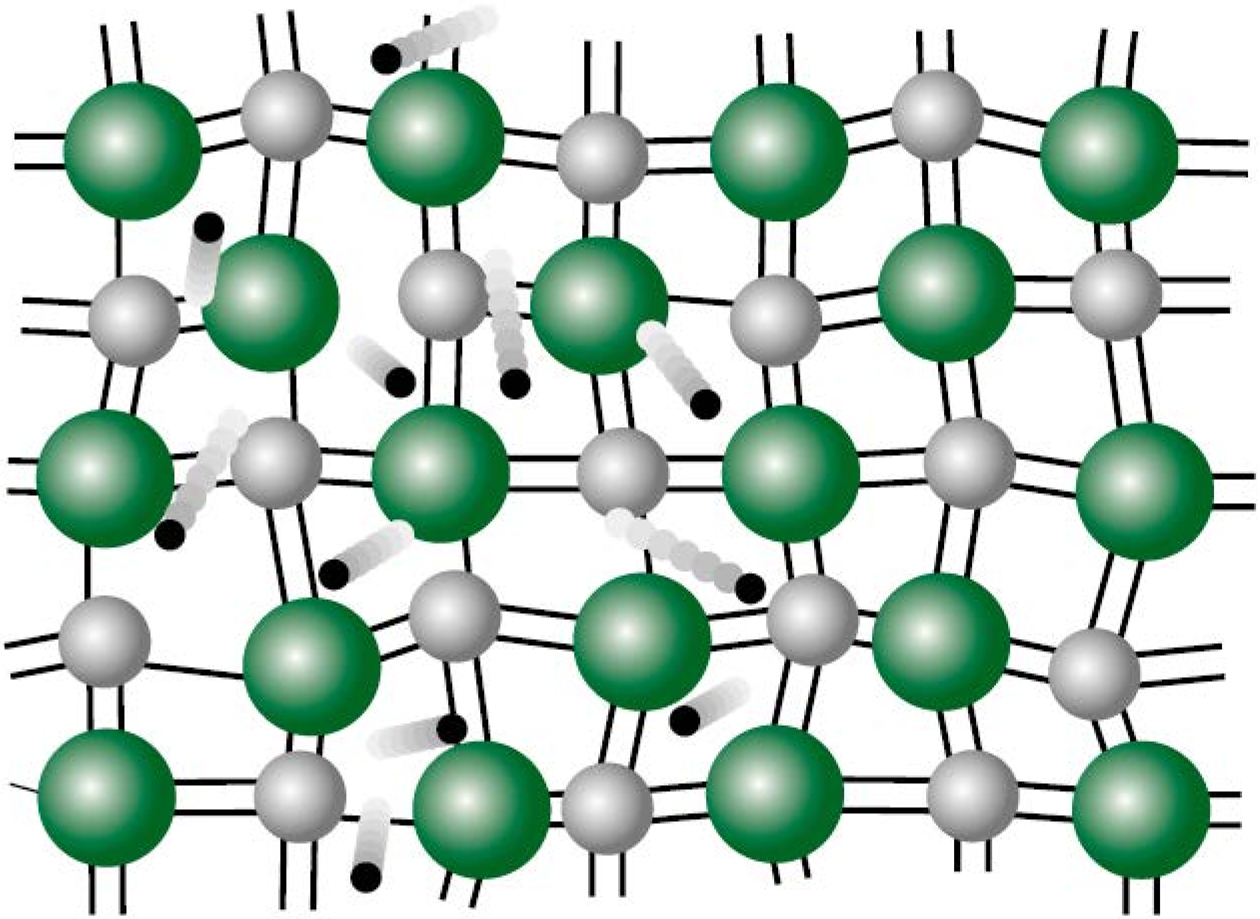

Accord. To E. Mazur

Non-thermal melting of Si

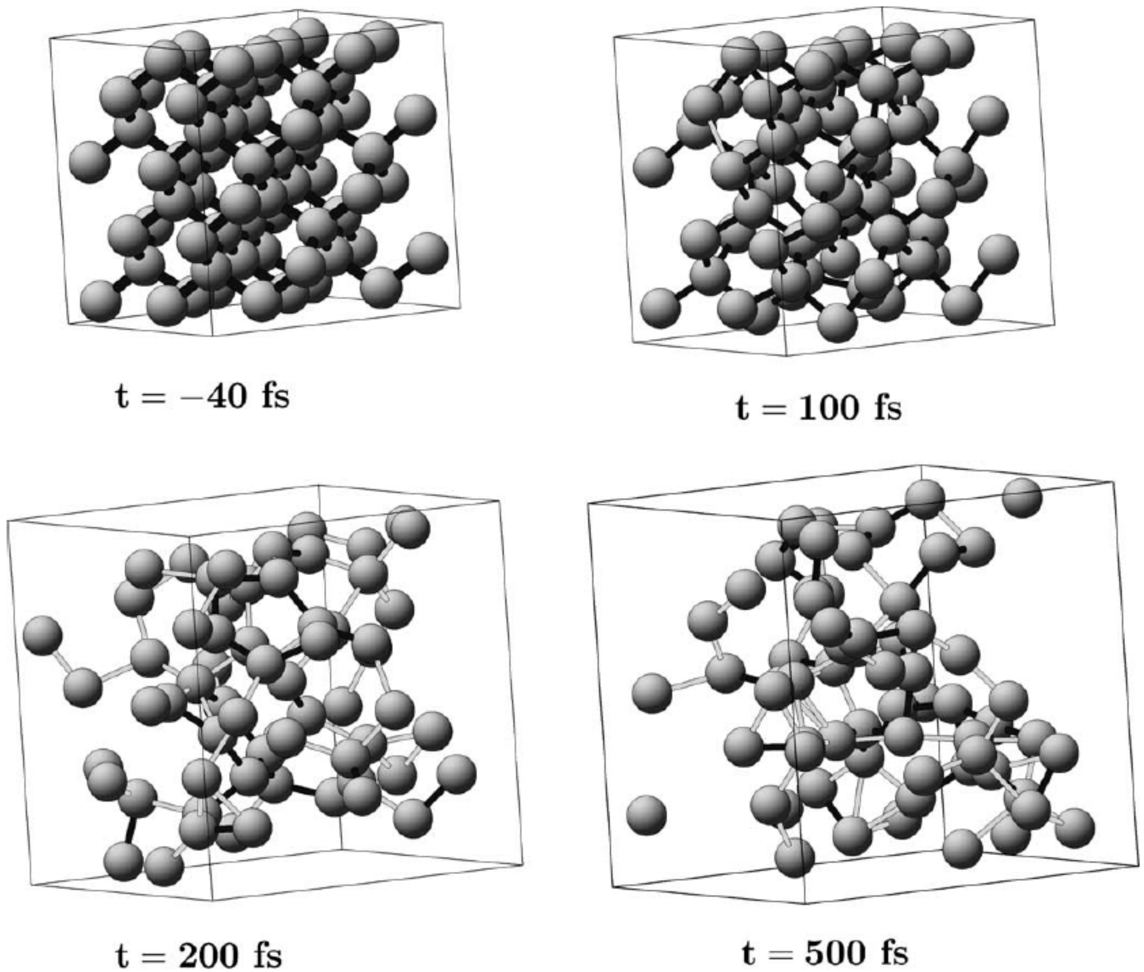

H.O. Jeschke, M.E. Garcia, M. Lenzner, J. Bonse, J. Krüger, W. Kautek, Appl. Surf. Sci. 197-198, p. 839, 2002.

X-ray diffraction: Non-thermal melting of InSb

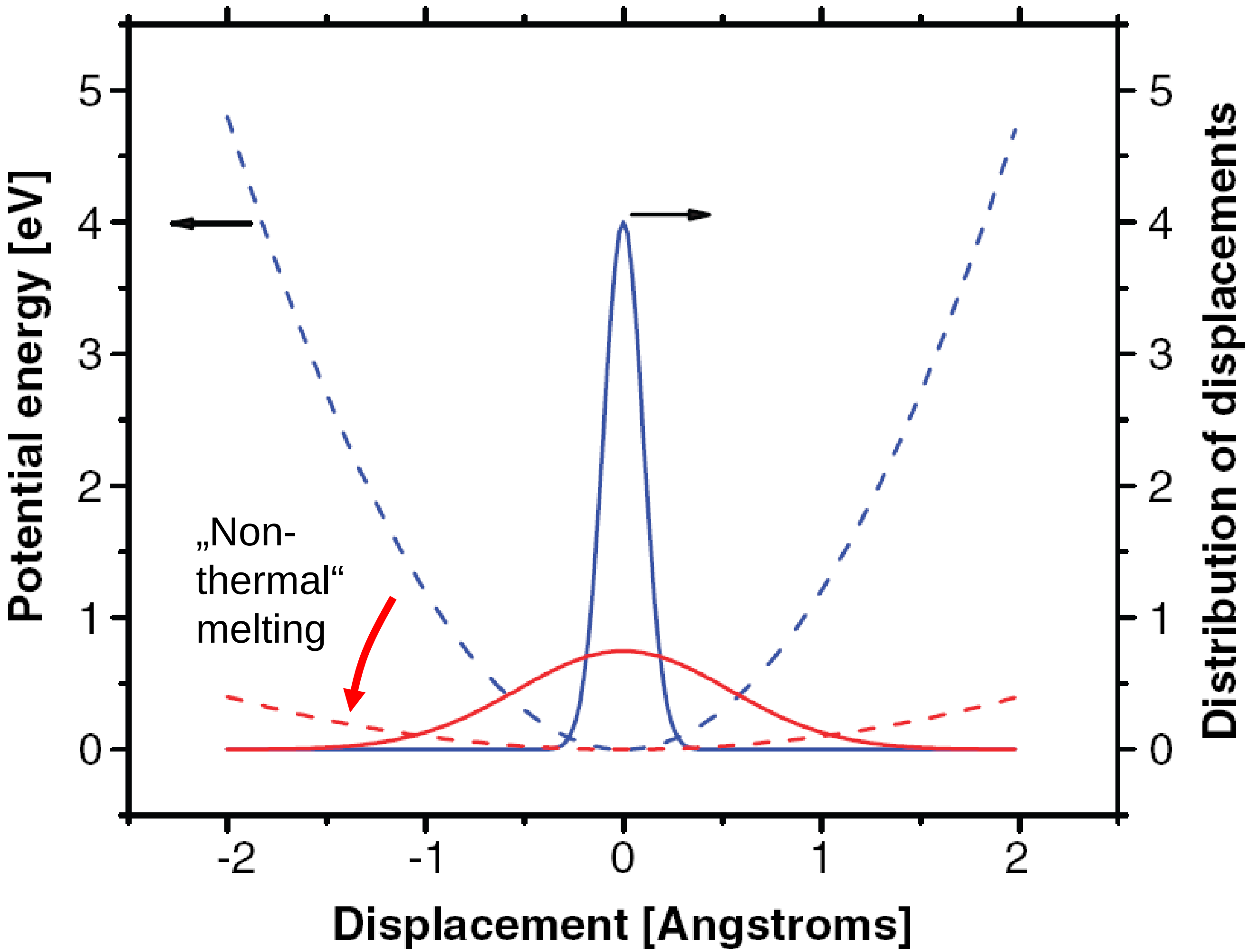

A. M. Lindenberg, 308 SCIENCE 208,392 (2005)

Bond Length and Electronic fs-Excitation of Si

- Molecular dynamics (MD) simulations on the basis of an electronic tight-binding Hamiltonian in real-space: **Rapid excitation of electrons within a few 10 fs**.
- Lattice dynamics on **time-dependent potential energy surfaces**.
- Massive **instability** in the crystal lattice due to perturbation of the **interatomic bonds**.

H.O. Jeschke, M.E. Garcia, M. Lenzner, J. Bonse, J. Krüger, W. Kautek, Appl. Surf. Sci. 197-198, p. 839, 2002.

Non-thermal melting: Si

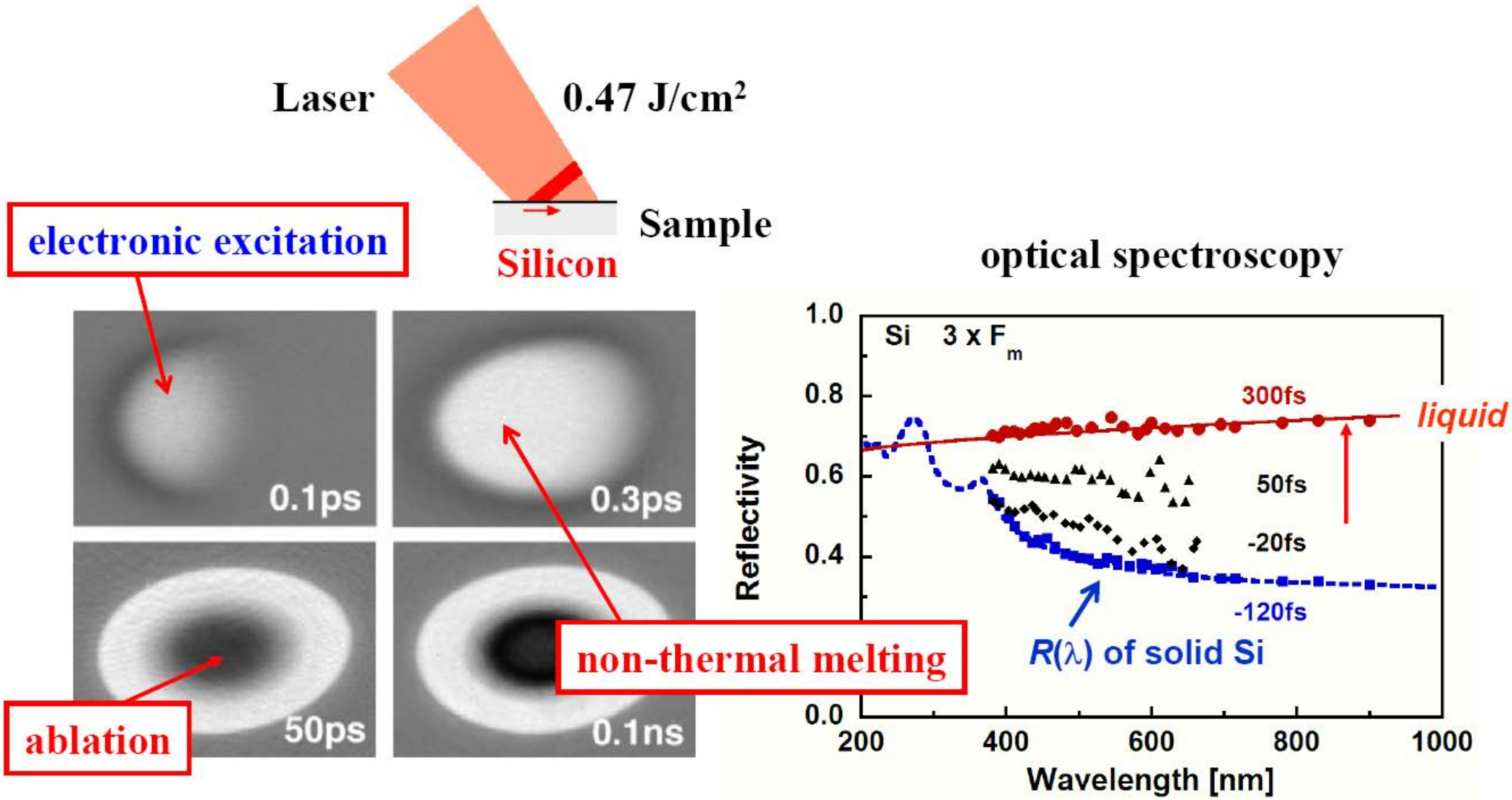

K. Sokolowski-Tinten et al., PRB 51, 14186 (1995), ibid. 58, R11805 (1998),

Time-resolved x-ray diffraction (TXRD)

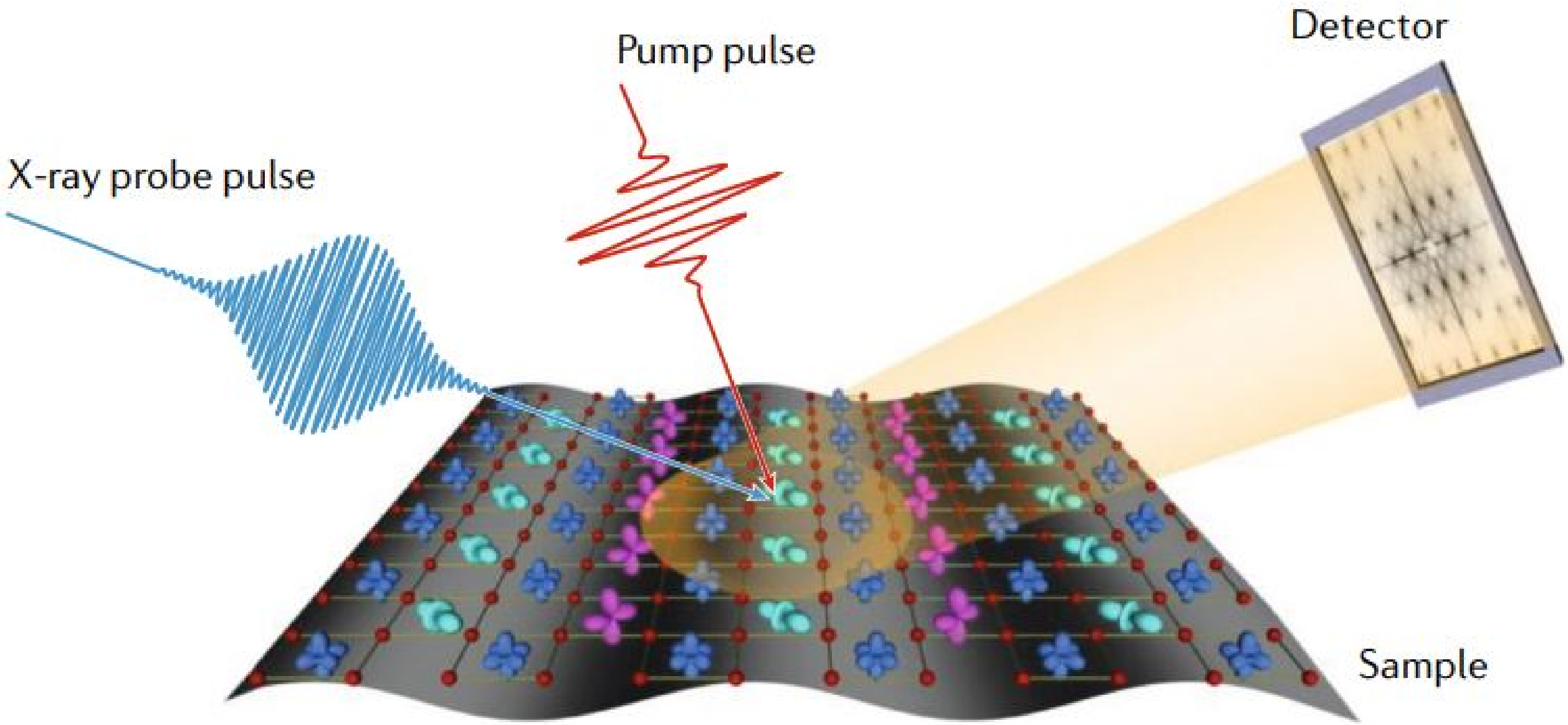

M. Buzzi, M. Först, R. Mankowsky, A. Cavalleri, Nature Reviews Materials, 3 (2018) 299-311.

X-ray diffraction: Non-thermal melting of Ge

170 nm Ge on Si; (111)-diffraction spot

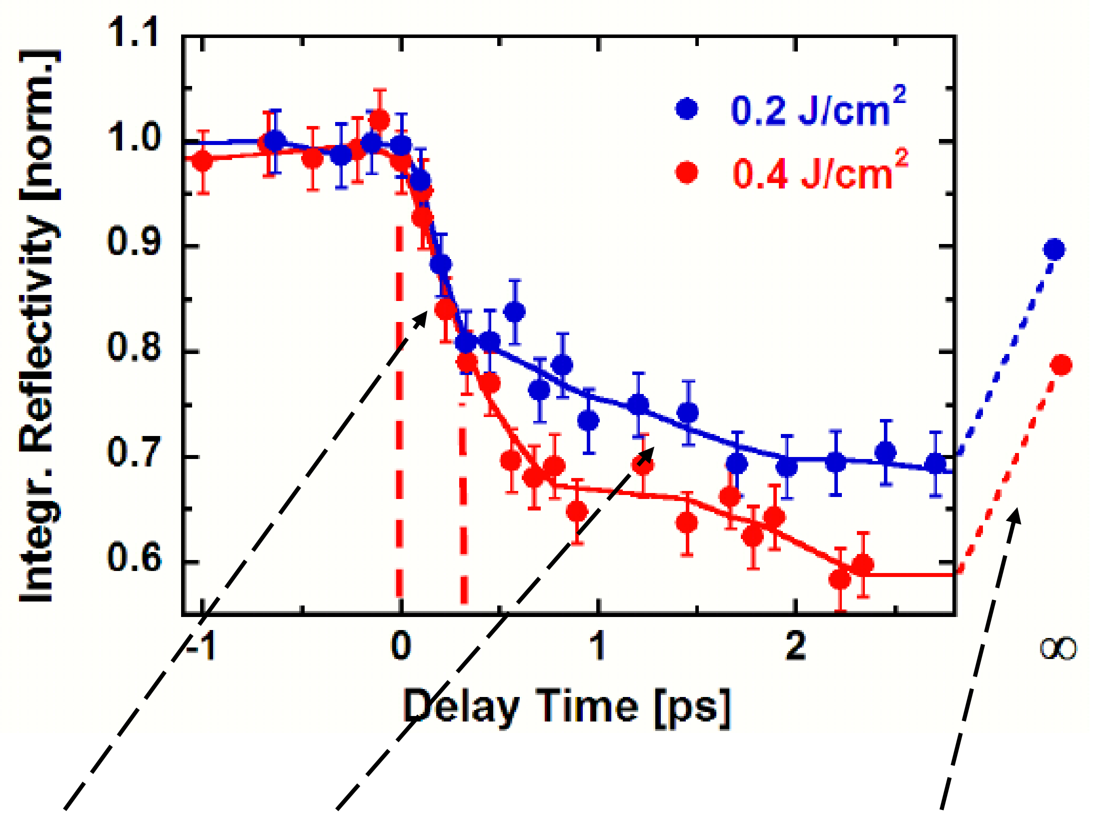

Non-thermal and thermal melting and subsequent re-crystallization

K.Sokolowski-Tinten et al., PRL 87, 225701 (2001)

Outline

- Excitation mechanisms of solids
- Metals: Two-temperature model
  - Fundamentals: Influence of density of states
  - Thin films
  - Metal ablation
  - Hot electron electrochemistry
- Dielectrics: Multiphoton and Avalanche Ionization
  - Dielectric ablation
  - Coulomb explosion
  - Non-thermal melting, X-ray
- Role of Defects
- Applications

Field enhancement by structural defects

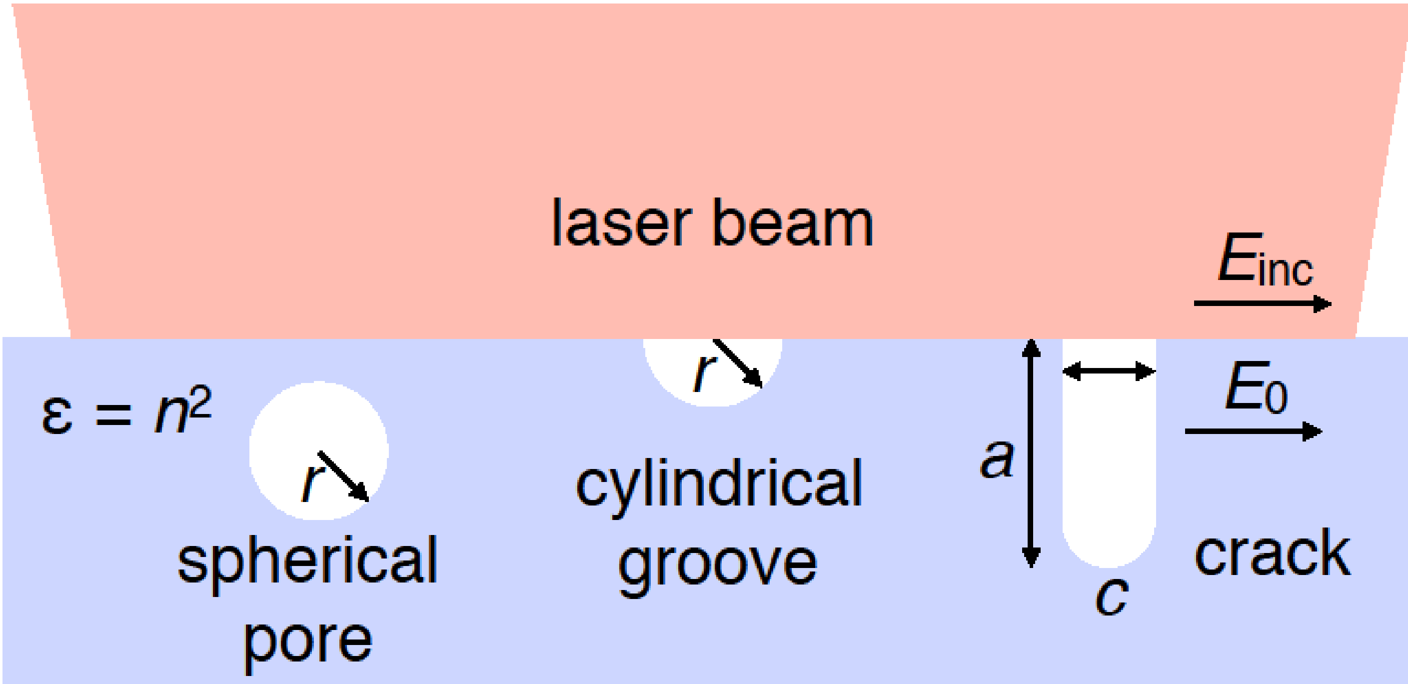

Representative geometries for **electric field enhancement** near pores, scratches, and incipient cracks.
Typical dimensions are r = 0.1 µm, c = 0.1 µm, and a = 1 µm

O. Armbruster, A. Naghilou, W. Kautek, Springer Series in Materials Science (2018), in print.
"The role of defects in pulsed laser matter interaction".

N. Bloembergen, Applied Optics, 12 (1973) 661-664

Threshold Fluence and Beam Diameter
Heat Accumulation Model

At higher repetition rate, the heat caused by laser irradiation accumulates.
When temperature reaches the critical temperature modification occurs.

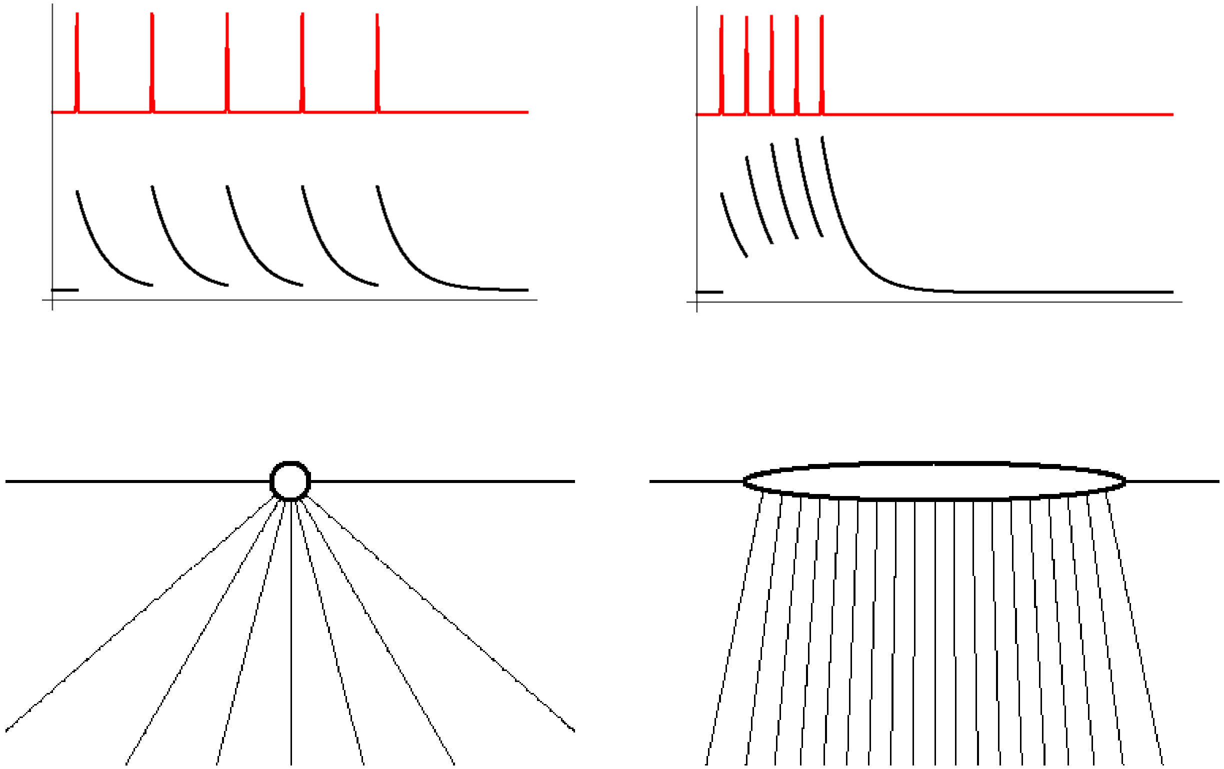

B. Kim, M. Feit, A. Rubenchik, E. Joslin, J. Eichler, P. Stoller, L. Da Silva," Effects of high repetition rate and beam size on hard tissue damage due to subpicosecond laser pulses" Appl. Phys. Lett. 76, 4001 (2000).

Threshold Fluence and Beam Diameter
Heat Accumulation Model

BBS Glass, 30 fs, 800 nm, 1000-on-1

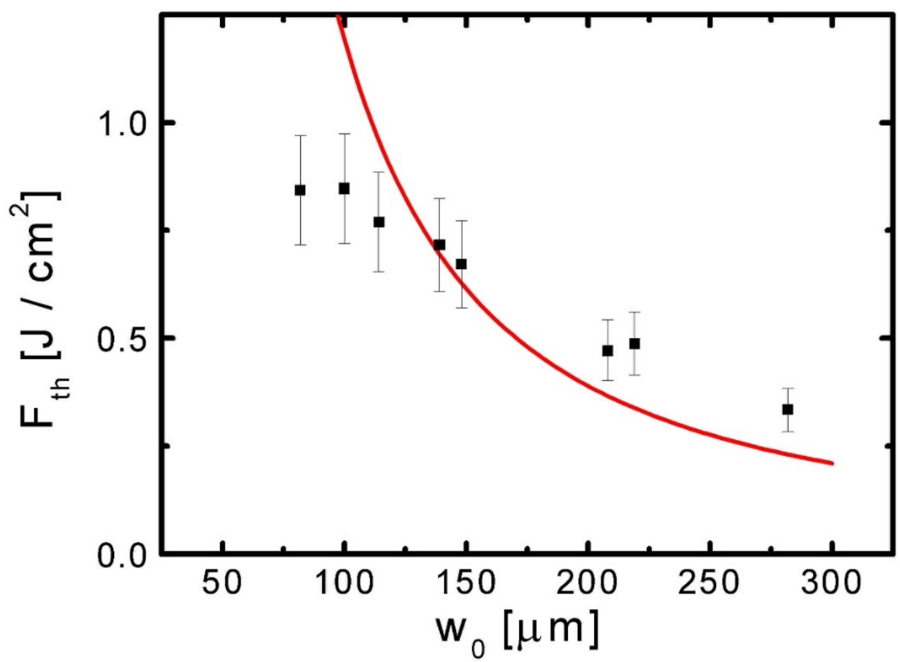

Fit Thermal Model

B. Kim, M. Feit, A. Rubenchik, E. Joslin, J. Eichler, P. Stoller, L. Da Silva," Effects of high repetition rate and beam size on hard tissue damage due to subpicosecond laser pulses" Appl. Phys. Lett. 76, 4001 (2000).

$$F_{th} = \frac{4c\rho dKT_c}{\alpha\omega_0^2 \nu_{rep} \ln\left(\frac{8NK}{\nu_{rep}\omega_0^2}\right)}$$

S. Martin, A. Hertwig, M. Lenzner, J. Krüger, W. Kautek
"Spot-size dependence of the ablation threshold in dielectrics for femtosecond laser pulses", Appl. Phys. A, 77, 883 (2003).

Threshold Fluence and Beam Diameter
Point Defect Model

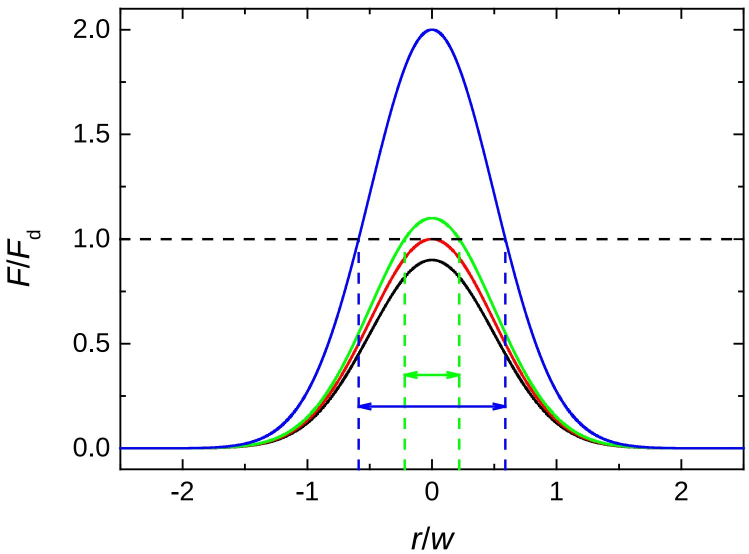

$$P_d = 1 - \left(\frac{\hat{F}}{F_d}\right)^{\left(-\frac{1}{2}\omega_0^2\ \pi\ \rho\right)}$$

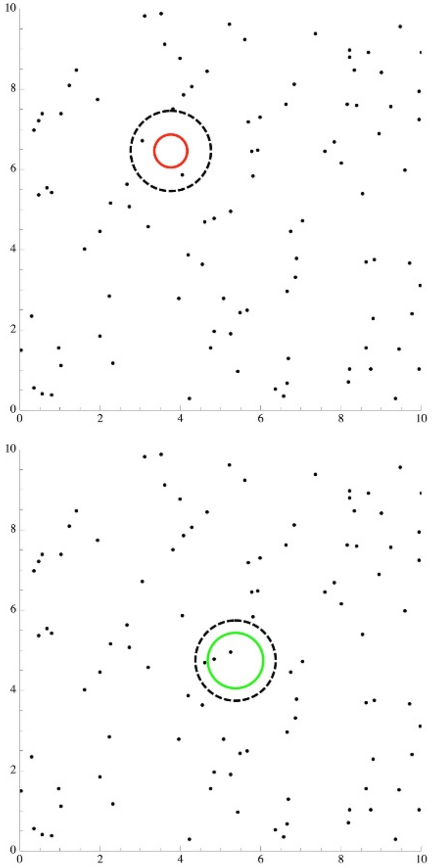

L. G. DeShazer, B. E. Newnamt, K. M. Leung „Role of coating defects in laser-induced damage to dielectric thin films” Appl. Phys. Lett. 23, 607 (1973)

Laser-generated defects

“Incubation”

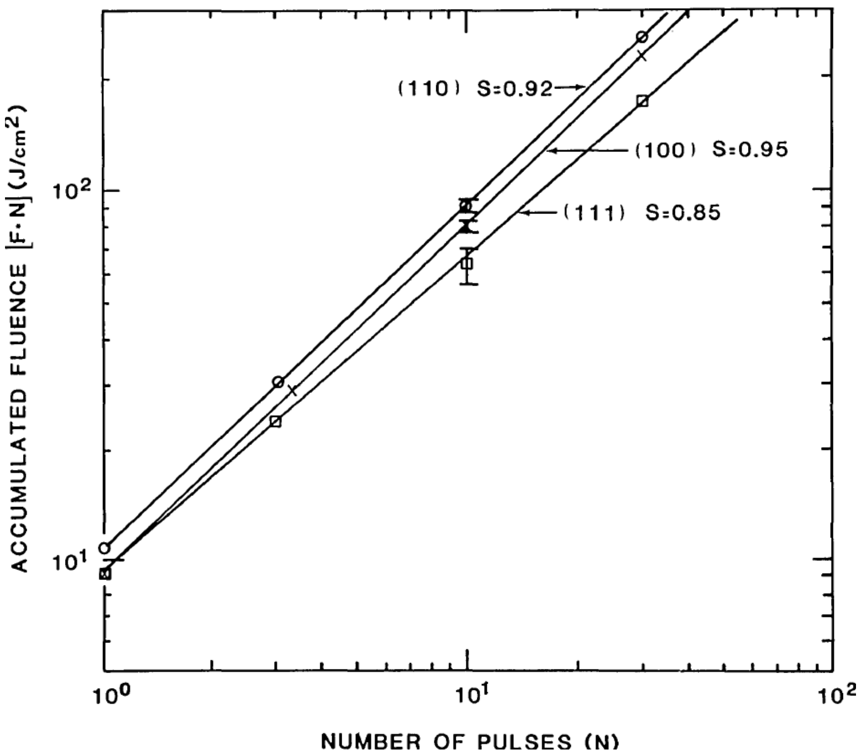

Damage fluence versus pulse number curves for various crystallographic orientations of chemically polished Cu

$$F_{th}(N) = F_{th}(1)\ N^{-\xi}$$

ξ: Empirical incubation parameter

O. Armbruster, A. Naghilou, W. Kautek, Springer Series in Materials Science (2018), in print.
“The role of defects in pulsed laser matter interaction”.

Y. Jee, M.F. Becker, R.M. Walser, Journal of the Optical Society of America B, 5 (1988) 648-659.

Laser-generated defects

PMMA

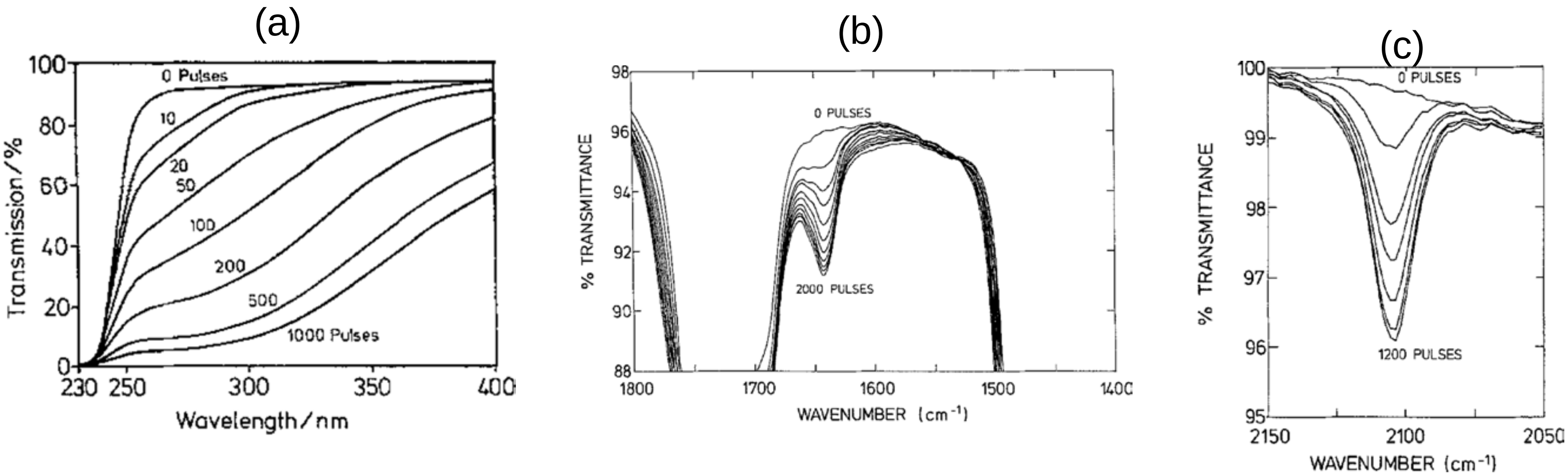

40 µm thick PMMA film at 248 nm, 40 mJ cm^{-2}.

(a) The UV spectrum of the same sample exhibits a **broad absorption** for wavelengths up to the visible.

(b) FT IR spectrum in the 1600 cm^{-1} region. Up to 2000 pulses, a peak, typical for **C=C double bonds**, grows in and reaches a photostationary equilibrium for higher pulse numbers.

(c) FT IR spectrum in the wavenumber region typical for the absorption of **cumulated double bonds** or triple bonds.

O. Armbruster, A. Naghilou, W. Kautek, Springer Series in Materials Science (2018), in print.
"The role of defects in pulsed laser matter interaction".

S. Küper, M. Stuke, Applied Physics A, 49 (1989) 211-215.

Laser-generated defects

Silver

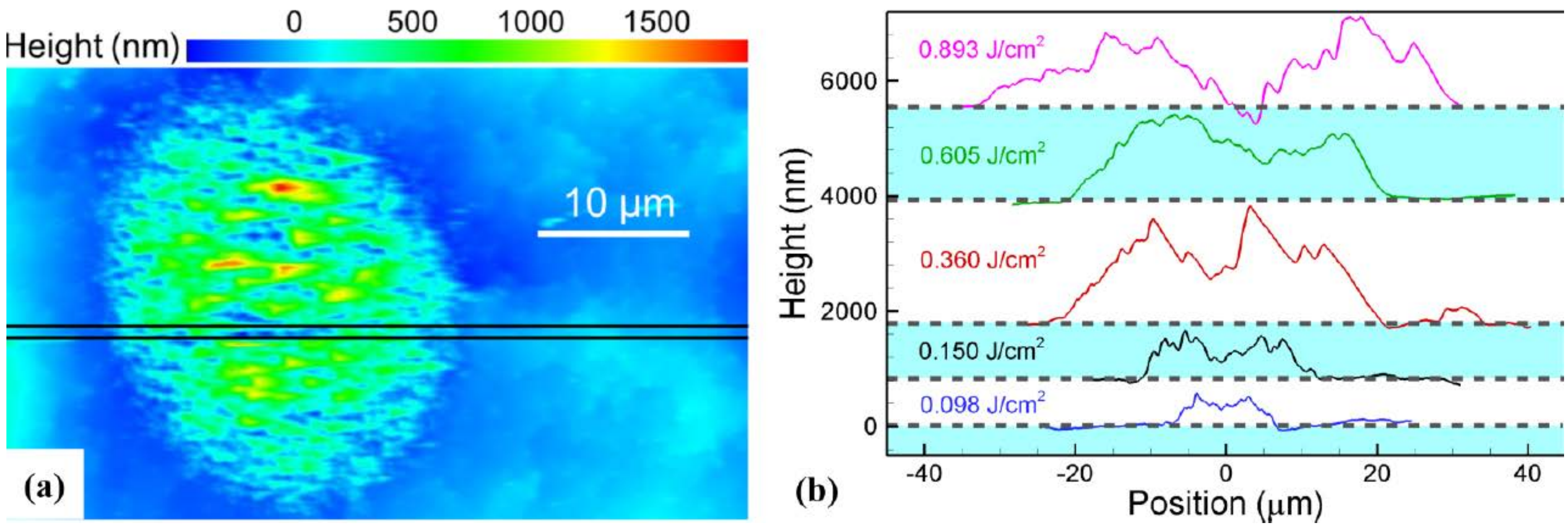

(a) AFM scan of a Ag (001) surface irradiated by a 100-fs laser pulse at an absorbed laser fluence of 0.15 J cm^{-2} (incident fluence: (4.87 ± 0.08) J cm^{-2}) below the threshold

(b) AFM line scans of several spots generated by irradiation at various absorbed fluences

O. Armbruster, A. Naghilou, W. Kautek, Springer Series in Materials Science (2018), in print.
“The role of defects in pulsed laser matter interaction”.

C. Wu, M.S. Christensen, J.-M. Savolainen, P. Balling, L.V. Zhigilei, Physical Review B, 91 (2015) 035413.

Laser-generated defects

Silver

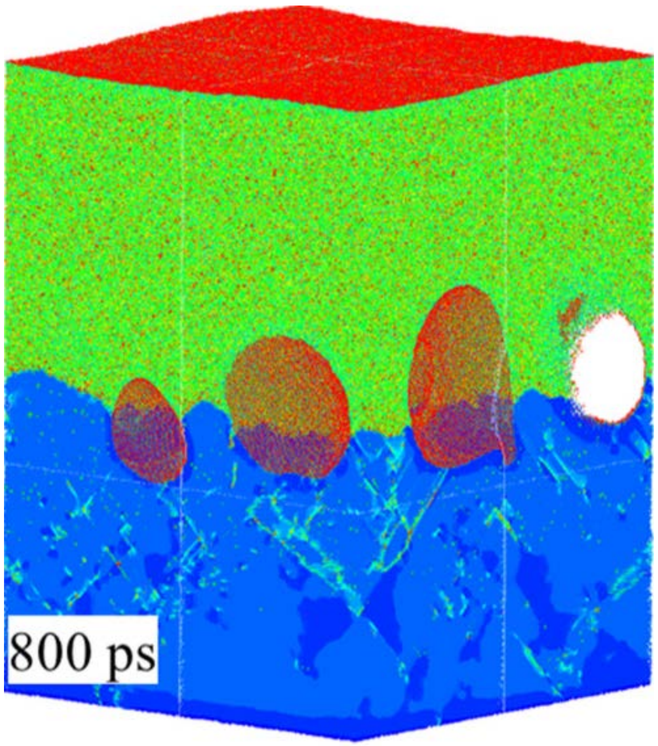

Snapshot of the atomic configuration after 800 ps generated in a TTM-MD simulation of an Ag (001) target irradiated by a 100 fs laser pulse at an absorbed fluence of 85 mJ cm^{-2}.

The atoms are colored by their potential energies, with the scale from -2.84 eV (blue) to -2.65 eV (red).

This scale ensures that most atoms in the crystalline part of the target are blue, the atoms in the molten part are green, and the **atoms on free surfaces are red**

O. Armbruster, A. Naghilou, W. Kautek, Springer Series in Materials Science (2018), in print.
“The role of defects in pulsed laser matter interaction”.

C. Wu, M.S. Christensen, J.-M. Savolainen, P. Balling, L.V. Zhigilei, Physical Review B, 91 (2015) 035413.

Laser-generated defects

Aluminium

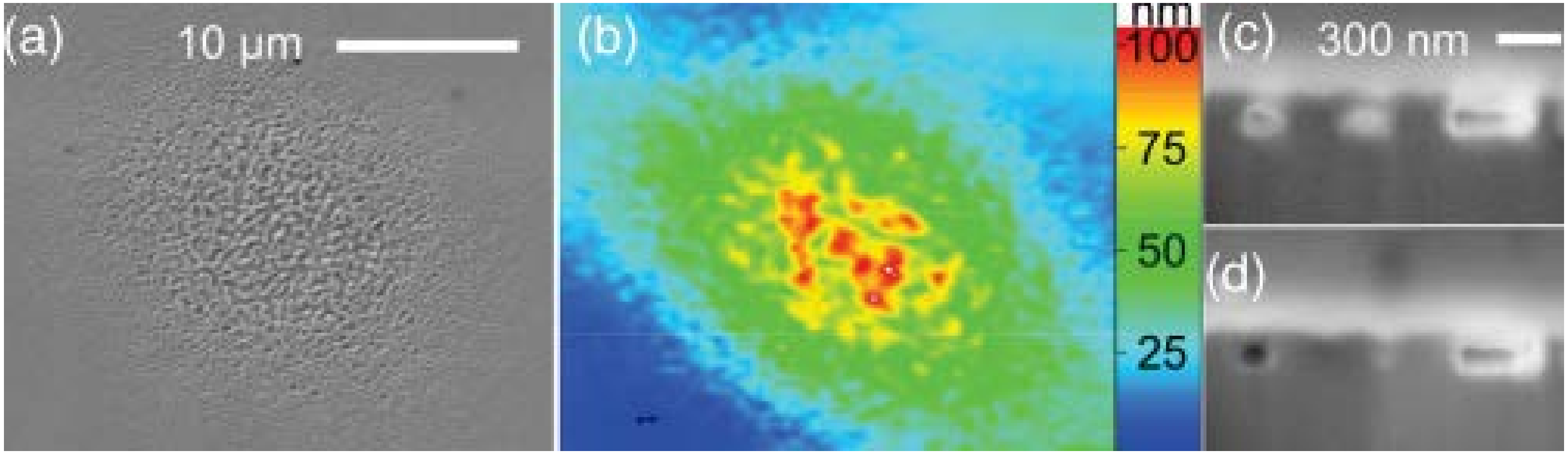

Swelling due to ultrafast irradiation at 0.79 J cm^{-2}.

(a) SEM

(b) AFM

(c) SEM images of the same spot after FIB milling. The bottom dark-gray area is the aluminum sample, while the top lighter gray stems from a protective tungsten layer.

(d) Same as (c) after additional 50 nm milling

O. Armbruster, A. Naghilou, W. Kautek, Springer Series in Materials Science (2018), in print. "The role of defects in pulsed laser matter interaction".

J.-M. Savolainen, M.S. Christensen, P. Balling, Physical Review B, 84 (2011) 193410.

Laser-generated defects

TiN

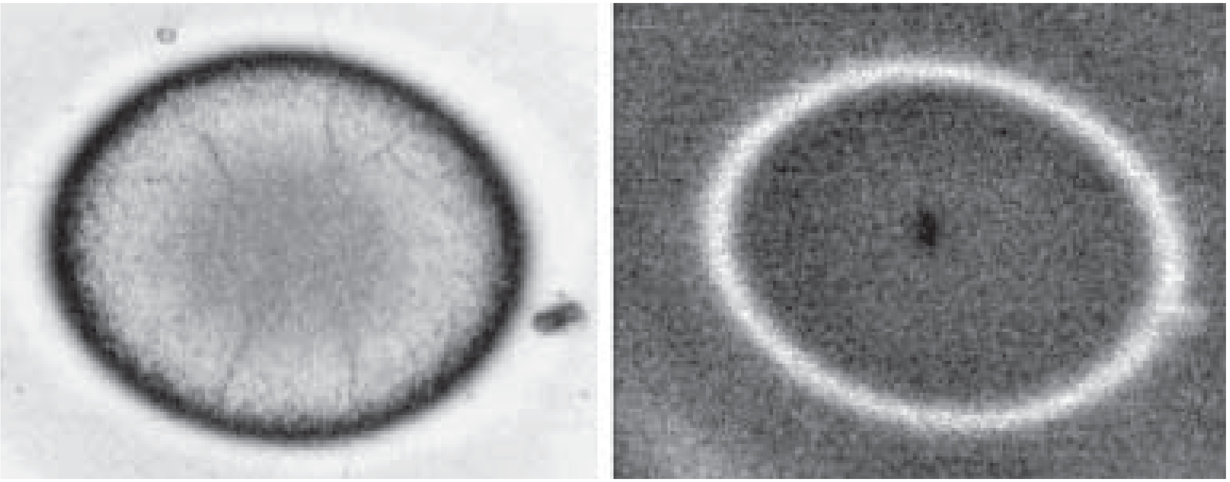

Oxygen map of femtosecond laser irradiated TiN

Scanning Auger electron microscopy (left) and AFM topography (right)

O. Armbruster, A. Naghilou, W. Kautek, Springer Series in Materials Science (2018), in print.
"The role of defects in pulsed laser matter interaction".

J. Bonse, H. Sturm, D. Schmidt, W. Kautek, Chemical, Applied Physics A, 71 (2000) 657-665.

Incubation:

Threshold fluences F_{th} vs. pulse number N

High Impact Polystyrene (HIPS)

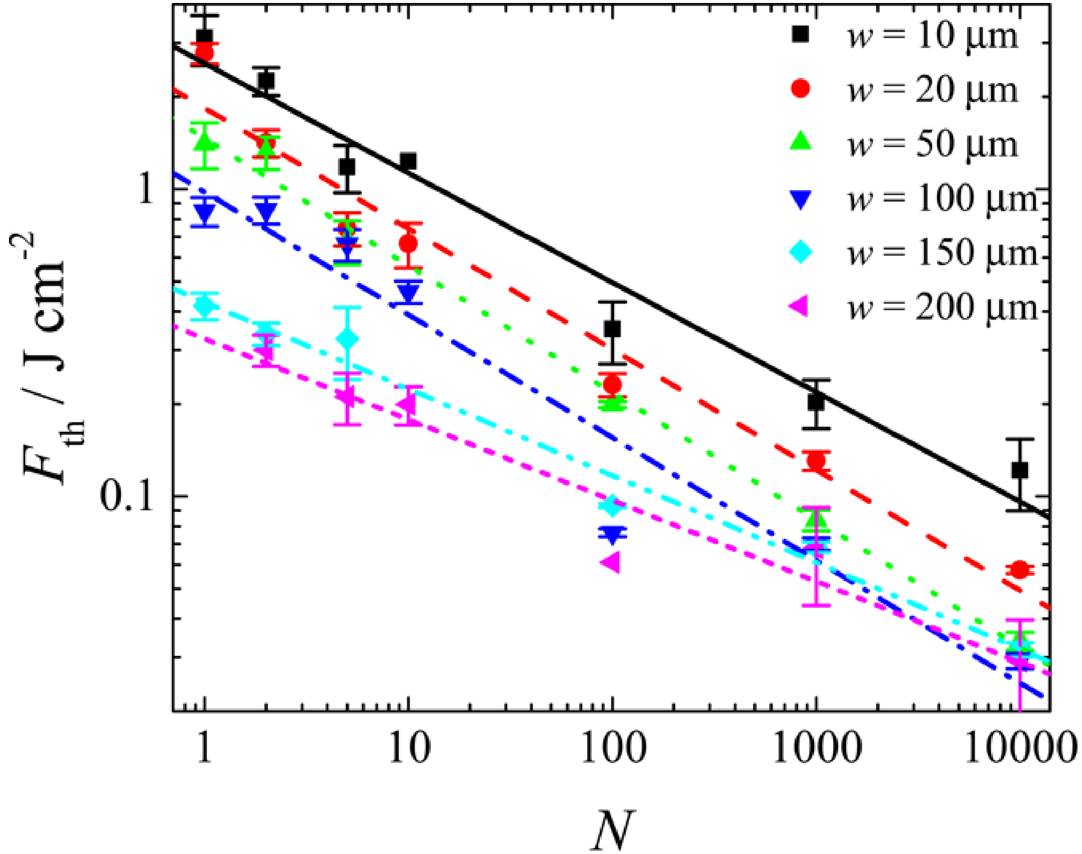

$$F_{\mathrm{th}}(N) = F_{\mathrm{th}}(1)N^{-\xi}$$

A. Naghilou, O. Armbruster, M. Kitzler, W. Kautek, J. Phys. Chem. C 119 (2015) 22992−22998

Beam Radius Determination
& Optically Active Low-Density Defects (LDD)

Optical Micrograph (upper left) & SEM (lower right)

N = 1; w = (50 ± 5) µm; F = (11 ± 2) J cm^{-2}.

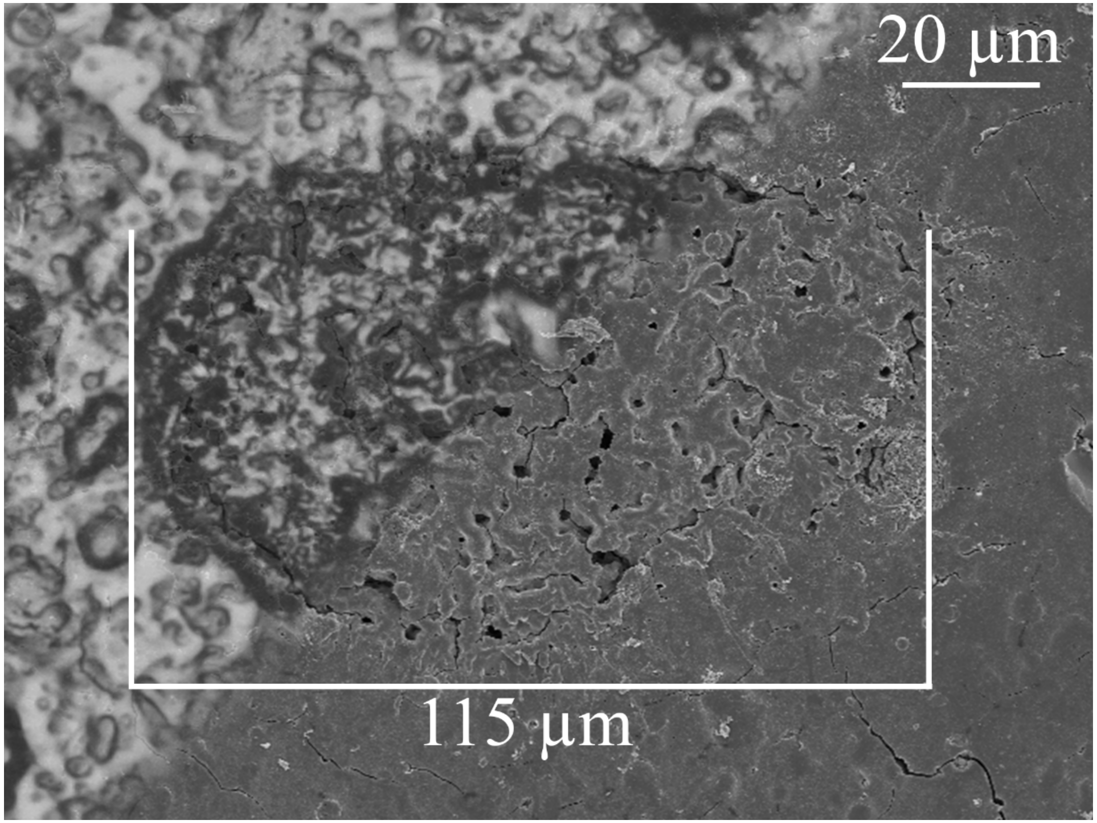

A. Naghilou, O. Armbruster, M. Kitzler, W. Kautek, J. Phys. Chem. C 119 (2015) 22992−22998

w-dependent Defect Model

$$F_{\text{th}}(N, w) = F_{\text{d}}(N) + (F_{\text{i}}(N) - F_{\text{d}}(N))\left(\frac{F_{\text{i}}(N)}{F_{\text{d}}(N)}\right)^{-1/2w^2\pi\sigma}$$

… lacks explanation for the reduction of F_{th} with N (“Incubation”)

DeShazer, L. G.; Newnam, B. E.; Leung, K. M., Appl. Phys. Lett. 1973, 23, 607-609.

Irradiation Area & Incubation:
High Impact Polystyrene (HIPS)

$$F_{th}(N,w) = F_d(N) + (F_i(N) - F_d(N))\left(\frac{F_i(N)}{F_d(N)}\right)^{-1/2w^2\pi\sigma}$$

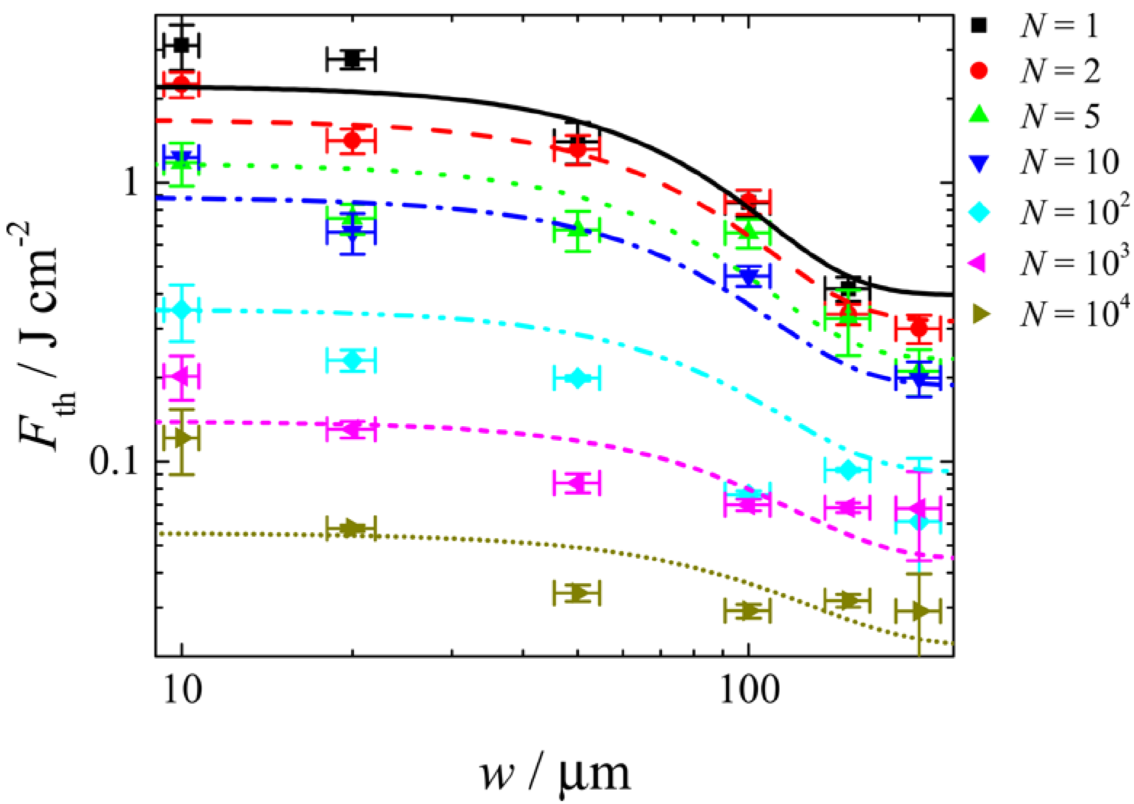

$$F_d(N) = F_d(1)N^{-\xi_d}$$

$$F_i(N) = F_i(1)N^{-\xi_i}$$

A. Naghilou, O. Armbruster, M. Kitzler, W. Kautek, J. Phys. Chem. C 119 (2015) 22992−22998

Irradiation Area & Incubation

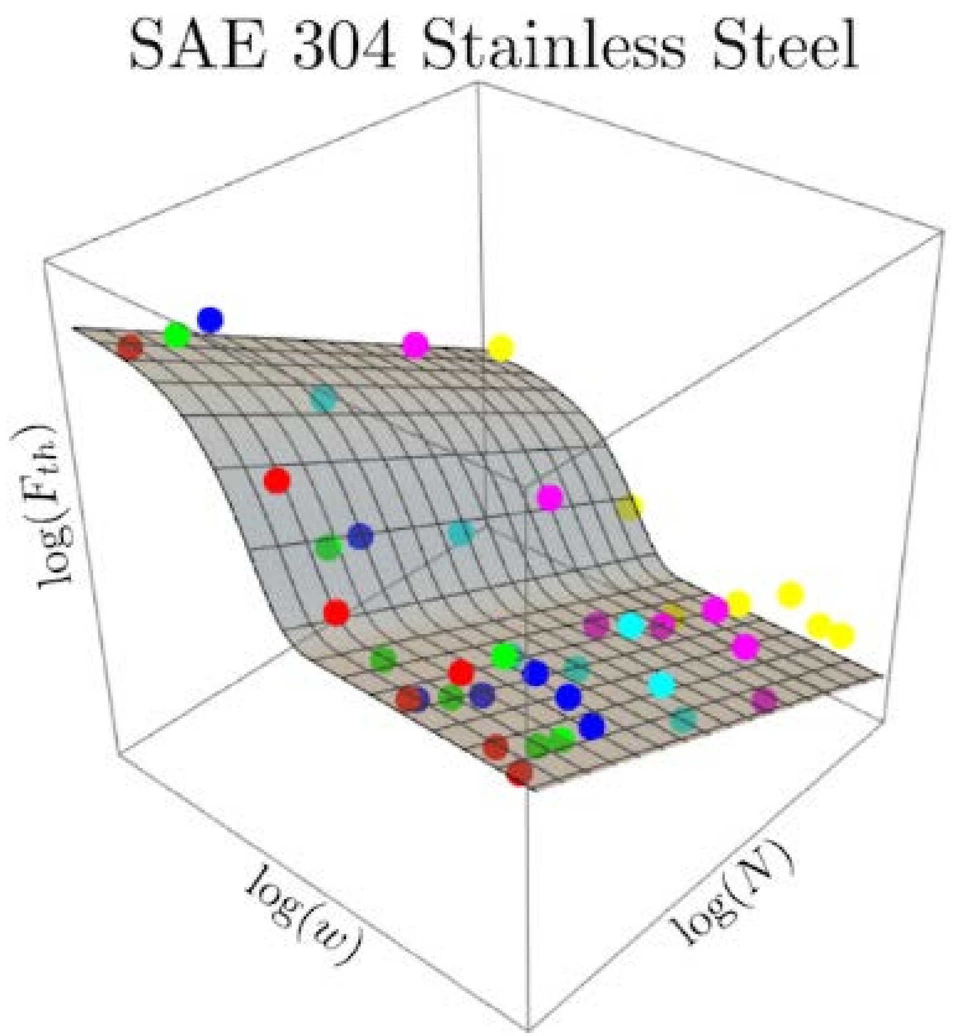

O. Armbruster, A. Naghilou, M. Kitzler, W. Kautek, Appl. Surf. Sci. 396 (2017) 1736–1740.

Irradiation Area & Incubation

High-impact Polystyrene (HIPS)

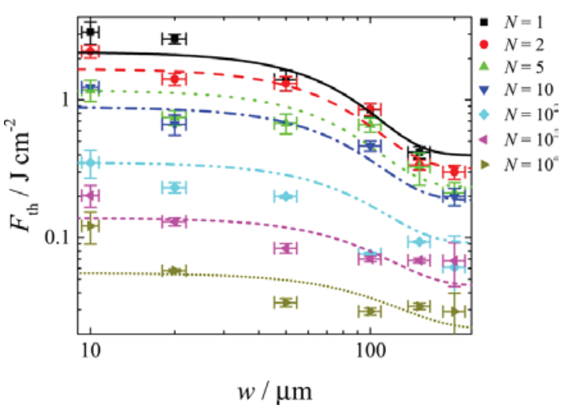

Silicon <111>

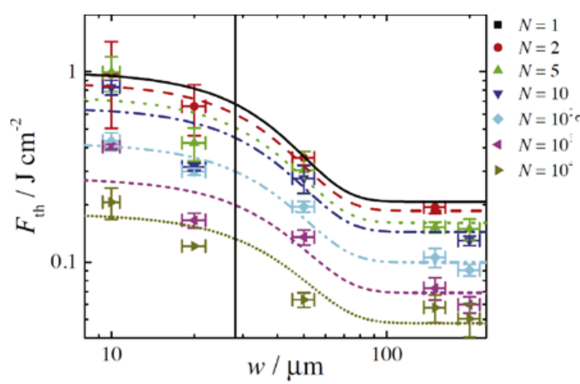

SAE 304 stainless steel

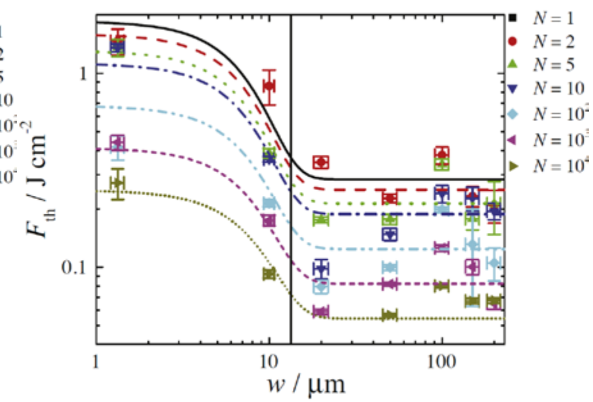

Sub-100 fs laser irradiation

O. Armbruster, A. Naghilou, W. Kautek, Springer Series in Materials Science (2018), in print. “The role of defects in pulsed laser matter interaction”.

O. Armbruster, A. Naghilou, M. Kitzler, W. Kautek, Appl. Surf. Sci. 396 (2017) 1736–1740.

Steel: Densities of LDDs

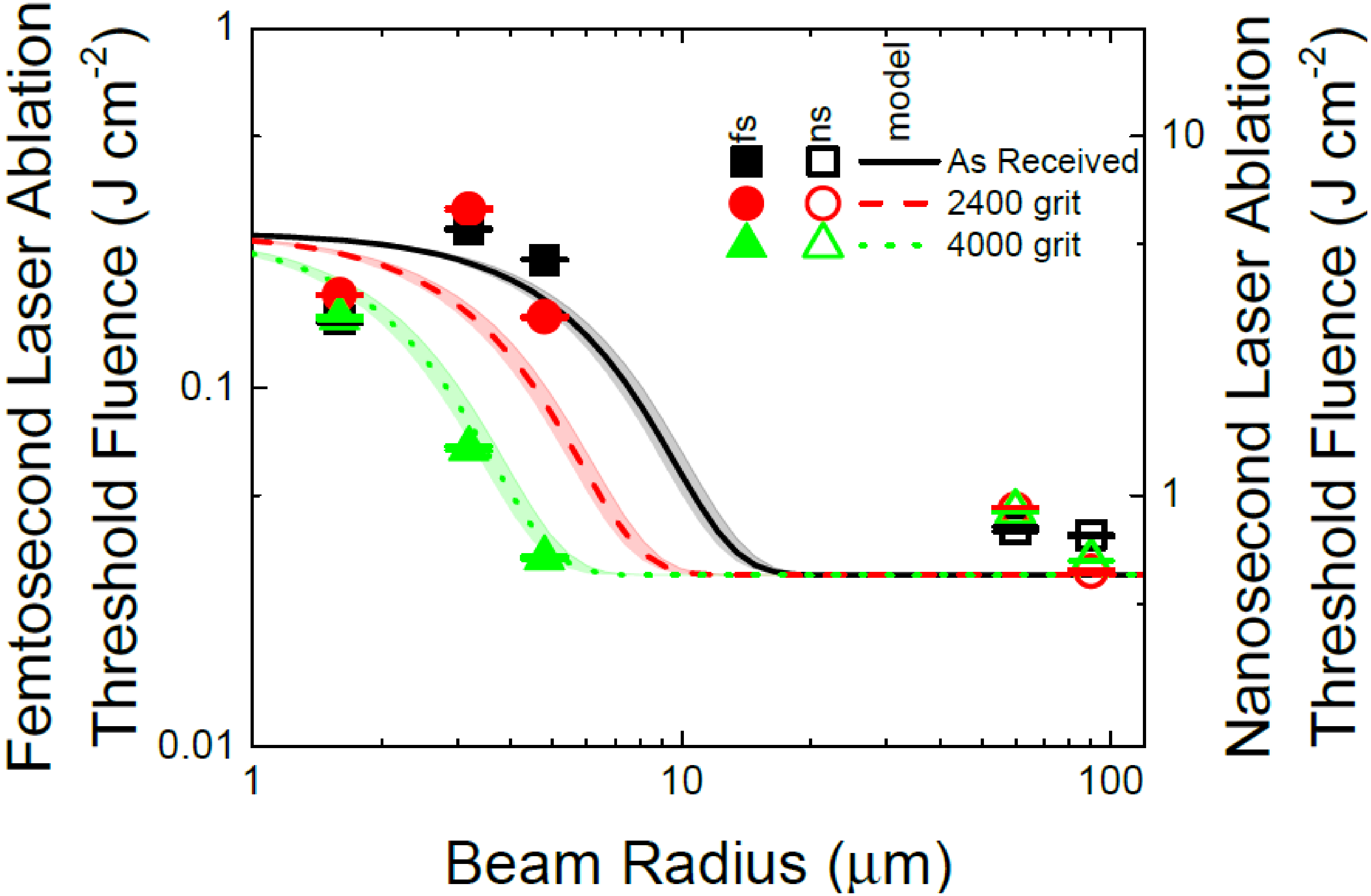

A. Naghilou, O. Armbruster, W. Kautek, App. Surf. Sci. 418 (2017) 487-490

Silicon: Densities of LDDs

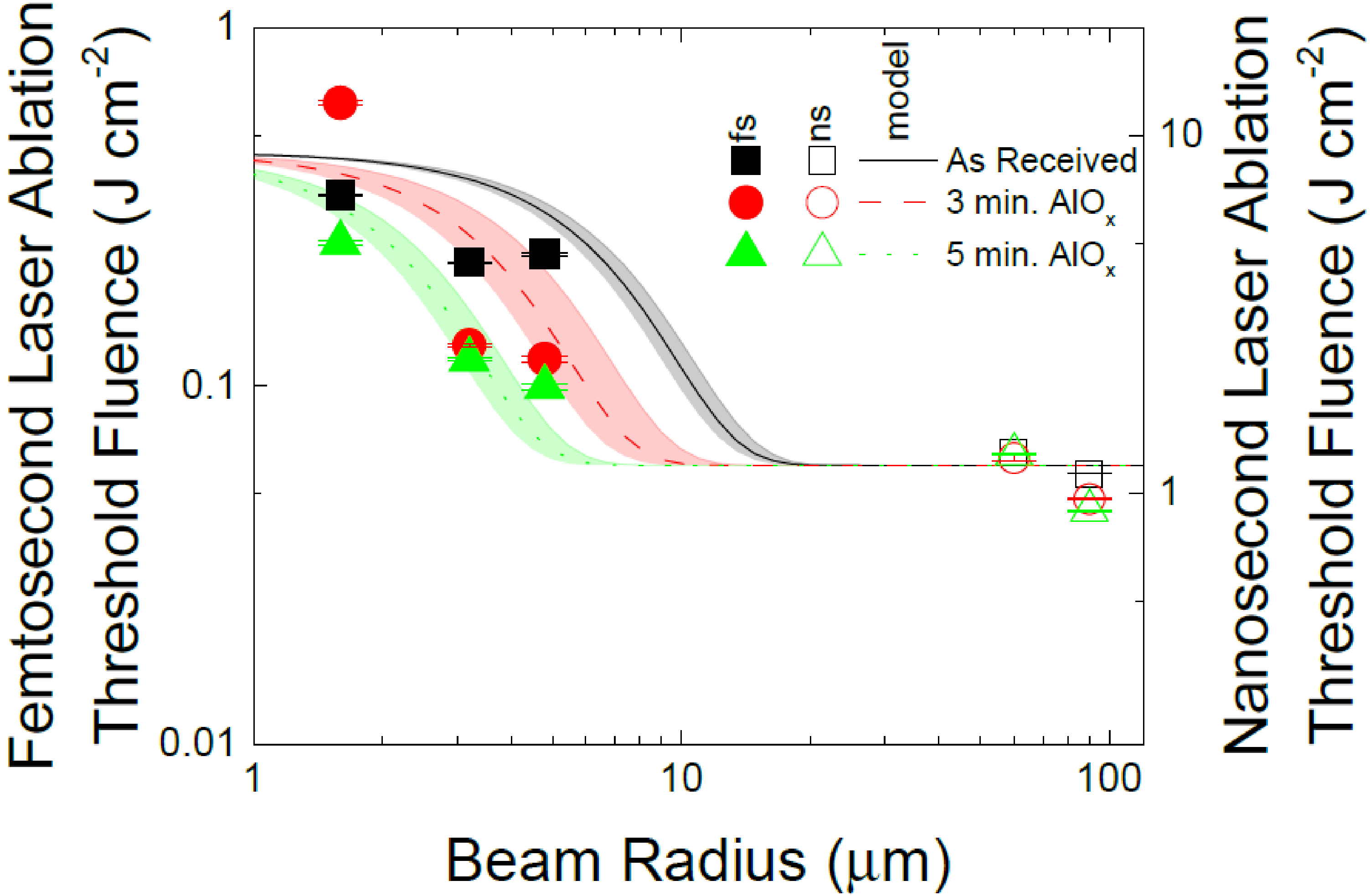

A. Naghilou, O. Armbruster, W. Kautek, App. Surf. Sci. 418 (2017) 487-490

Threshold Fluence and Beam Diameter
Point Defect Model

- Generic model:
  Defect model extended to account for **incubation**
- Large beam radii: spot covers finite number of optically active **low-density defects (LDD)**, separation above the wavelength
- Small beam radii: interaction with optically active **high-density defects (HDD)**, separation below wavelength.
- New model currently being systematically examined with a wide range of solid materials: metals, semiconductors…

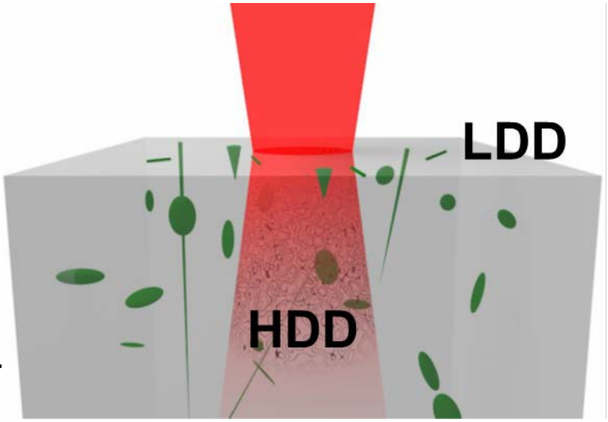

A. Naghilou, O. Armbruster, M. Kitzler, W. Kautek, J. Phys. Chem. C 119 (2015) 22992−22998

Summary:
Non-thermal electronic and structural dynamics in semiconductors and dielectrics

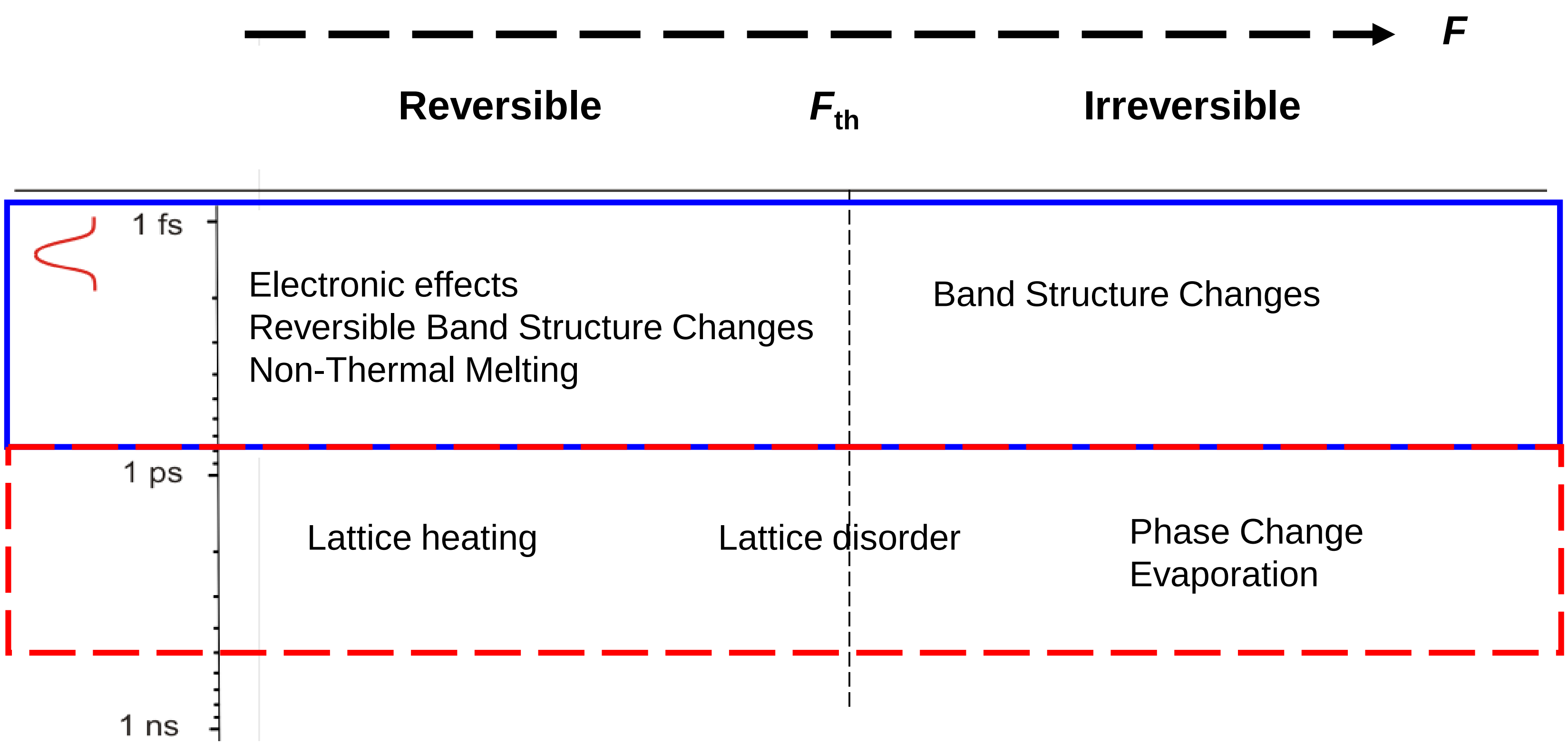

W. Kautek and M. Forster, Springer Series in Materials Science 135 (2010) 89-214.
W. Kautek and O. Armbruster, Springer Series in Materials Science 191 (2014) 43-66.

Outline

- Excitation mechanisms of solids
- Metals: Two-temperature model
  - Fundamentals: Influence of density of states
  - Thin films
  - Metal ablation
  - Hot electron electrochemistry
- Dielectrics: Multiphoton and Avalanche Ionization
  - Dielectric ablation
  - Coulomb explosion
  - Non-thermal melting, X-ray
- Role of Defects
- Applications

Ophthalmic Applications

fs-Laser Applications: 1991

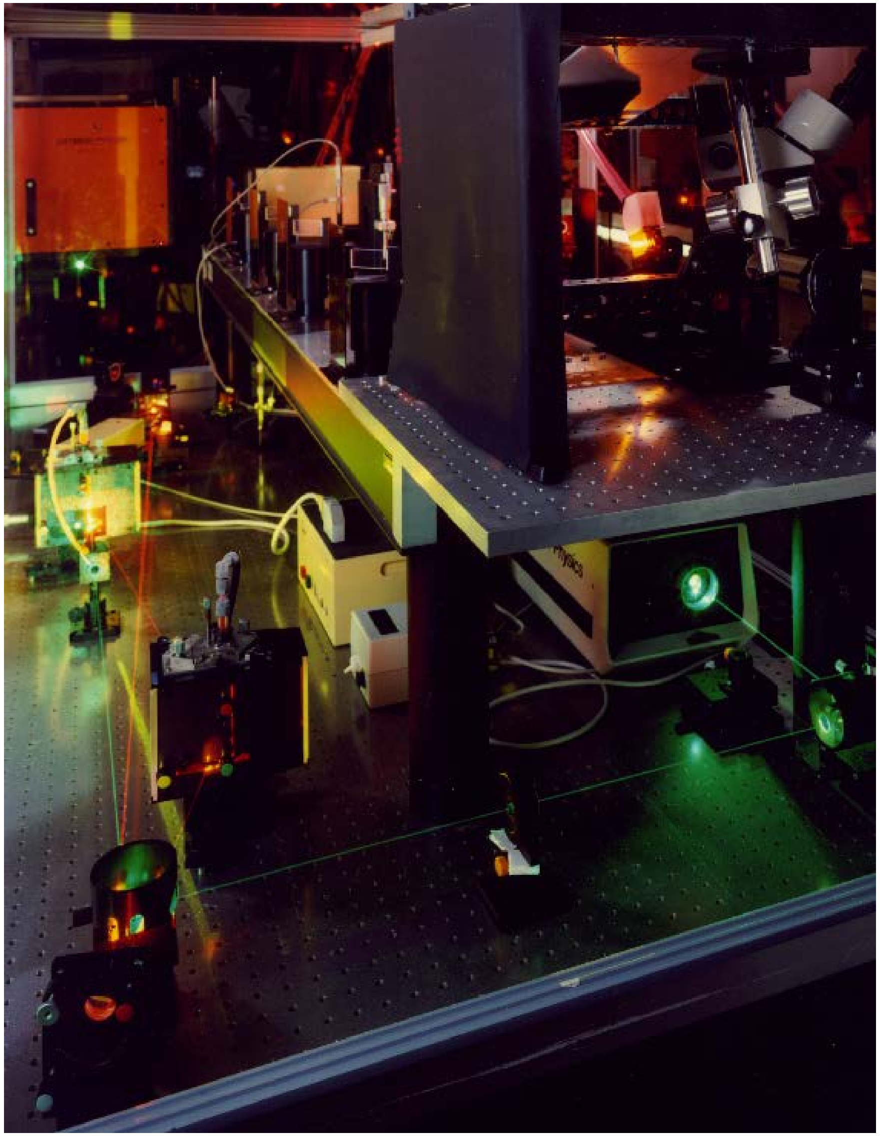

BAM

300 fs (CPM)

632 nm

First 300 fs Laser Ablation of Human Corneas

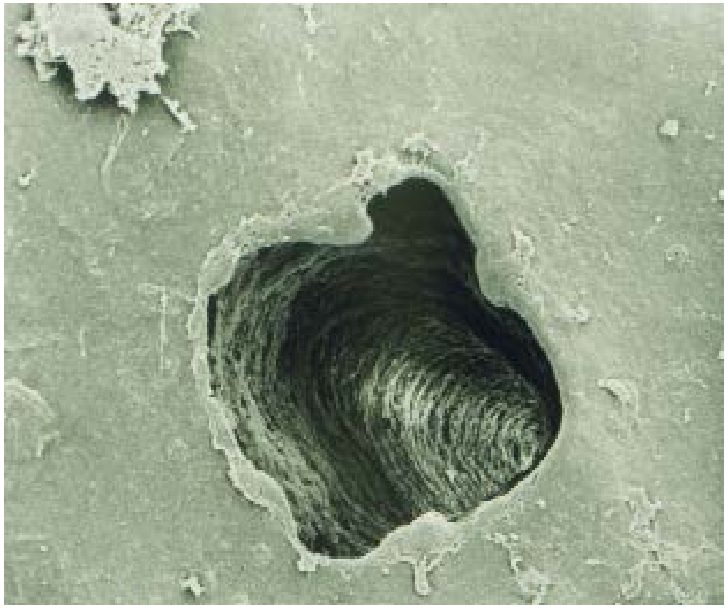

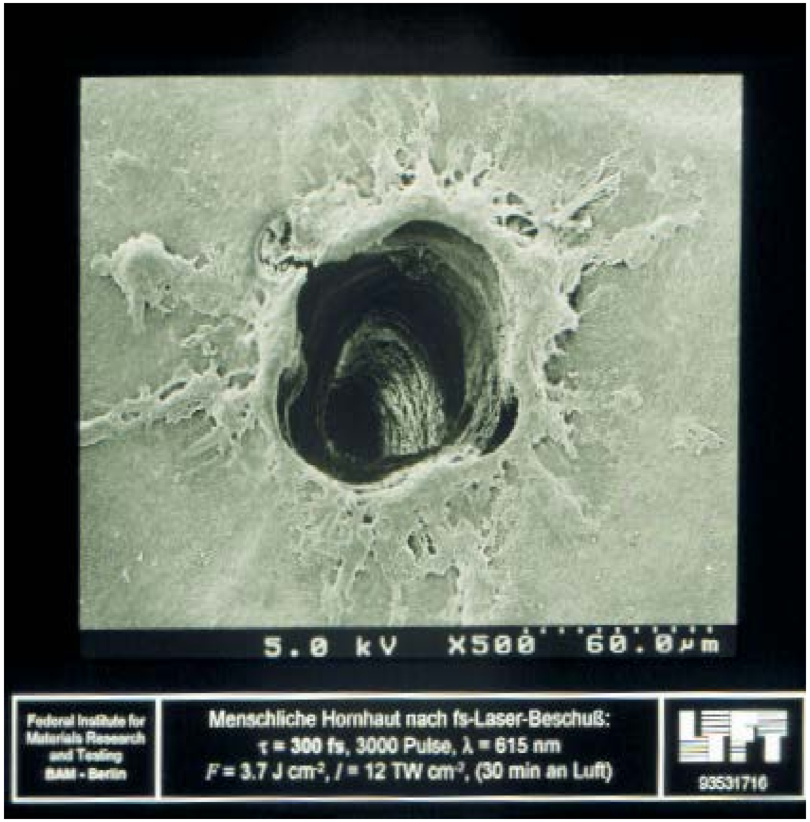

Kautek W., Mitterer S., Krüger J., Husinsky W., Grabner G.:
Femtosecond-Pulse Laser Ablation of Human Corneas
Applied Phys. A 57: 1-6 (1994)

Two Photon Excitation of Collagen

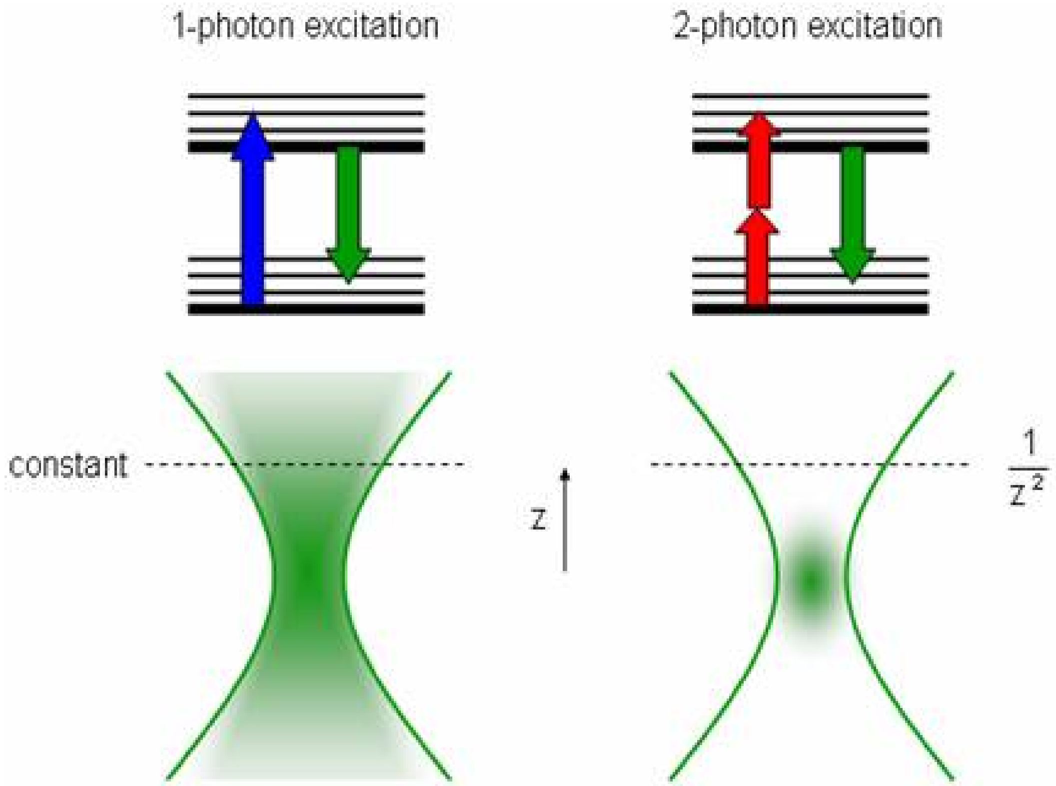

$$\frac{dn_p}{dt} = \delta N F^2$$

According to J. Mertz, Boston University

300 fs Laser Ablation of Human Corneas

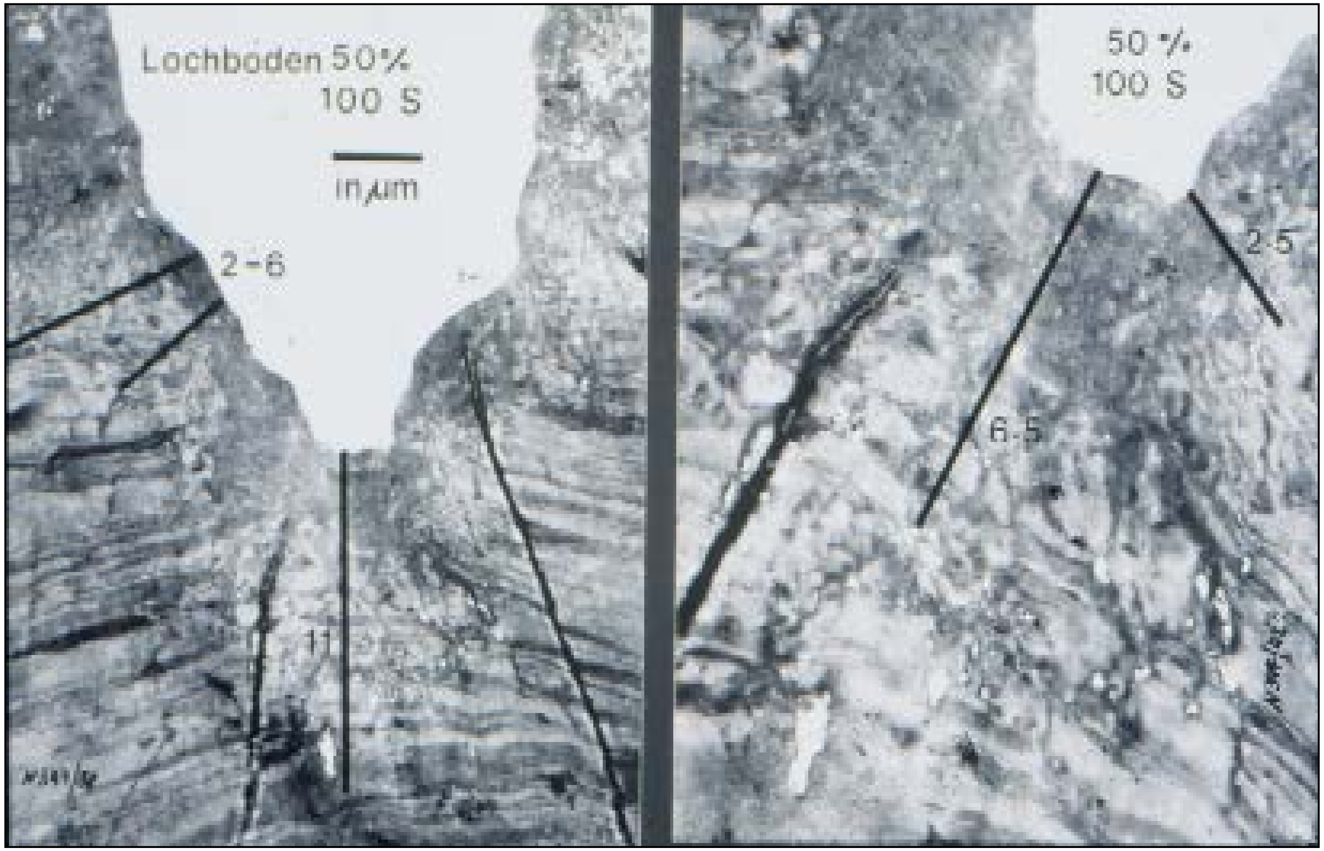

Kautek W., Mitterer S., Krüger J., Husinsky W., Grabner G.:
Femtosecond-Pulse Laser Ablation of Human Corneas
Applied Phys. A 57: 1-6 (1994)

30 fs Laser Ablation of Human Corneas

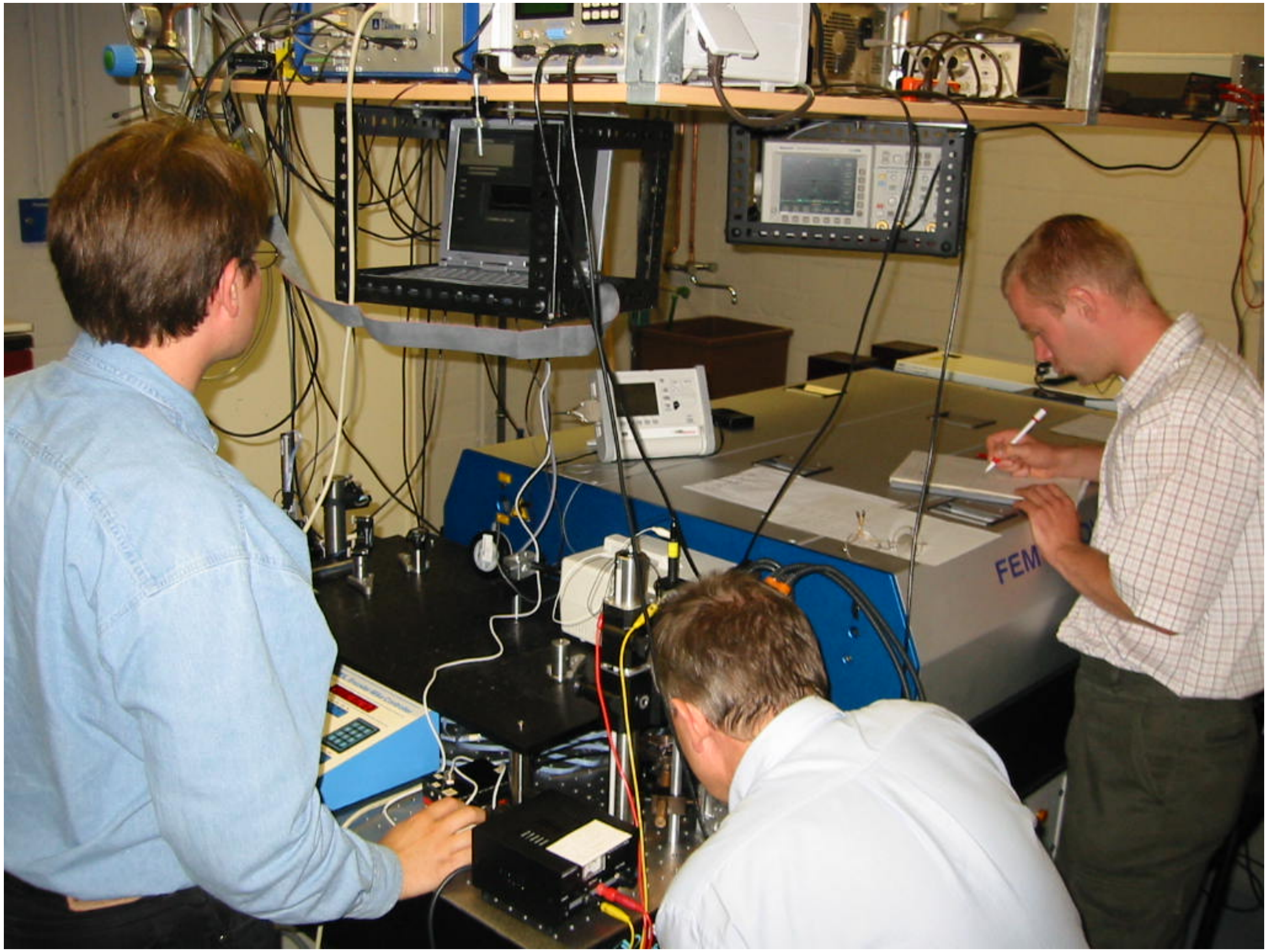

D. Gruber, W. Husinsky, G. Grabner, I. Baumgartner, J. Scholmann, J. Krüger, W. Kautek,
"Laser in Medicine", (Eds.) W. Waidelich, G. Staehler, R. Waidelich, Springer Verlag, Heidelberg 1996, S. 397-400.

G. Grabner, A. Hertwig, S. Martin, J. Krüger, H. Hönigsmann, F. Trautinger, W. Kautek, to be published.

30 fs Laser Corneal Surgery

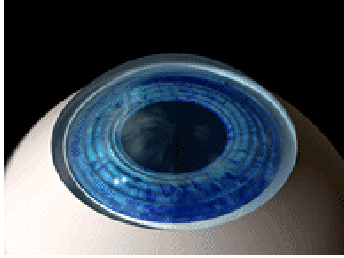

D. Gruber, W. Husinsky, G. Grabner, I. Baumgartner, J. Scholmann, J. Krüger, W. Kautek, "Laser in Medicine", (Eds.) W. Waidelich, G. Staehler, R. Waidelich, Springer Verlag, Heidelberg 1996, S. 397-400.

G. Grabner, A. Hertwig, S. Martin, J. Krüger, H. Hönigsmann, F. Trautinger, W. Kautek, to be published.

Corneal Surgery

Prof. Dr. Günther Grabner
Landesklinik für Augenheilkunde und Optometrie, Salzburg

PARACELSUS
MEDIZINISCHE PRIVATUNIVERSITÄT

fs-LASIK (fs-Laser in situ Keratomileusis)

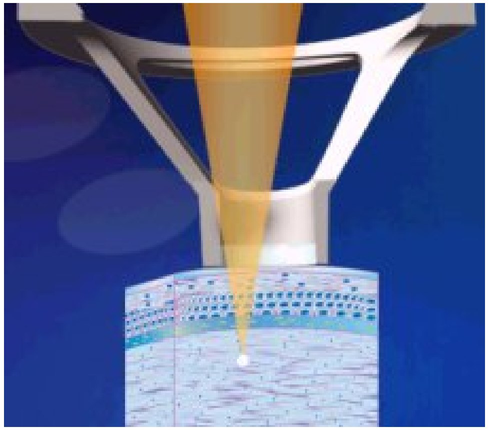

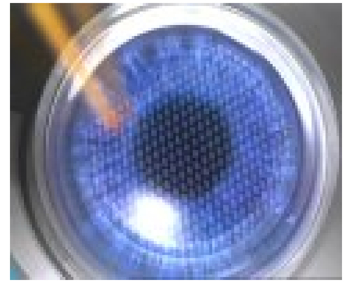

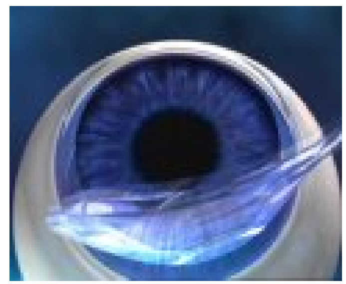

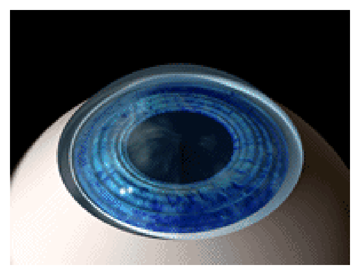

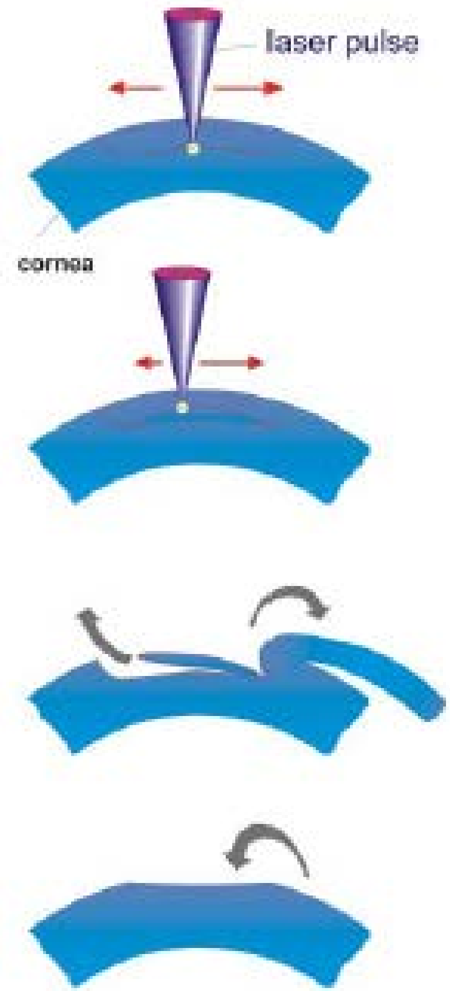

Prof. Dr. Günther Grabner
Landesklinik für Augenheilkunde und Optometrie, Salzburg

Paracelsus
Medizinische Privatuniversität

Nanotechnology Applications

Apertureless scanning near-field optical lithography

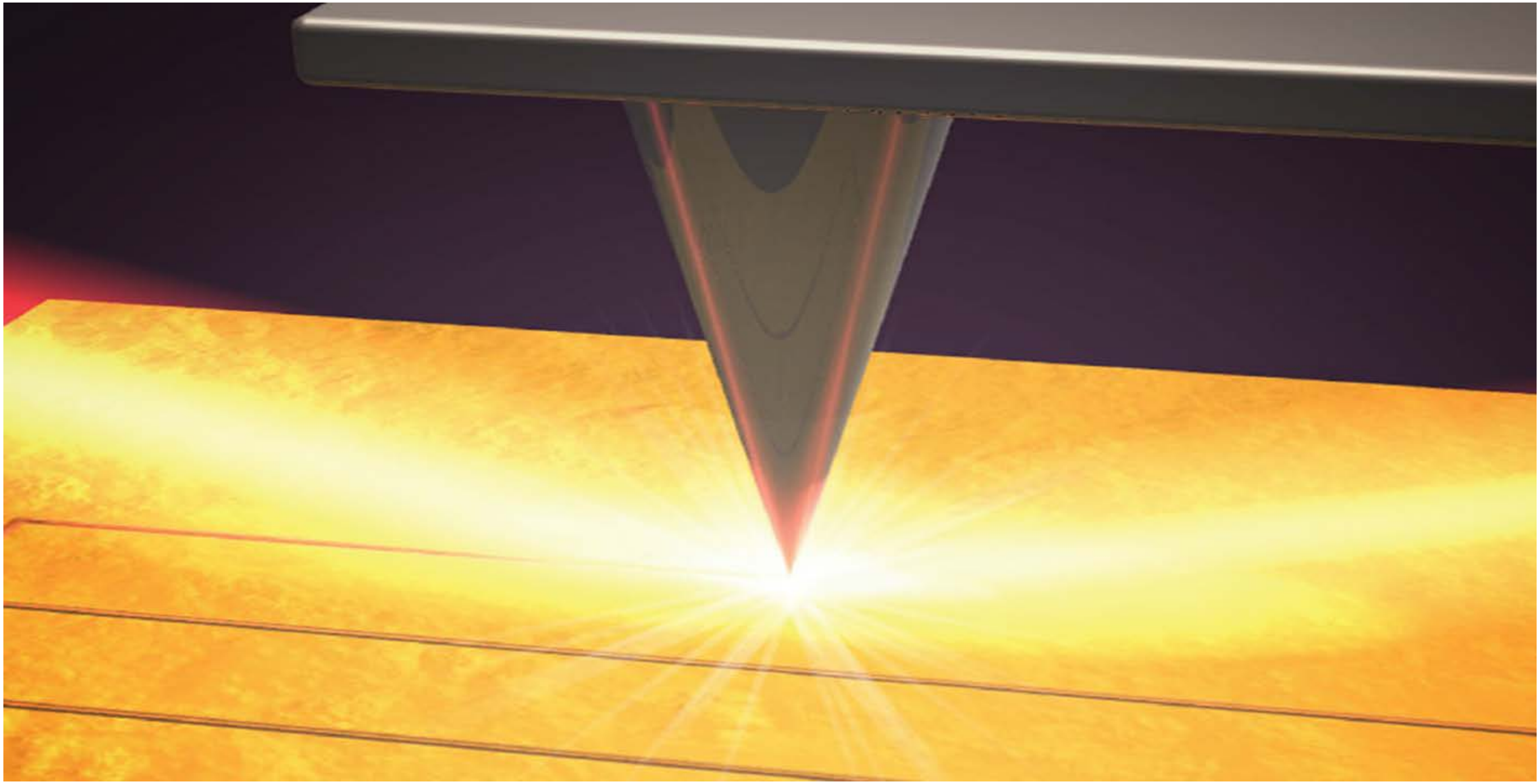

C. Huber, A Trügler, U. Hohenester, Y. Prior, W. Kautek, Phys. Chem. Chem. Phys. 16 (2014) 2289-2296
I. Falcón Casas and W. Kautek, Springer Series in Materials Science 309 (2020) 113-132.

Femtosecond near-field nanolithography: experimental setup

- Yb-doped fiber laser
- 1040 nm wavelength
- 150 fs temporal length
- 50 MHz repetition rate

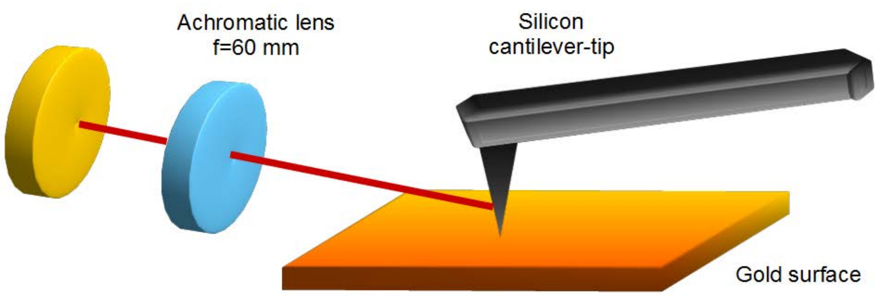

- Polarization control
- Angle of incidence
- Laser focal spot radius ~ 50 µ

I. Falcón Casas, W. Kautek ,Nanomaterials 8 (2018) 20-31
I. Falcón Casas and W. Kautek, Springer Series in Materials Science 309 (2020) 113-132

Near-field simulations

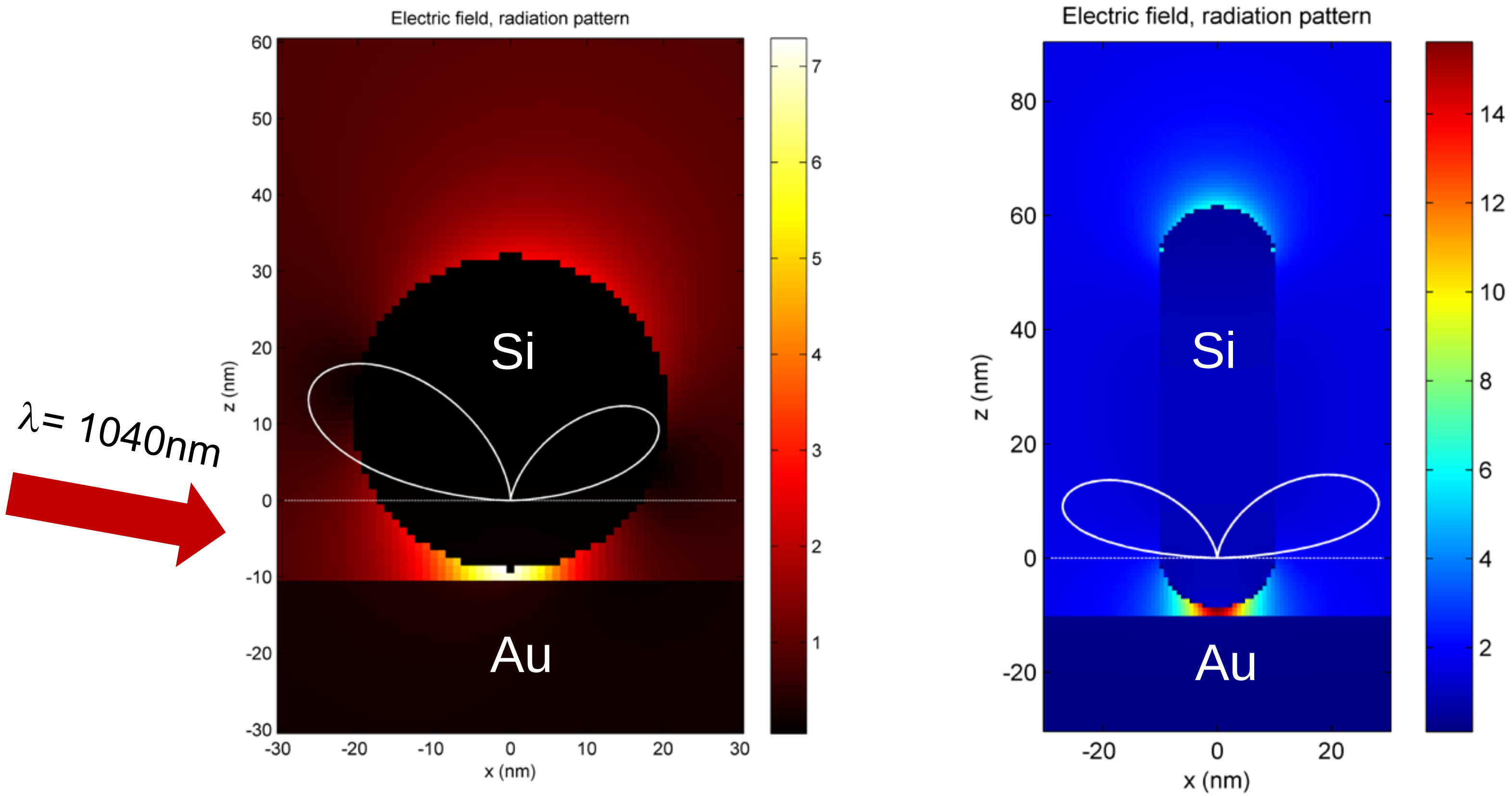

Enhancement factors ~ 10 (sphere), 15-200 (rod)

I. Falcón Casas, W. Kautek, Nanomaterials 8 (2018) 536

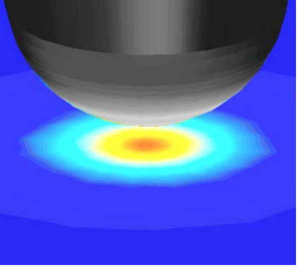

Boundary Element Method: Field enhancement study

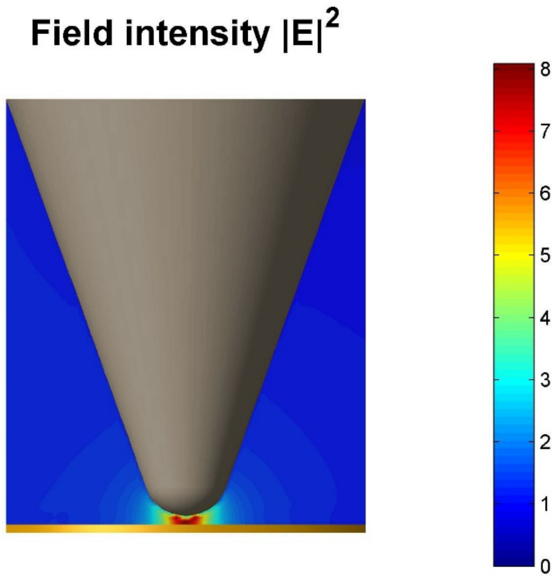

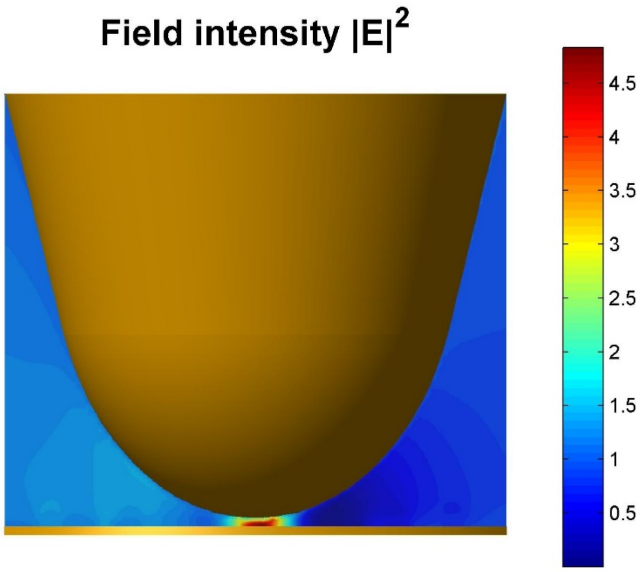

Field enhancement of a **silicon** tip with a radius of **curvature of 10 nm**

Field enhancement of a **gold-coated tip** with a radius of **curvature of 65 nm**

C. Huber, A Trügler, U. Hohenester, Y. Prior, W. Kautek, Phys. Chem. Chem. Phys. 16 (2014) 2289-2296

Theoretical Investigation
Thermo-mechanical study

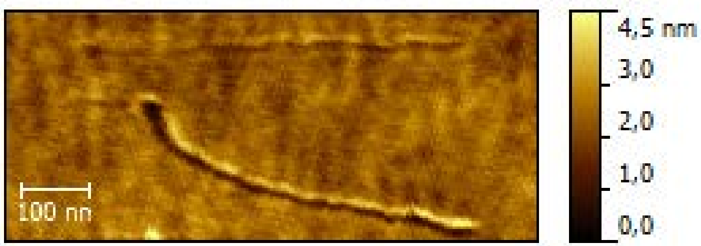

Experimental verification of the tip displacement due to laser heating

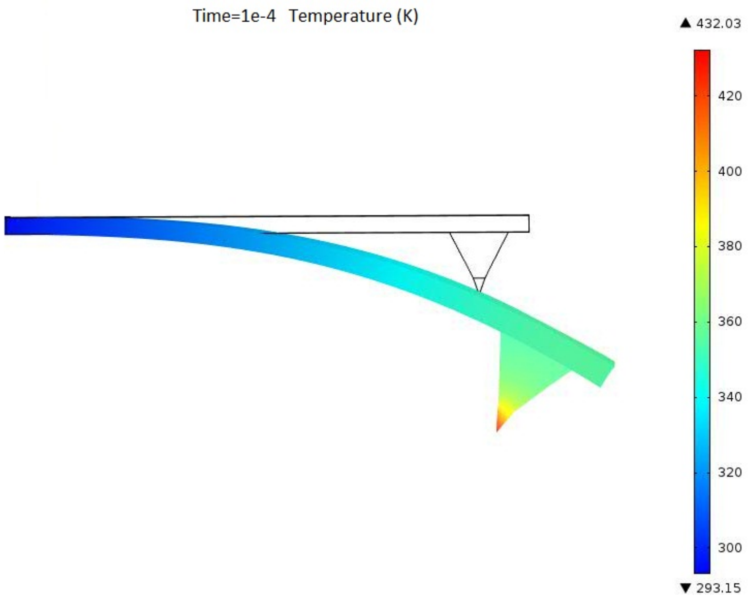

Software package: COMSOL Multiphysics 4.1

Tip displacement (x 1000)
with reflective coating
after 0.1 ms at 432 K.

C. Huber, A Trügler, U. Hohenester, Y. Prior, W. Kautek, Phys. Chem. Chem. Phys. 16 (2014) 2289-2296

Apertureless scanning near-field optical lithography

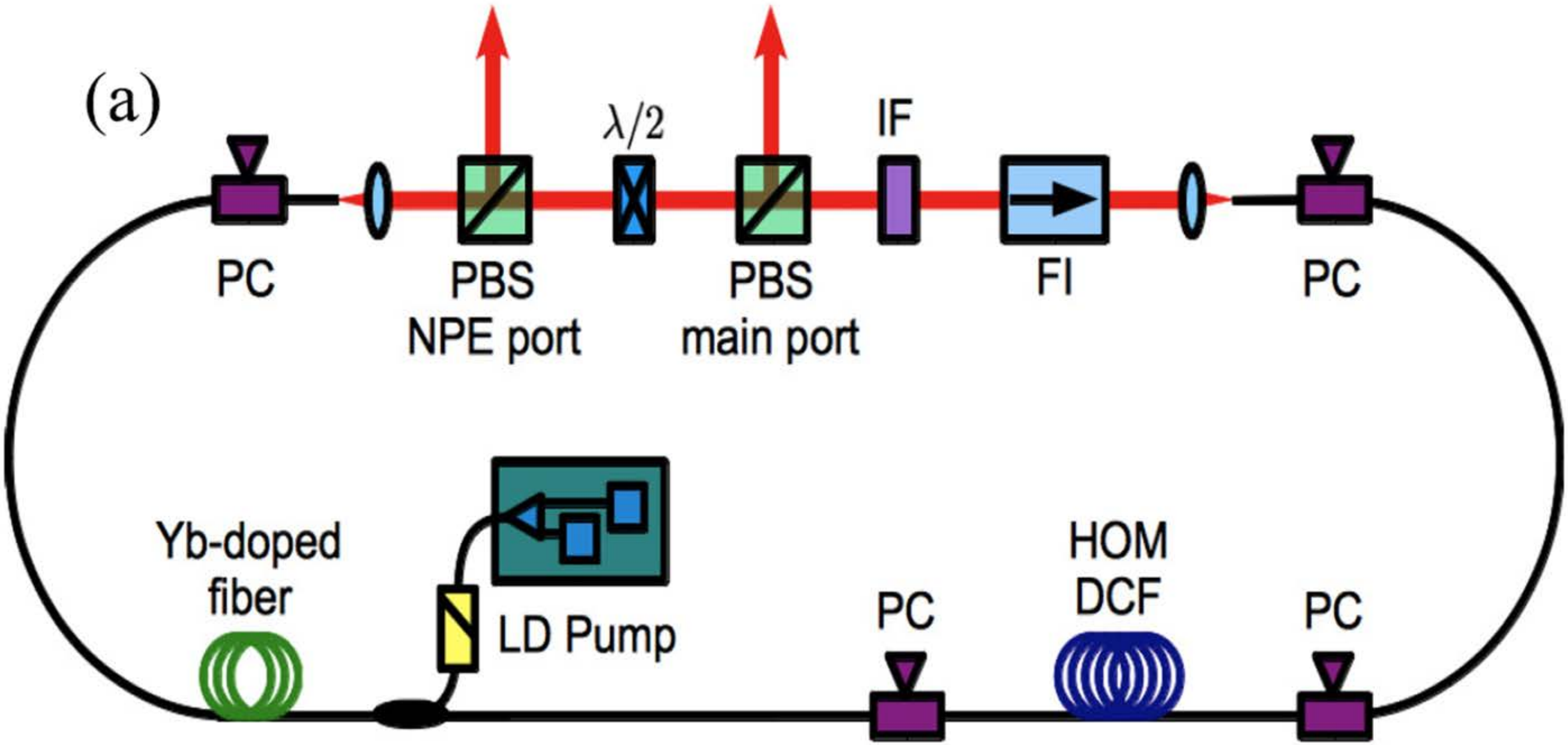

Fiber laser cavity. PC: polarization controller, HOM: higher-order mode,
FI: Faraday isolator, IF: 10nm FWHM interference filter, PBS: polarizer beamsplitter, LD: laser diode.

A.J. Verhoef, L. Zhu, S. Møller Israelsen, L. Grüner-Nielsen, A. Unterhuber,
W. Kautek, K. Rottwitt, A. Baltuška, and A. Fernández, Optics Express 23 (2015) 36139-36145

Apertureless scanning near-field optical lithography

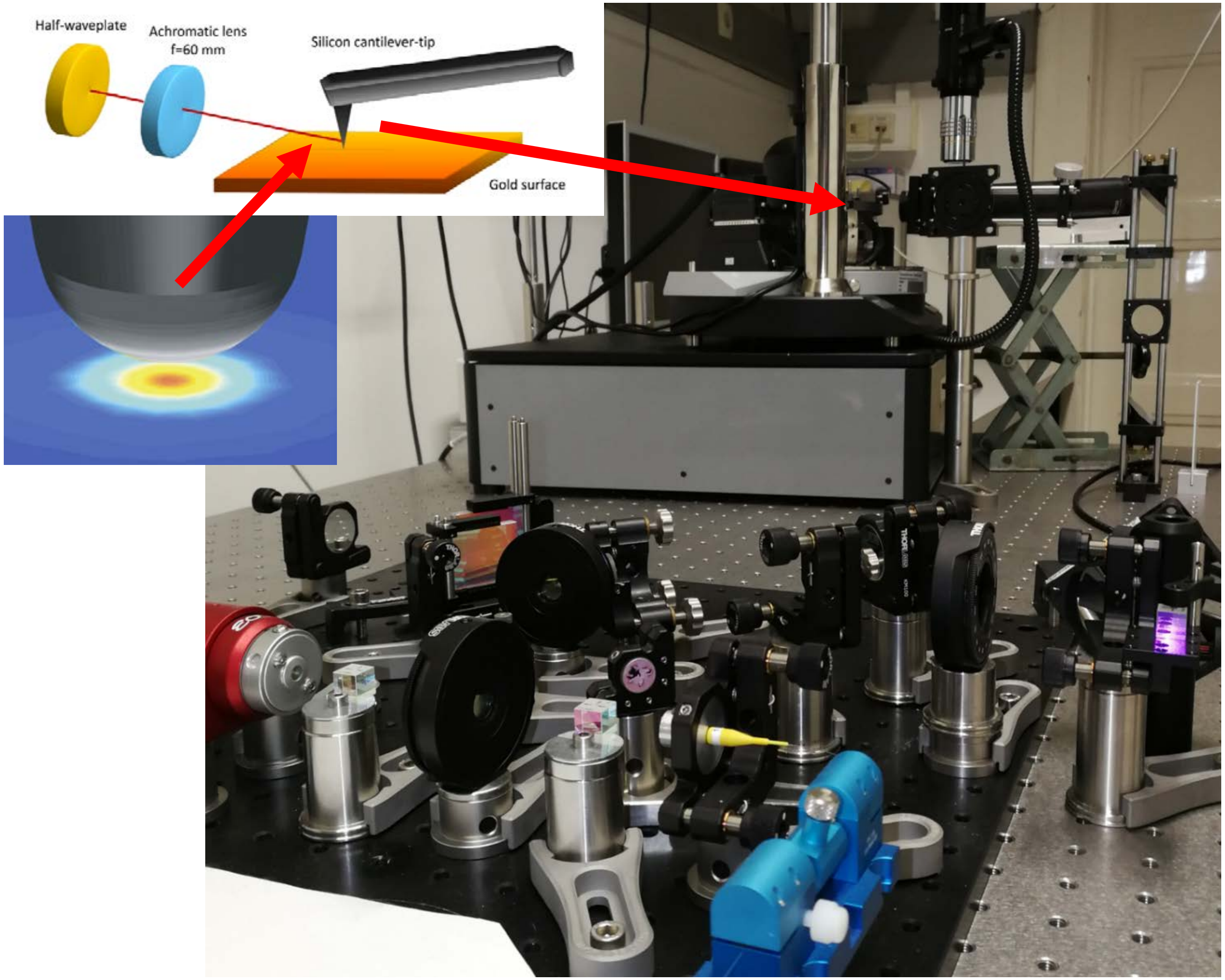

I. Falcón Casas, W. Kautek ,Nanomaterials 8 (2018) 20-31
I. Falcón Casas and W. Kautek, Springer Series in Materials Science 309 (2020) 113-132

Apertureless scanning near-field optical lithography: Nanolithography on Au nanofilms

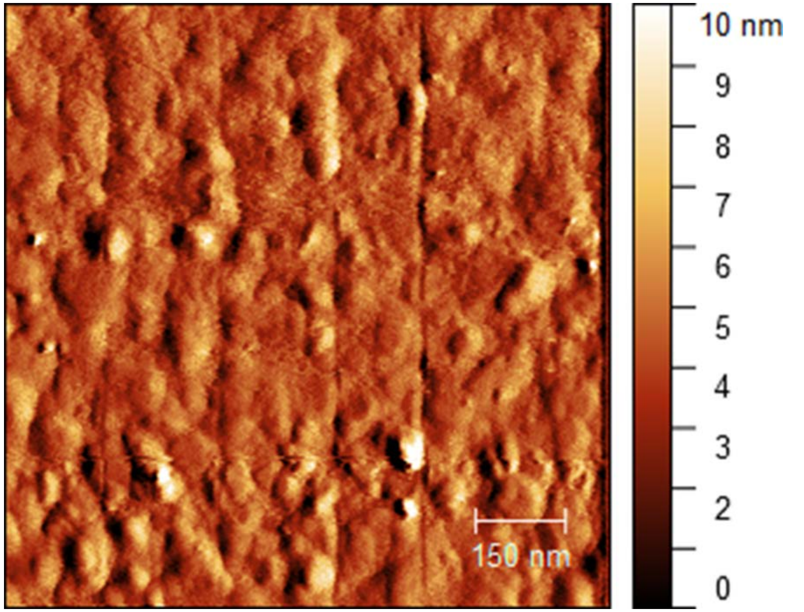

Laser Power	Width	Depth
3 mW	12 nm	0.4 nm
12 mW	15 nm	0.5 nm
25 mW	16 nm	0.7 nm
35 mW	16 nm	1.5 nm

I. Falcón Casas, W. Kautek ,Nanomaterials 8 (2018) 20-31
I. Falcón Casas and W. Kautek, Springer Series in Materials Science 309 (2020) 113-132

Below far-field threshold fluence

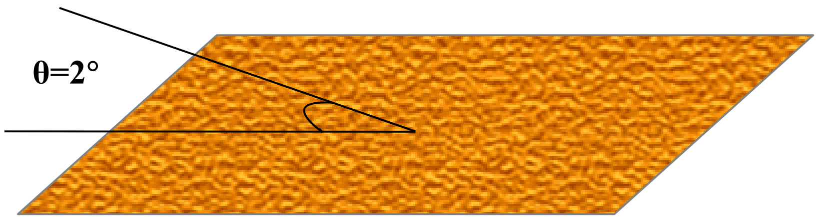

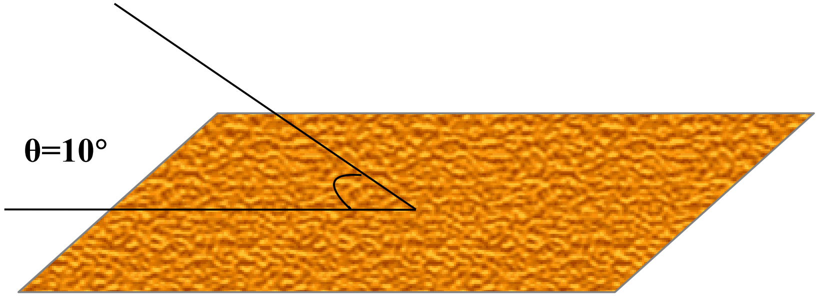

Angle of incidence θ	$I_0 \cos^2(\theta) / I_0$	F (mJ/cm^2)	F(x°)/F (2°)	Near-field modification	Far-field modification
2°	0.035	0.008	1	X	-
10°	0.174	0.038	5	-	X
90°	1	0.219	29	-	X

I. Falcón Casas, W. Kautek, Nanomaterials 8 (2018) 536

Boundary Element Method: Field enhancement vs. Polarisation angle

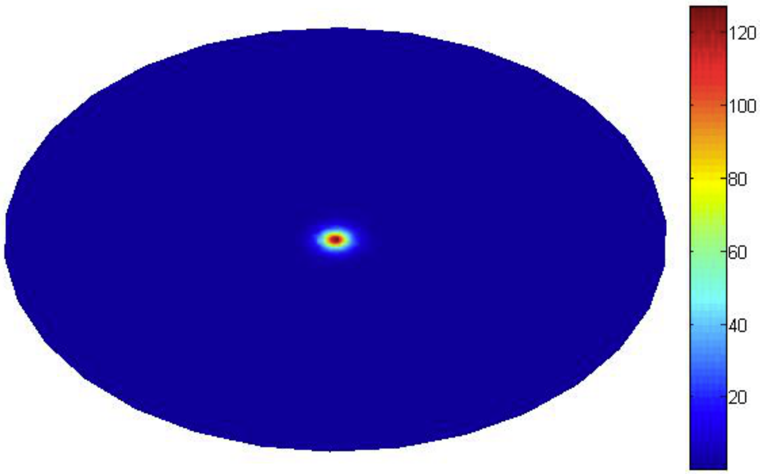

p-polarization

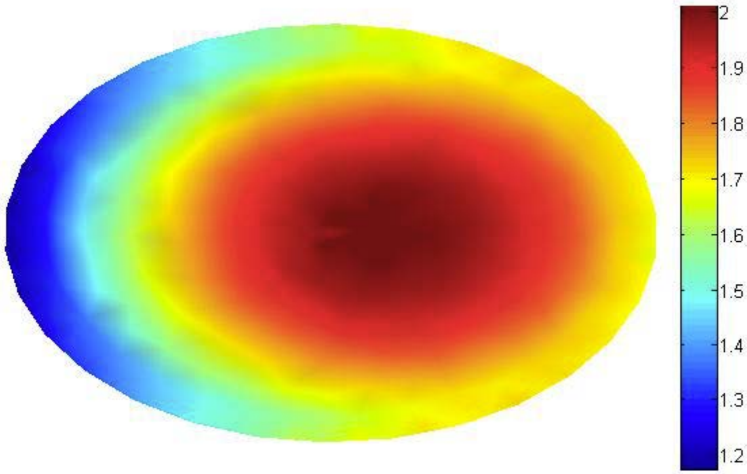

s-polarization

I. Falcon Casas and W. Kautek, in *Laser micro-nano-nanomanufacturing and 3D microprinting*, Springer (2019), in print

Boundary Element Method: Field enhancement vs. Polarisation angle

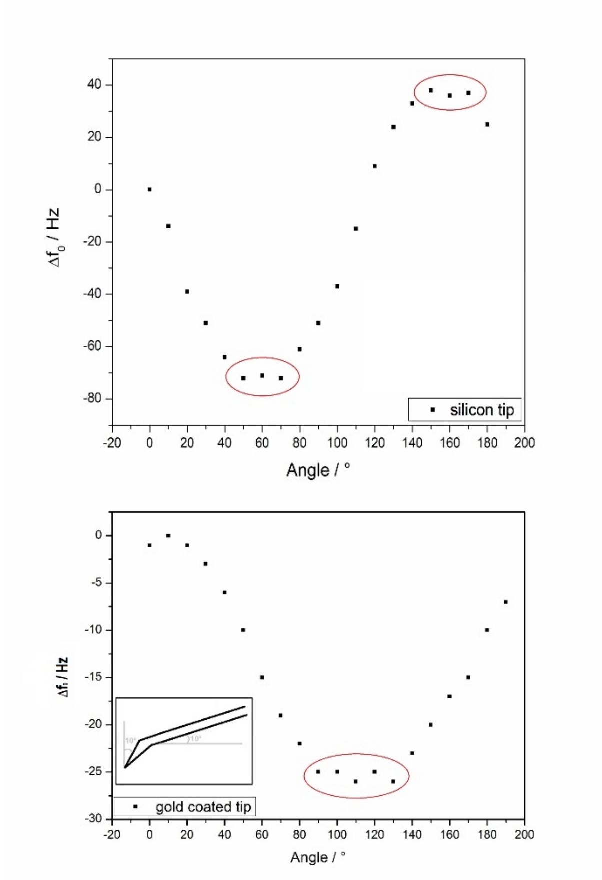

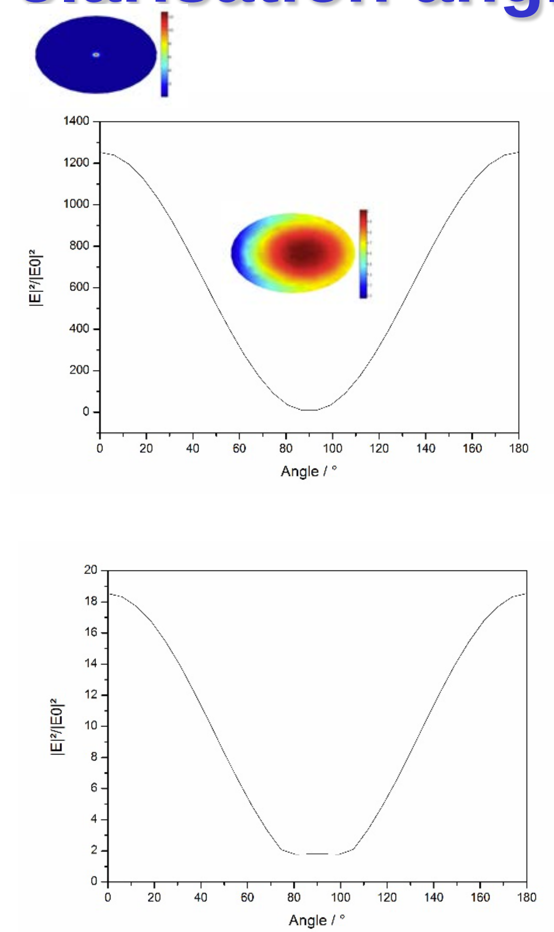

Experimental results of the polarisation angle dependency of a silicon tip and a gold coated tip

Theoretical results of the polarisation angle dependency of a silicon tip with and without substrate

C. Huber, A Trügler, U. Hohenester, Y. Prior, W. Kautek, Phys. Chem. Chem. Phys. 16 (2014) 2289-2296
I. Falcón Casas and W. Kautek, Springer Series in Materials Science 309 (2020) 113-132

Mechanical scratching

MEH-PPV, Poly[2-methoxy-5-(2-ethylhexyloxy)-1,4-phenylenevinylene]

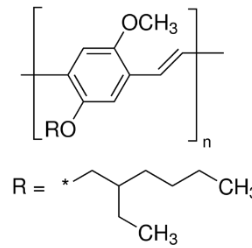

Cantilever
with **high spring constant**:
k = 5 N/m (vs. 0.4 N/m in aSNOM)

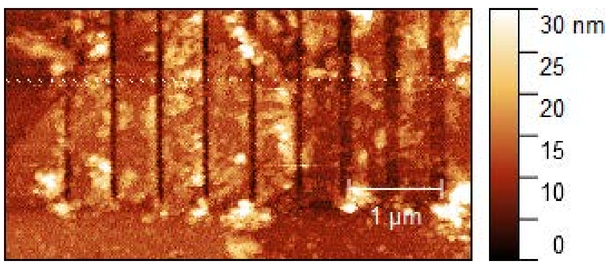

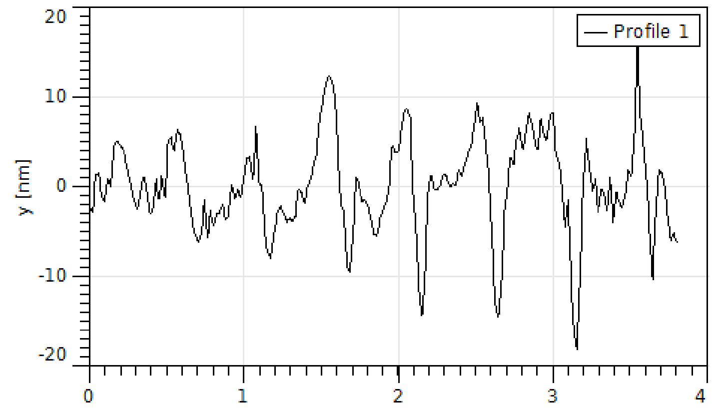

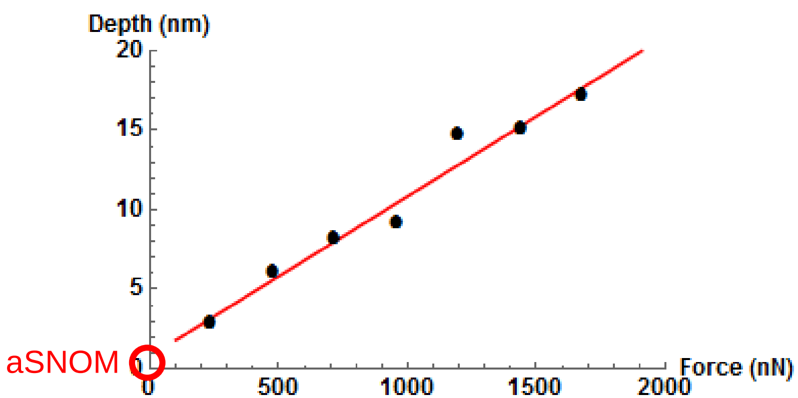

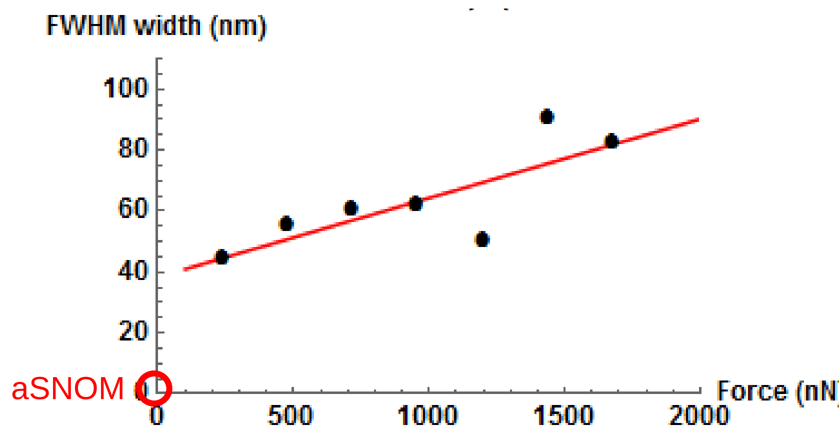

I. Falcon Casas and W. Kautek, Springer Series in Materials Science 309 (2020) 113-132

Nanolithography depending on intensity: Photoresist (AZ4620)

p-polarization

s-polarization

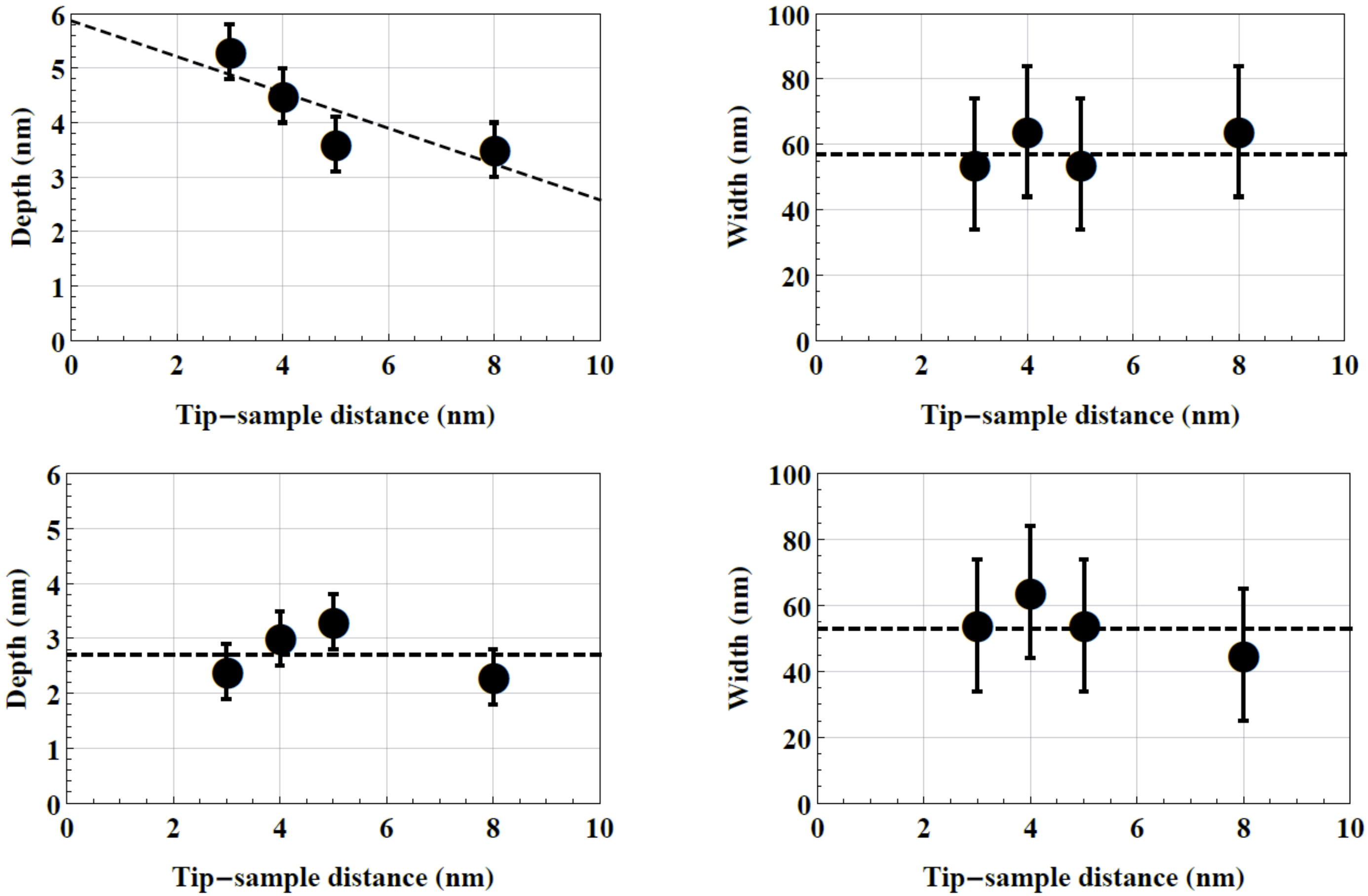

I. Falcon Casas and W. Kautek, Springer Series in Materials Science 309 (2020) 113-132

Laser Generation of NPs:
Breast Cancer Diagnosis

Breast Cancer Diagnosis

© Siemens Healthcare GmbH

- X-ray Mammography
- Magnetic Resonance Imaging (MRI)
- Computer X-ray Tomography (CT)
- Ultrasonography (US)
- Positron Emission Tomography (PET)

Breast Cancer Diagnosis

- X-ray Mammography

- Magnetic Resonance Imaging (MRI)
- Computer X-ray Tomography (CT)
- Ultrasonography (US)
- Positron Emission Tomography (PET)

Breast Cancer Diagnosis

- X-ray Mammography

- Magnetic Resonance Imaging (MRI)
- Computer X-ray Tomography (CT)
- Ultrasonography (US)
- Positron Emission Tomography (PET)

Breast MRI

Contrast-enhanced Magnetic Resonance Imaging (CEMRI): **Gadolinium III chelates** as CAs.

Motivation

Au and Ag NPs, quantum dots, carbon nanotubes, hollow polymer NPs loaded with dyes and fluorophores

Polymer NPs, porous NPs and liposomes loaded with radioactive tracers

Commercial preparations of NPs of **superparamagnetic iron oxide**

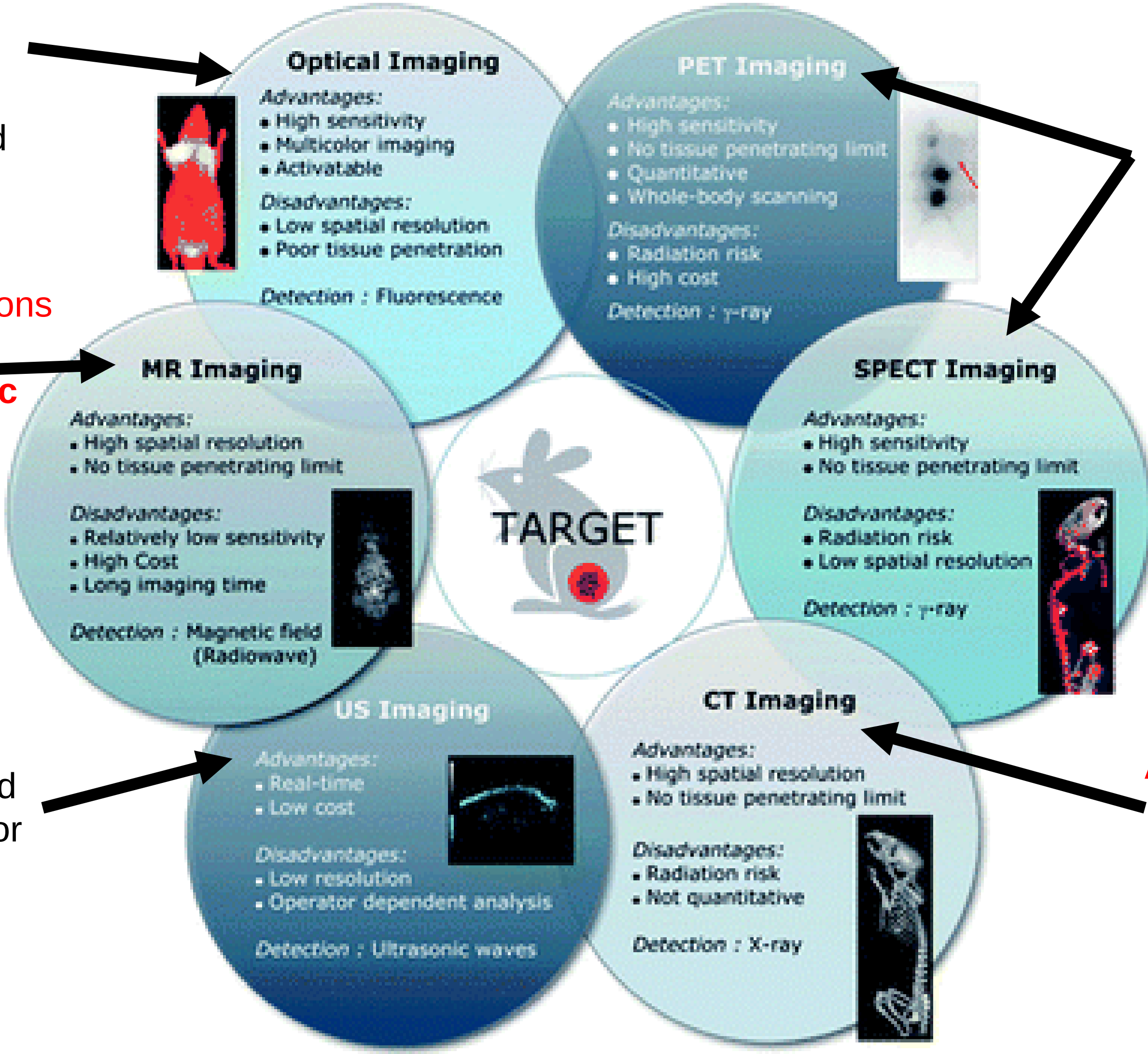

Commercial Microparticles (microbubbles) for echography image and commercial Au NPs for photoacoustic image

Commercial **Au NPs** and NPs of elements with **high atomic number (Bi, Ta, Yb)**

Generation of nanoparticles from binary oxide ceramics by laser ablation in liquid

"Laser ablation synthesis in solutions (LASiS)"

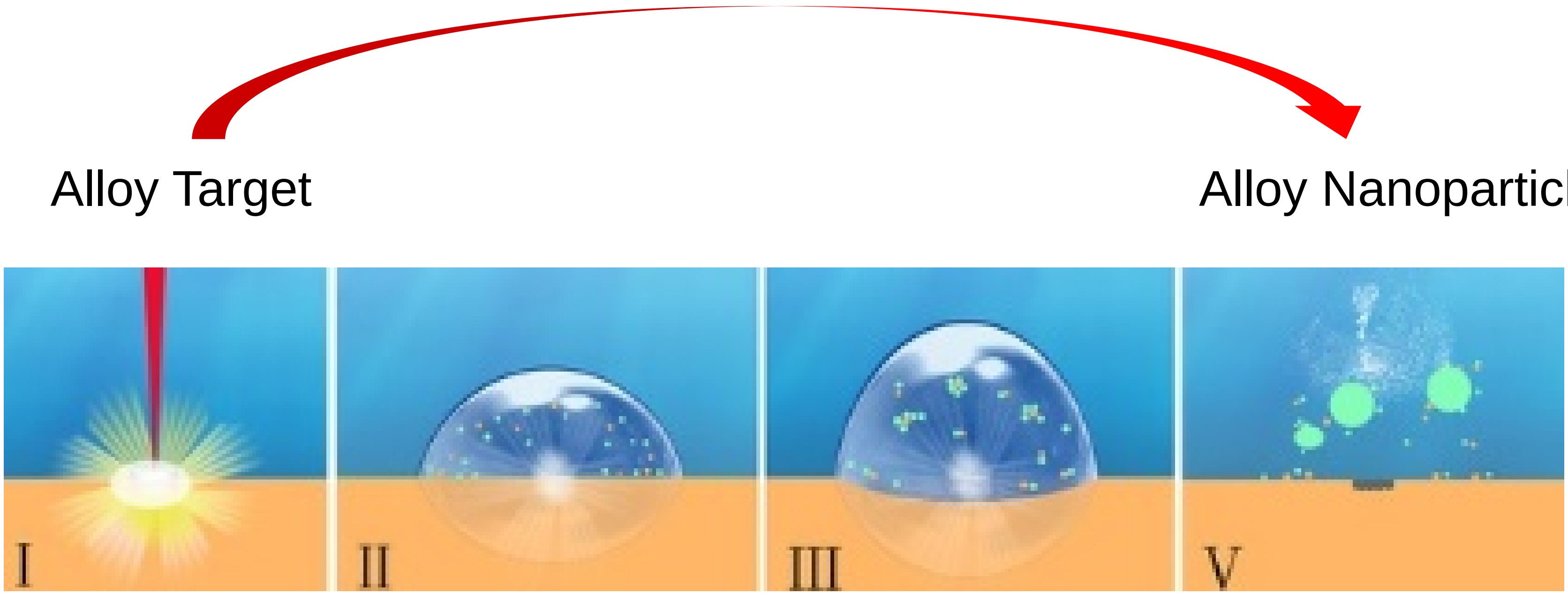

Figure from Stephan Barcikowski

Before Cavitation Impact in liquid: Primary and secondary nanoparticle

400 Jm^{-2}

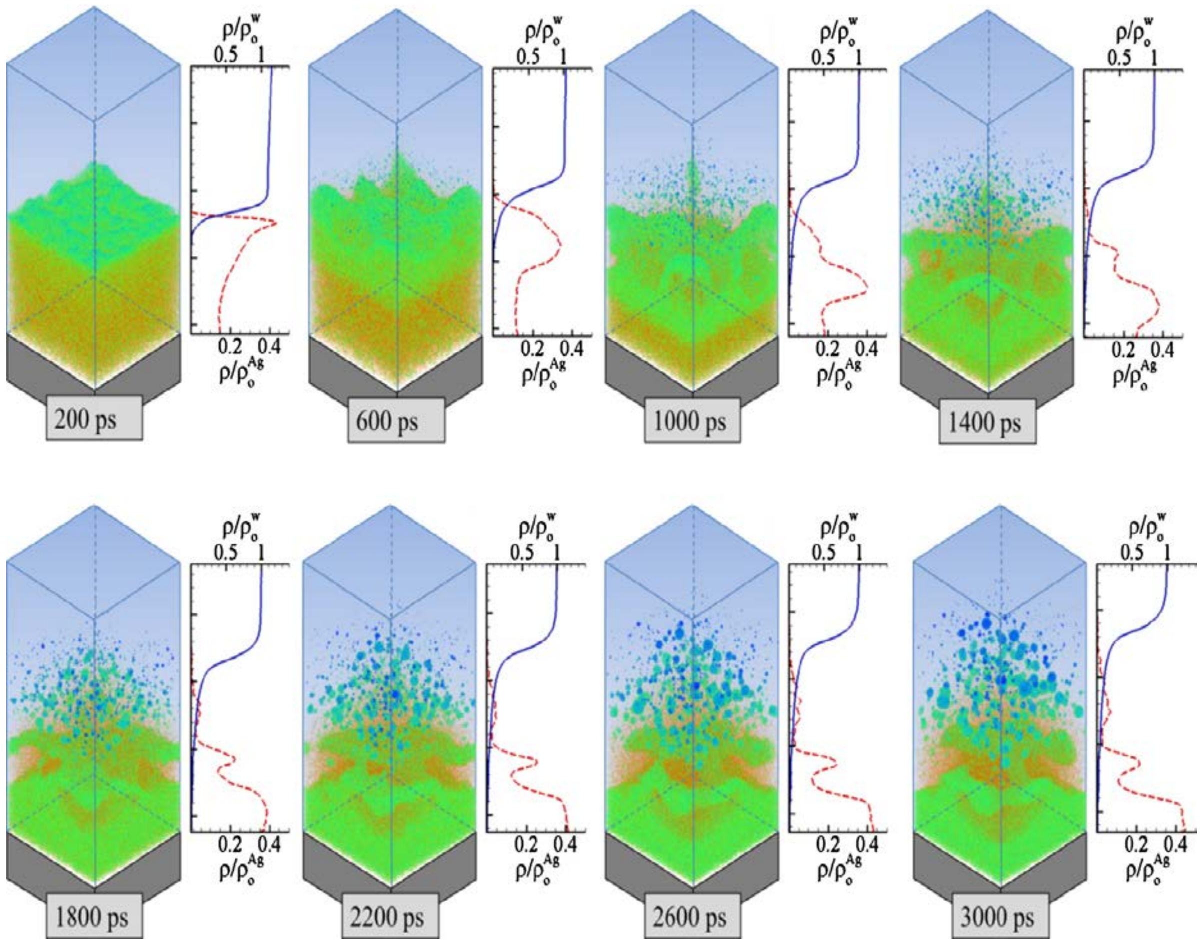

Ag thin film illuminated by 40 fs laser pulse

C.-Y. Shih, C. Wu, M.V. Shugaev, L.V. Zhigilei, Journal of Colloid and Interface Science, DOI http://dx.doi.org/10.1016/j.jcis.2016.10.029 (2017)

High power femtosecond laser pulse oscillator

Modified Femtosource XL, Femtolasers Produktions: GmbH, 60 fs, 800 nm, 11 MHz

Laser ablation synthesis in solutions (LASiS) of binary oxide ceramics in water and ethanol

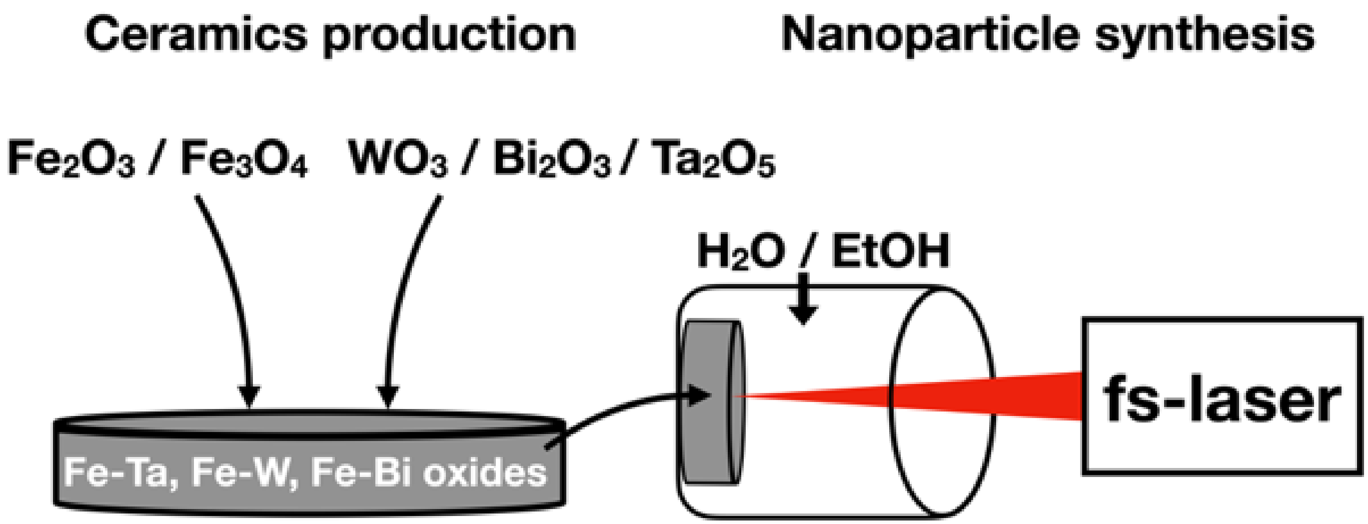

A. Naghilou, O. Bomati-Miguel, A. Subotic, R. Lahoz, M. Kitzler-Zeiler, C. Radtke, M.A. Rodríguez, W. Kautek, Ceram. Int. 47 (2021) 29363-29370

Bulk ceramic production

- Ceramic reaction-sintering method
- Iron oxide powders mixed with Ta_2O_5, WO_3, Bi_2O_3
  Stoichiometric to obtain $FeTaO_4$, Fe_2WO_6, $FeBiO_3$
- Attrition milling for 2 h
  (Y_2O_3 stabilized ZrO_2, 1 mm diameter balls)
- Cylindrical bulk samples by biaxial pressing at 100 MPa
  (10 mm in height and 15 mm in diameter).
- 10ºC/min heating rate and 2 h at
  1400ºC Fe-Ta
  1050ºC Fe-W
  750ºC Fe-Bi

A. Naghilou, O. Bomati-Miguel, A. Subotic, R. Lahoz, M. Kitzler-Zeiler, C. Radtke, M.A. Rodríguez, W. Kautek, Ceram. Int. 47 (2021) 29363-29370

XRD and EDX analysis of binary metal oxide target ceramics

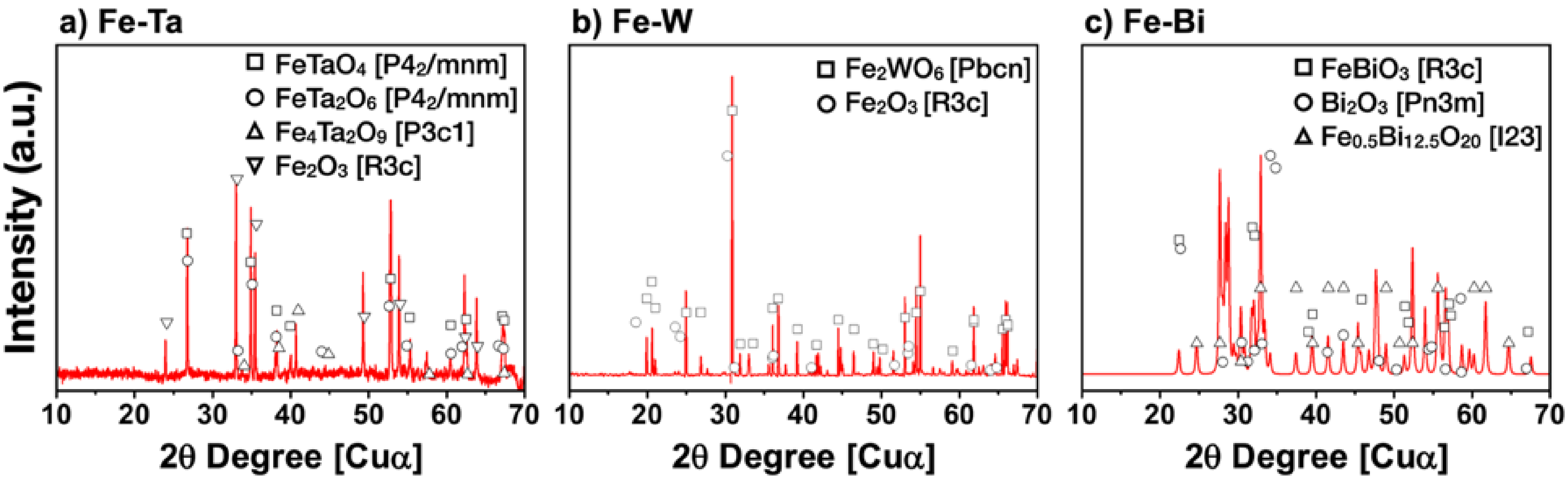

	Fe (at.%)	O (at.%)	Ta (at.%)	W (at.%)	Bi (at.%)	ME/Fe	O/(ME+Fe)
Fe-Ta	11±3	70±2	18±2	-	-	1.7±0.4	2.4±0.3
Fe-W	19±2	70±3	-	11±1	-	0.6±0.1	2.4±0.2
Fe-Bi	7±3	82±7	-	-	10±4	1.4±0.8	4.7±1.4

A. Naghilou, O. Bomati-Miguel, A. Subotic, R. Lahoz, M. Kitzler-Zeiler, C. Radtke, M.A. Rodríguez, W. Kautek, Ceram. Int. 47 (2021) 29363-29370

Me-Oxide Alloy Targets

$FeTaO_4$

Fe_2WO_6

$FeBiO_3$

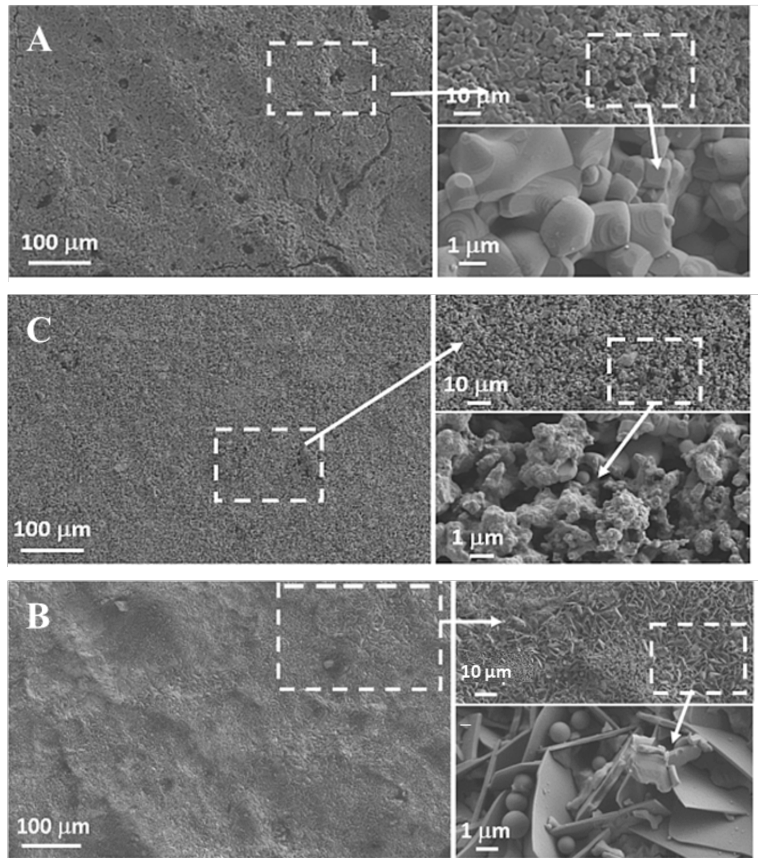

	Fe(%)	O(%)	Ta(%)	W(%)	Bi (%)	Me/Fe		O/(Me+Fe)	
							Formula		Formula
$FeTaO_4$	10.32	70.36	18.32	-	-	1.8	1.0	2.5	2.0
Fe_2WO_6	18.74	70.39	-	10.9	-	0.6	0.5	2.4	2.0
$FeBiO_3$	6.48	82.29	-	-	9.97	1.5	1.0	5	1.5

A. Naghilou, O. Bomati-Miguel,
A. Subotic, R. Lahoz, M. Kitzler-Zeiler,
C. Radtke, M.A. Rodríguez, W. Kautek,
Ceram. Int. 47 (2021) 29363-29370

Squared diameters of ablated areas fitted with D^2-ln$F$

$$D^2 = 2w_0^2 \ln \frac{F_0}{F_{\mathrm{th}}}$$

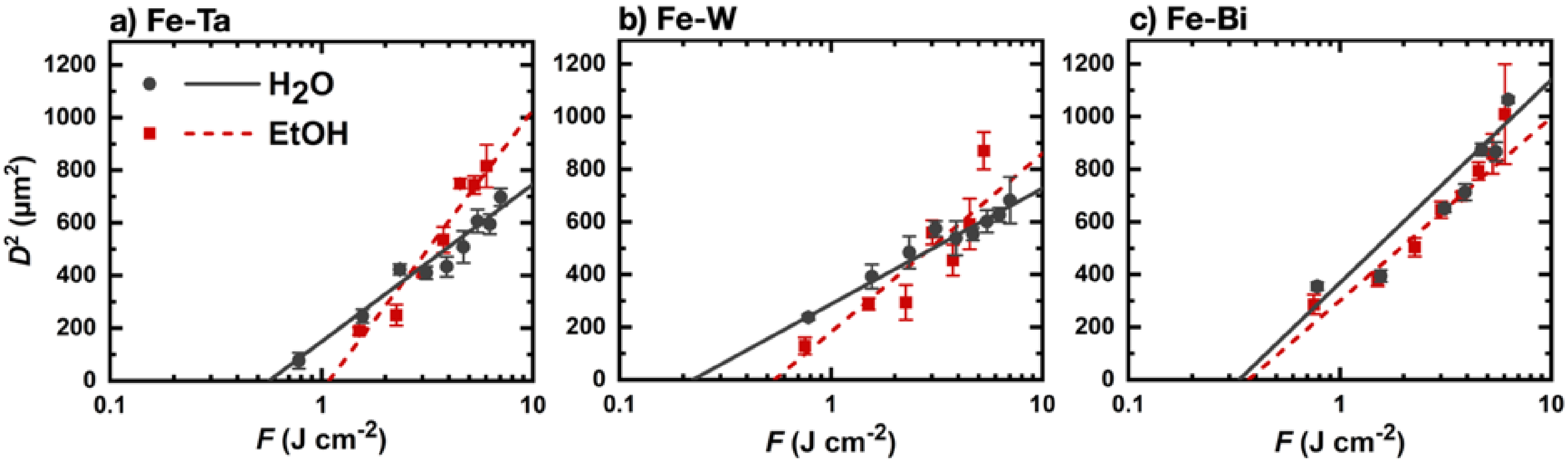

A. Naghilou, O. Bomati-Miguel, A. Subotic, R. Lahoz, M. Kitzler-Zeiler, C. Radtke, M.A. Rodríguez, W. Kautek, Ceram. Int. 47 (2021) 29363-29370

F_{th} deduced from the D^2-ln$F$ data

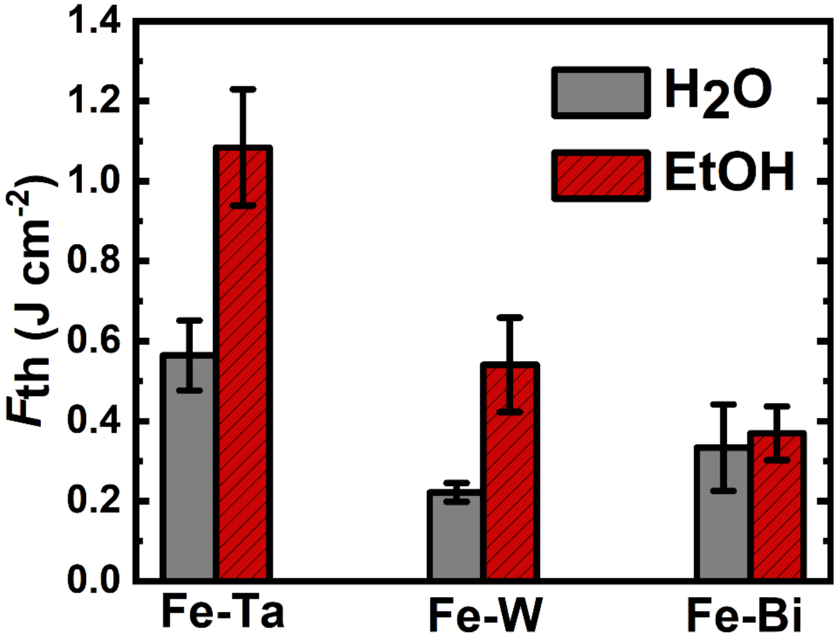

Plasma-induced dissociation of **ethanol**, facilitating the formation of solid **carbon particles** and longer **hydrocarbon molecules** which **absorb** part of the laser radiation.

A. Naghilou, O. Bomati-Miguel, A. Subotic, R. Lahoz, M. Kitzler-Zeiler, C. Radtke, M.A. Rodríguez, W. Kautek, Ceram. Int. 47 (2021) 29363-29370

F_{th} deduced from the D^2-ln$F$ data

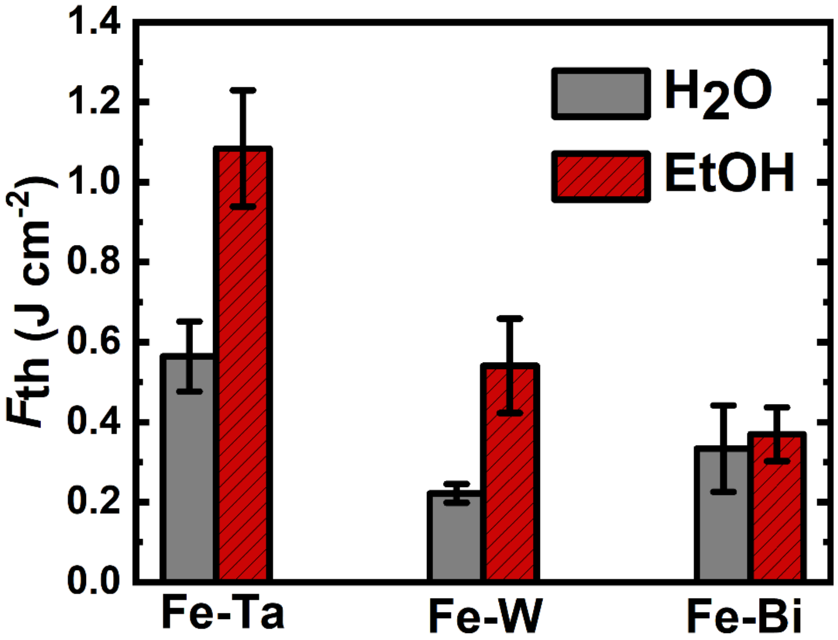

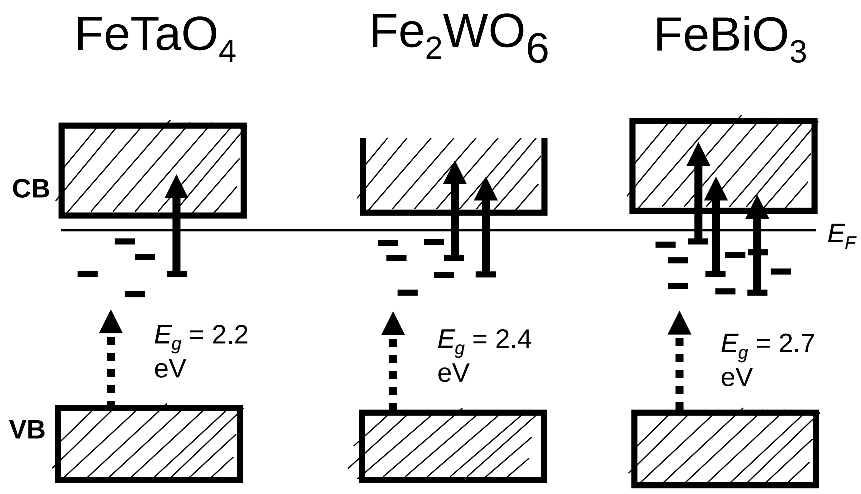

Laser: 1.55 eV!
1 and 2 photon excitation
Excitation depends on **defect density**

A. Naghilou, O. Bomati-Miguel, A. Subotic, R. Lahoz, M. Kitzler-Zeiler, C. Radtke, M.A. Rodríguez, W. Kautek, Ceram. Int. 47 (2021) 29363-29370

EDX of NPs

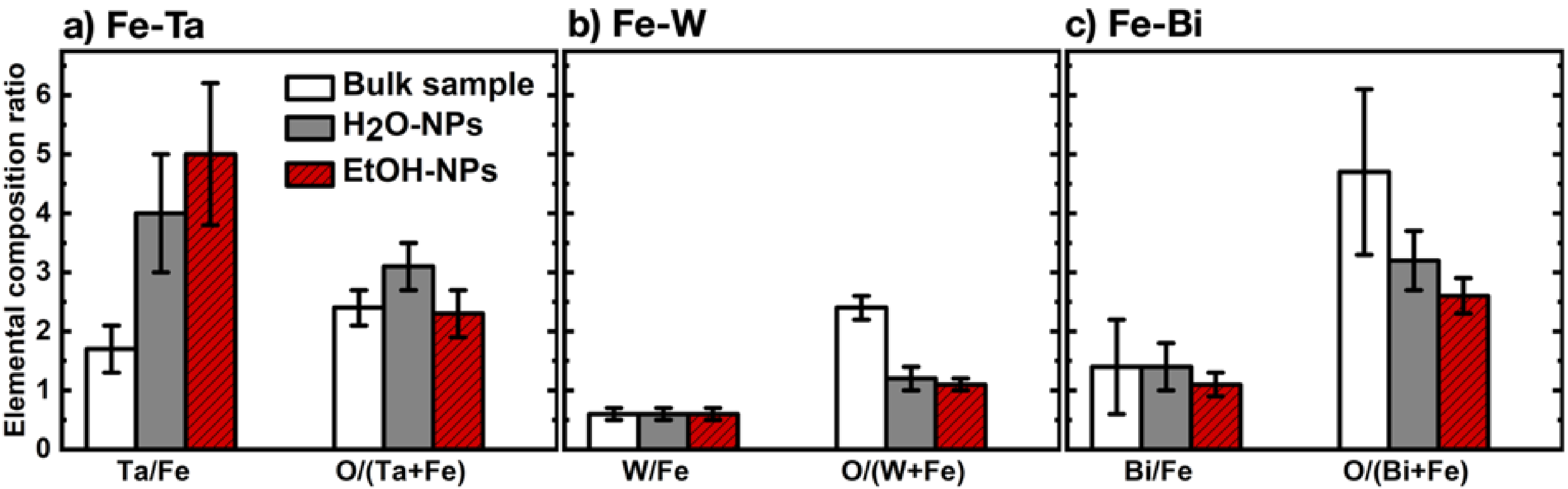

A. Naghilou, O. Bomati-Miguel, A. Subotic, R. Lahoz, M. Kitzler-Zeiler, C. Radtke, M.A. Rodríguez, W. Kautek, Ceram. Int. 47 (2021) 29363-29370

TEM and SAED patterns of NPs from H_2O

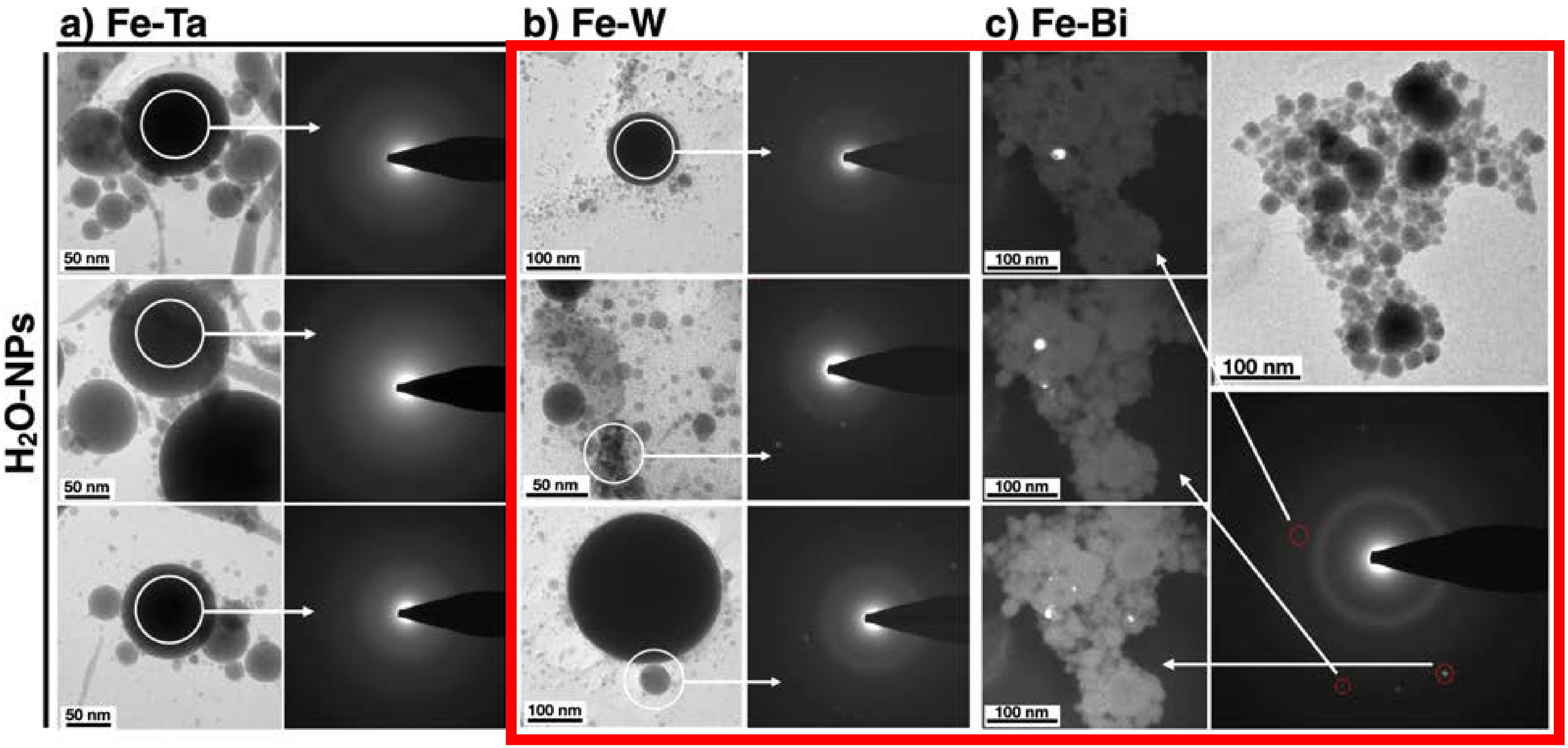

0.5% citric acid aqueous solution
N = 1206 pulse overlap, F = 3.90 J cm^{-2}.

A. Naghilou, O. Bomati-Miguel, A. Subotic, R. Lahoz, M. Kitzler-Zeiler, C. Radtke, M.A. Rodríguez, W. Kautek, Ceram. Int. 47 (2021) 29363-29370

TEM and SAED patterns of NPs from Ethanol

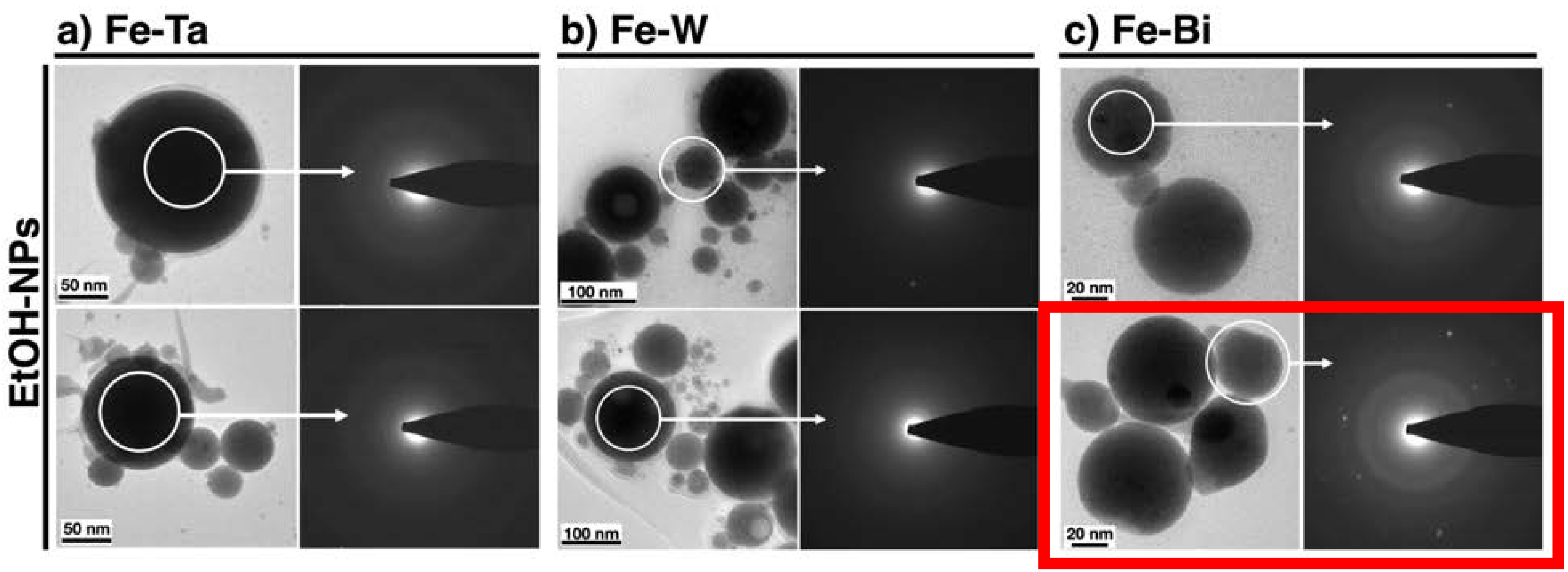

0.5% citric acid ethanol solution

N = 1221 pulse overlap and F = 3.77 J cm^{-2}

A. Naghilou, O. Bomati-Miguel, A. Subotic, R. Lahoz, M. Kitzler-Zeiler, C. Radtke, M.A. Rodríguez, W. Kautek, Ceram. Int. 47 (2021) 29363-29370

Schematic comparison of crystallinity of produced NPs in water and ethanol

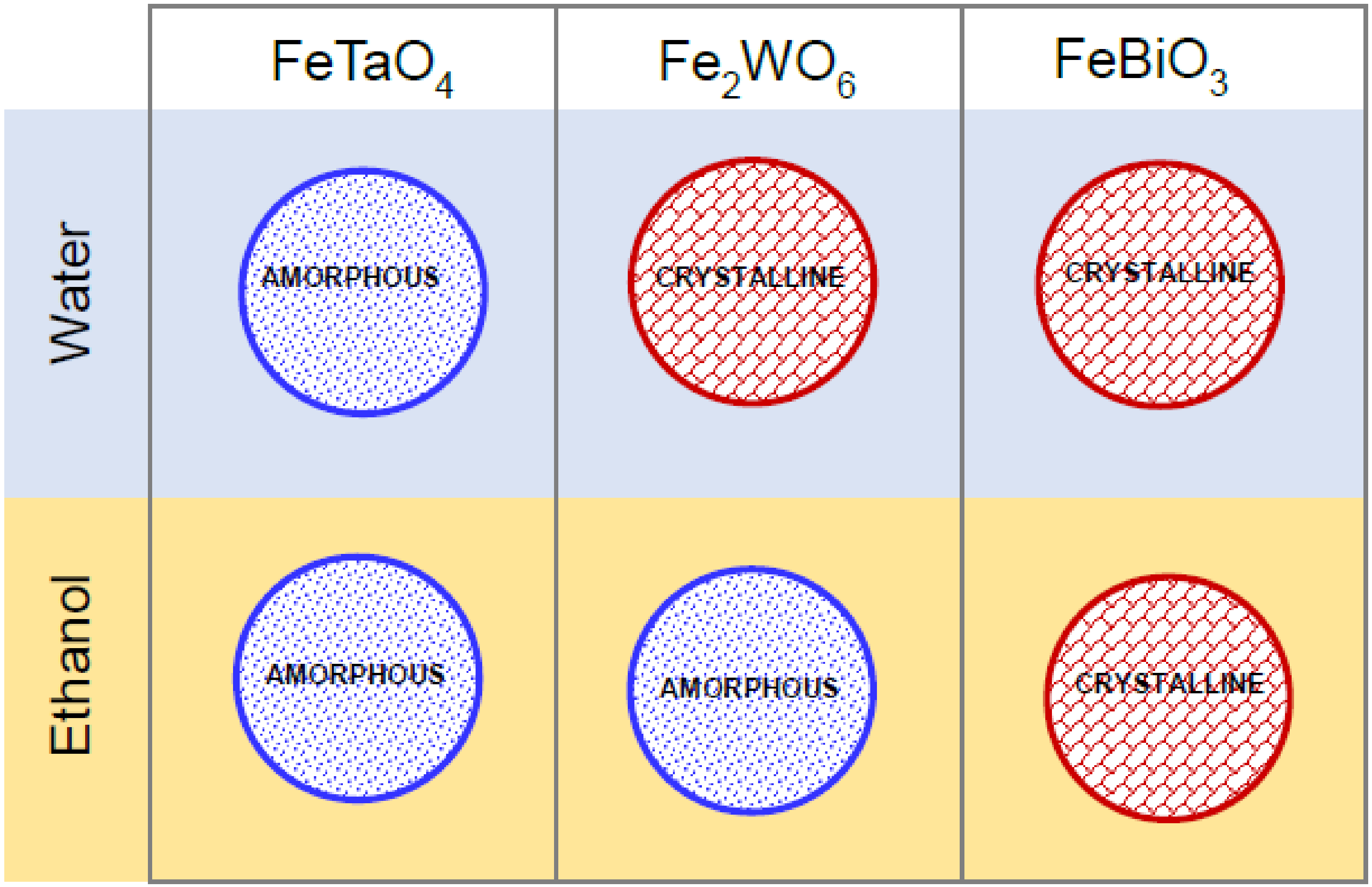

A. Naghilou, O. Bomati-Miguel, A. Subotic, R. Lahoz, M. Kitzler-Zeiler, C. Radtke, M.A. Rodríguez, W. Kautek, Ceram. Int. 47 (2021) 29363-29370

Femtosecond laser reduction of graphene oxide

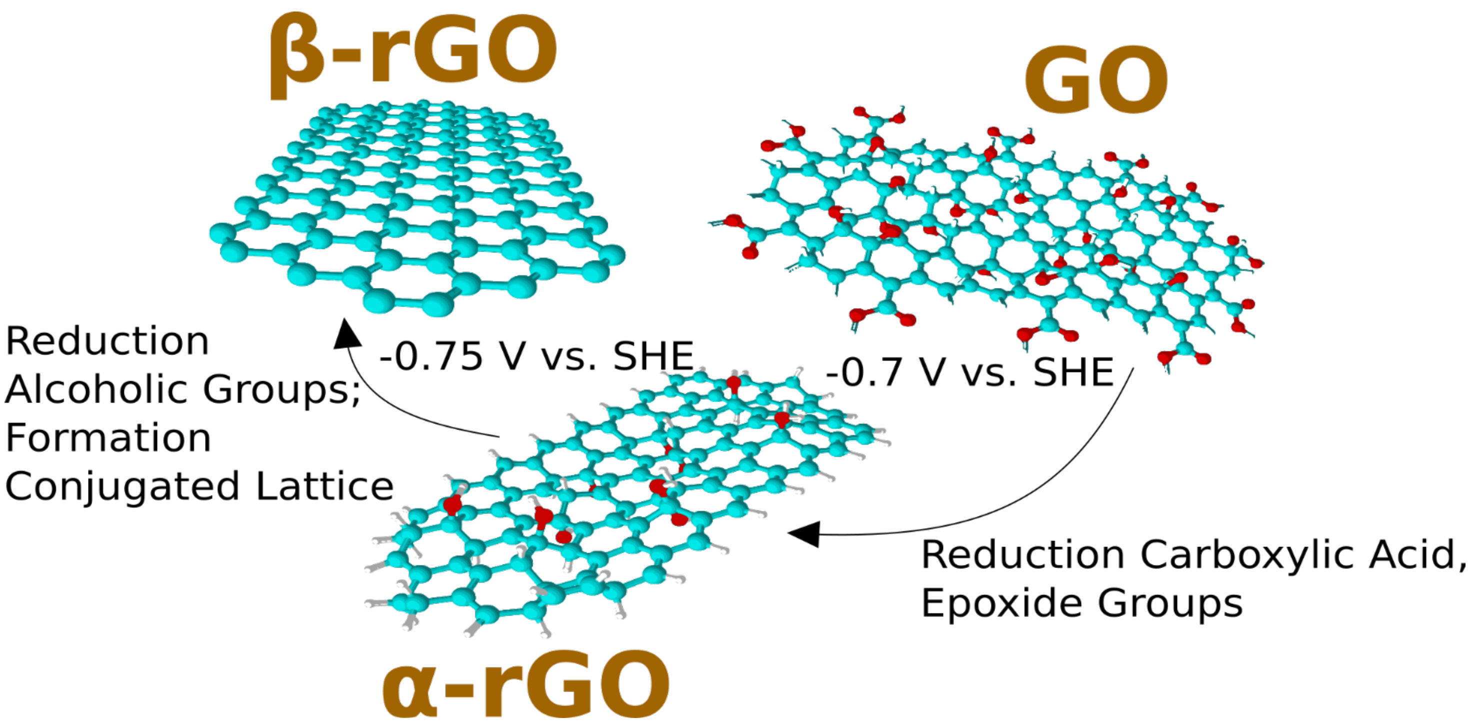

M. Pfaffeneder-Kmen, F. Bausch, G. Trettenhahn, W. Kautek, J. Phys. Chem. C 120 (2015) 15563–15568.
M. Pfaffeneder-Kmen, I. Falcon Casas, A. Naghilou, G. Trettenhahn, W. Kautek, Electrochim. Acta 255 (2017) 160-167.

Graphene Oxide Reduction with a fs-Laser

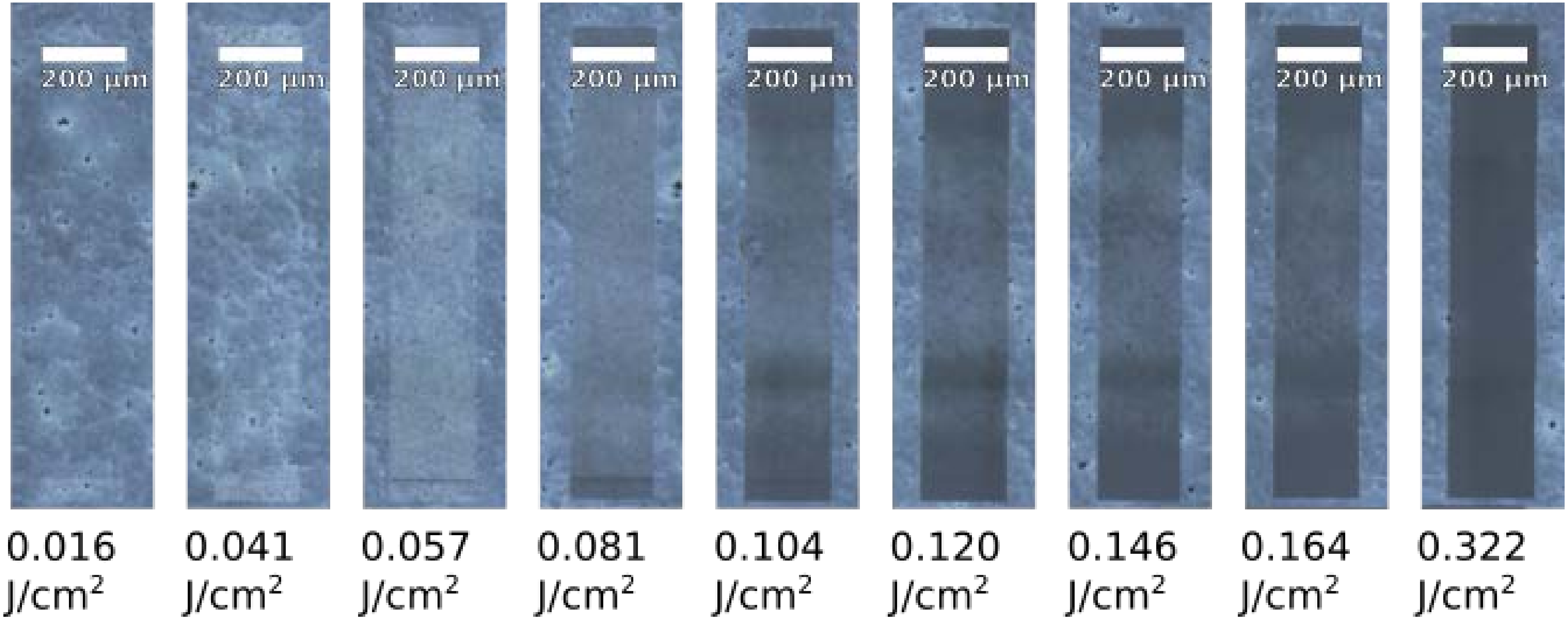

M. Pfaffeneder-Kmen, I. Falcon Casas, A. Naghilou, G. Trettenhahn, W. Kautek, in publication.

Graphene Oxide Reduction with a fs-Laser:
Bandgap, Raman, Conductivity

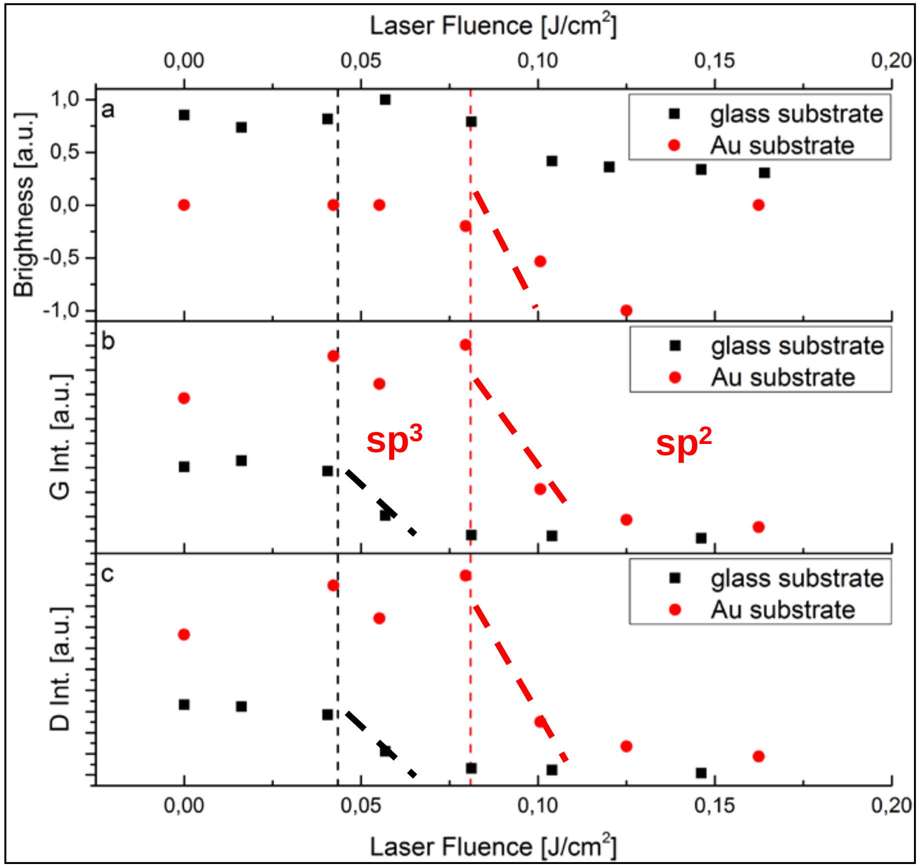

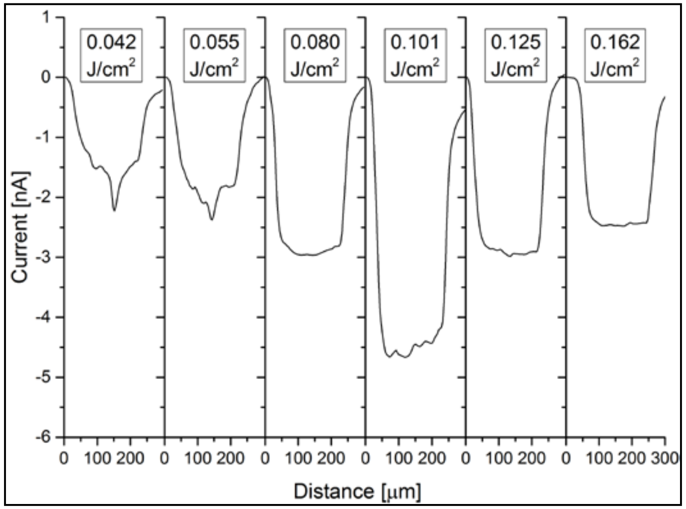

M. Pfaffeneder-Kmen, I. Falcon Casas, A. Naghilou, G. Trettenhahn, W. Kautek, in publication.

Near-field femtosecond laser reduction of graphene oxide

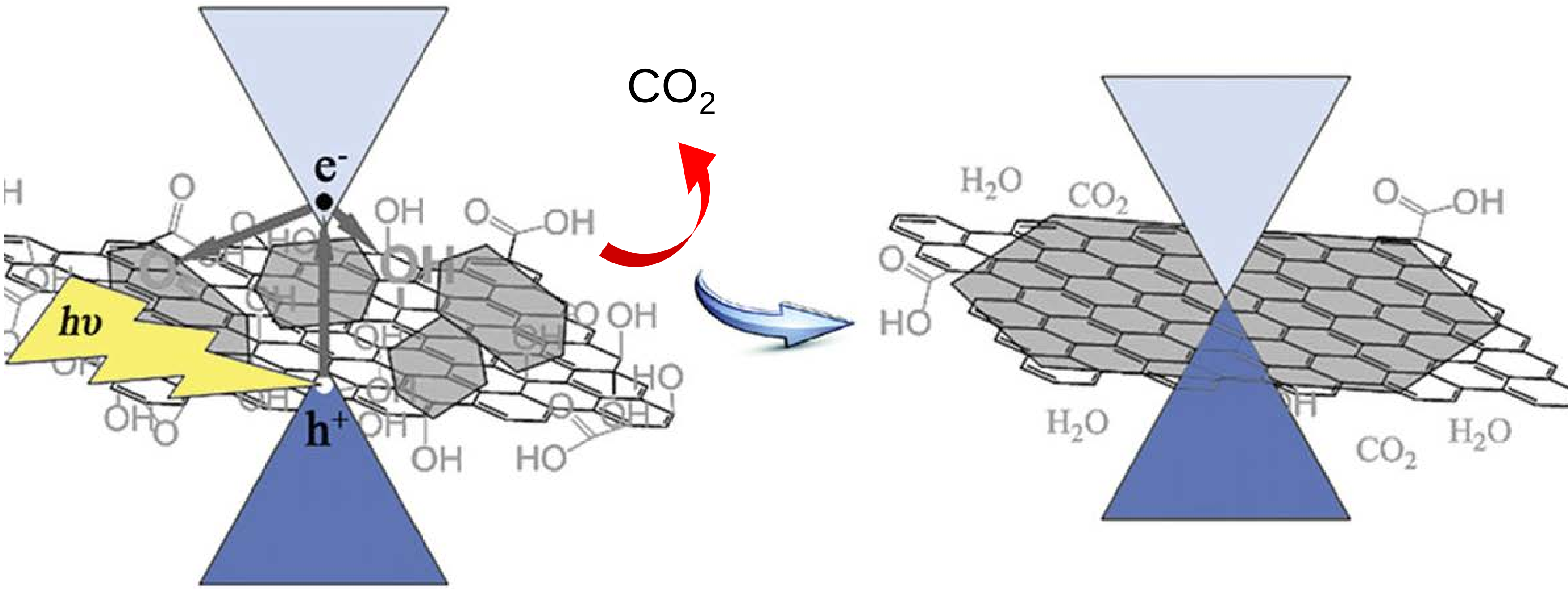

Energy dissipation and phase transformations following excitation by ultrashort laser pulses

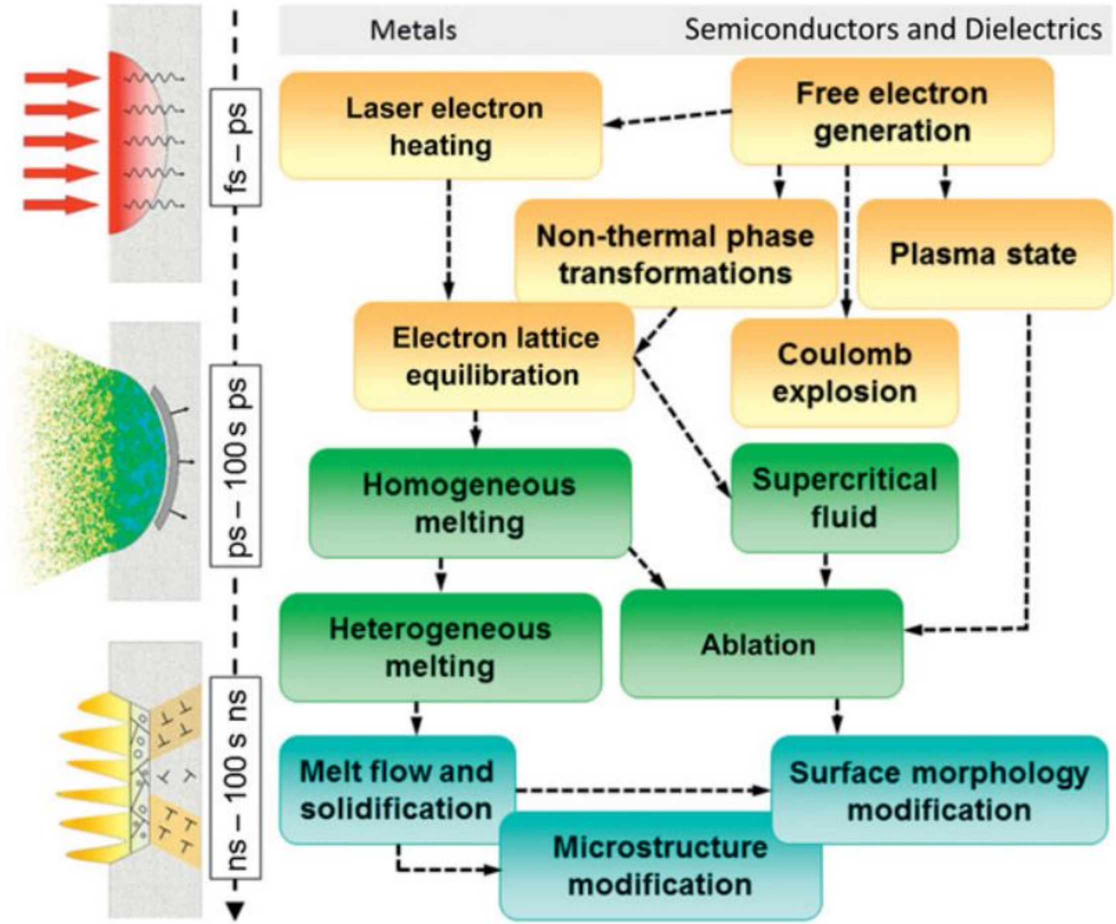

M.V. Shugaev, C. Wu, O. Armbruster, A. Naghilou, N. Brouwer, D.S. Ivanov, T.J.-Y. Derrien, N.M. Bulgakova, W. Kautek, B. Rethfeld, L.V. Zhigilei, MRS Bulletin 41 (2016) 960–968.

Handbook

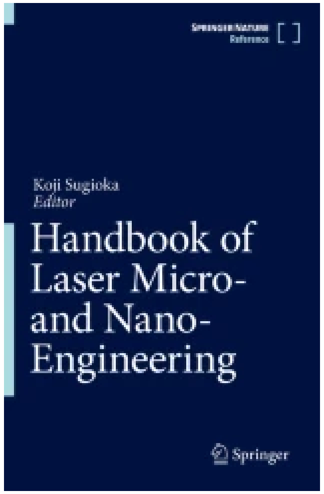

"Handbook of Laser Micro- and Nano-Engineering"
Ed. K. Sugioka, Springer International Publishing, Cham 2021

Authors:
Nadezhda M. Bulgakova, Leonid Zhigilei, Peter Balling,
Wolfgang Kautek, Maxim V. Shugaev, Antonio Miotello,
Marta Castillejo, Koji Sugioka, Jörn Bonse, Jörg Krüger,
Minghui Hong, Hiroyuki Niino, Craig B. Arnold, Saulius Juodkazis,
Alberto Piqué, Mangirdas Malinauskas, Bilal Gökce,
Costas P. Grigoropoulos, Jan J. Dubowski, Boris N. Chichkov,
…. et al.

Lecture References

Text Books edited by

International School on Lasers in Materials Science (SLIMS)

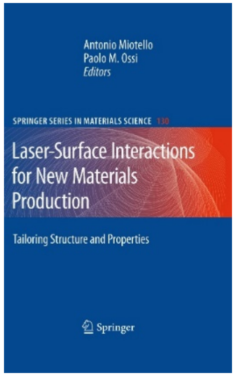

"Laser-Surface Interactions for New Materials Production: Tailoring Structure and Properties"
(Eds.) A Miotello, P.M. Ossi
Springer Series in Materials Science **130** (2010)
Springer-Verlag Berlin Heidelberg 2010
https://link.springer.com/book/10.1007/978-3-642-03307-0

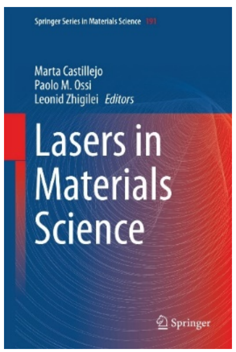

"Lasers in Materials Science"
(Eds.) M. Castillejo, P.M. Ossi, L. Zhigilei
Springer Series in Materials Science **191** (2014)
Springer International Publishing Switzerland 2014
https://link.springer.com/book/10.1007/978-3-319-02898-9

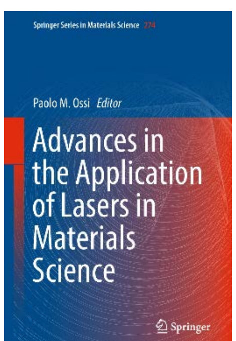

"Advances in the Application of Lasers in Materials Science"
(Ed.) P.M. Ossi
Springer Series in Materials Science 274 (2018)
Springer Nature Switzerland AG 2018
https://link.springer.com/book/10.1007/978-3-319-96845-2